

Air Infiltration through Revolving Doors

Lin Du

A Thesis

in

The Department

of

Building, Civil and Environmental Engineering

Presented in Partial Fulfillment of the Requirements
for the Degree of Master of Applied Science (Building Engineering) at

Concordia University

Montreal, Quebec, Canada

December, 2009

© Lin Du, 2009



Library and Archives
Canada

Published Heritage
Branch

395 Wellington Street
Ottawa ON K1A 0N4
Canada

Bibliothèque et
Archives Canada

Direction du
Patrimoine de l'édition

395, rue Wellington
Ottawa ON K1A 0N4
Canada

Your file *Votre référence*
ISBN: 978-0-494-67309-6
Our file *Notre référence*
ISBN: 978-0-494-67309-6

NOTICE:

The author has granted a non-exclusive license allowing Library and Archives Canada to reproduce, publish, archive, preserve, conserve, communicate to the public by telecommunication or on the Internet, loan, distribute and sell theses worldwide, for commercial or non-commercial purposes, in microform, paper, electronic and/or any other formats.

The author retains copyright ownership and moral rights in this thesis. Neither the thesis nor substantial extracts from it may be printed or otherwise reproduced without the author's permission.

In compliance with the Canadian Privacy Act some supporting forms may have been removed from this thesis.

While these forms may be included in the document page count, their removal does not represent any loss of content from the thesis.

AVIS:

L'auteur a accordé une licence non exclusive permettant à la Bibliothèque et Archives Canada de reproduire, publier, archiver, sauvegarder, conserver, transmettre au public par télécommunication ou par l'Internet, prêter, distribuer et vendre des thèses partout dans le monde, à des fins commerciales ou autres, sur support microforme, papier, électronique et/ou autres formats.

L'auteur conserve la propriété du droit d'auteur et des droits moraux qui protègent cette thèse. Ni la thèse ni des extraits substantiels de celle-ci ne doivent être imprimés ou autrement reproduits sans son autorisation.

Conformément à la loi canadienne sur la protection de la vie privée, quelques formulaires secondaires ont été enlevés de cette thèse.

Bien que ces formulaires aient inclus dans la pagination, il n'y aura aucun contenu manquant.


Canada

ABSTRACT

Air Infiltration through Revolving Doors

Lin Du

For large public buildings, conventional swing or sliding doors provide openings on the ground floor causing significant amount of energy losses through doorway. The configuration of revolving doors keeps the entrance closed at all times while allowing large number of people to pass through. Therefore, revolving doors are widely used as a solution to reduce the undesired air infiltration caused by the entrance and minimize the energy needs for heating and cooling.

A 1/10 reduced-scale model was designed for the laboratory measurements of the air infiltration caused by the movement of revolving doors. The revolving door was installed on a well-insulated airtight box, placed in a climatic chamber in which the winter outdoor conditions were controlled. A heater was installed inside the box to maintain the indoor environment at a constant temperature. Experiments were performed at different rotation speeds of the revolving door. The air infiltration rates due to the door rotation at different indoor-outdoor temperature differences were calculated based on the energy balance equation of the air inside the box. The experimental results were compared with those from very limited previous studies.

Correlation-based models of the volumetric air flow rate expressed by the rotation speed and dimensionless temperature indexes around the door were obtained at different seal conditions. The models established on the base of the experimental data provide an easy

way to calculate the part of air infiltration rate caused by the motion of a revolving door in prototype. The energy loss due to the rotation of door, based on the new experiments, was also compared with those based on previous data.

ACKNOWLEDGEMENTS

First of all, I would like to show my greatest appreciation to my supervisors, Dr. R. Zmeureanu and Dr. T. Stathopoulos, for providing me opportunity and financial assistance for my Master studies. Thank you for your patience, suggestions and encouragement in all the time of research and writing of this thesis.

Many thanks are due to Mr. J. Hrib and Mr. L. Demers. Thank you for help me build the experimental model. I cannot remember how many times I called you when something went wrong and you always came to fix the problems. My experiments could not be finished without your help.

More particularly, endless thanks should go to my beloved family. Even though you are far away in China, I know that all of you stay with me in my heart. Thank you so much for the constant support, from financially to mentally.

Last but not the least I wish to express a sense of gratitude to my best friend in Montreal, Kenny Wakeling. Your support and encouragement gave me strength to overcome all the difficulties. Finally, I want to thank my other friends, Jing Li, Laurent Magnier, and Xiaotian Chen for all their help and support during my study and research.

Table of Contents

LIST OF FIGURES	viii
LIST OF TABLES	xii
NOMENCLATURE	iv
CHAPTER 1 INTRODUCTION	1
1.1. Revolving Doors	1
1.2. Research Objectives	2
1.3. Thesis Outline	3
CHAPTER 2 LITERATURE REVIEW	5
2.1. Standards	5
2.2. Full-Scale Study	6
2.3. Full-scale measurement.....	10
2.4. Reduced-scale model.....	12
2.5. Analytical Model.....	14
2.6. Estimation of Energy Savings by Using Revolving Doors.....	18
2.7. Conclusion.....	18
CHAPTER 3 DESIGN OF THE REDUCED-SCALE MODEL	20
3.1. Similitude and Modeling Methodologies	20

3.1.1.	Similitude.....	20
3.1.2.	Dimensionless Group.....	21
3.1.3.	Scale Ratios.....	22
3.2.	Design of Experiment.....	23
3.2.1.	Field Study.....	23
3.2.2.	Dimensions of the Experimental Model	27
3.3.	Experimental Approach.....	29
3.3.1.	Measurement of Air Temperature.....	34
3.3.2.	Measurement of Electric Power Input	37
3.3.3.	Identification of the Overall UA-value of the Insulated Box	38
3.3.4.	Setup of Infrared Camera.....	39

CHAPTER 4 EXPERIMENTAL RESULTS AND DISCUSSION..... 411

4.1.	Data Measurement and Analysis.....	41
4.1.1.	Experimental Results	41
4.1.2.	Error Analysis.....	48
4.1.3.	Conversion of the Experimental Results to the Prototype Air Infiltration Rate.....	54
4.1.4.	Discussion.....	56
4.1.5.	Air Infiltration through Revolving Door with Different Conditions of Seals.....	60

4.2. Dimensionless Expression of Temperature Distribution	61
4.3. Infrared Images	69
4.4. Correlation-Based Models.....	73
4.5. Conclusion.....	77
CHAPTER 5 CONCLUSIONS AND RECOMMENDATIONS FOR FUTURE WORK	79
5.1. Summary and Conclusions.....	79
5.2. Future Work	81
References	83
Appendix A: Air Velocities inside the Climatic Chamber	85
Appendix B: Instantaneous Calculation Method of Experimental Air Infiltration.....	90
B-1. Heat loss through the envelope	90
B-2. Tests with one layer of insulation	91
B-3. Tests after two layers of insulation	93
B-4. The instantaneous method.....	95
Appendix C: Measured Temperatures and Dimensionless Temperatures around the Experimental Revolving Door.....	101

Appendix D: Correlation-based Models Obtained from Experimental	
Data.....	107

LIST OF FIGURES

Fig. 2-1: Infiltration through new and worn door seals (door is not rotating) (Schutrum et al., 1961).....	7
Fig. 2-2: Infiltration vs. rpm and indoor-outdoor air temperature difference for motor-operated revolving door (air leakage past seals deducted) (Schutrum et al., 1961).....	8
Fig. 2-3: Infiltration through manually-operated revolving doors (air movement 35 fpm indoors, air leakage past door seals deducted) (Schutrum et al., 1961).....	9
Fig. 2-4: Comparison of the air leakage of four doors and results of Schutrum et al. (1961) (Zmeureanu et al., 2001).....	11
Fig. 2-5: Schematic displacement as a result of the movement of the door (Schijndel et al., 2003).....	16
Fig. 3-1: Frequency of occurrence of rotation speed of the revolving doors from field study.....	26
Fig. 3-2: Average rotation speed vs. traffic rate from the field study.....	26
Fig. 3-3: Dimensions of the experimental box and revolving door without outside insulation (dimensions are in cm).....	27
Fig. 3-4: Box position inside the environmental chamber (dimensions are in cm).....	28
Fig. 3-5: Dimensions of the experimental model (dimensions are in cm).....	29
Fig 3-6: Experimental instrumentation setup.....	34
Fig. 3-7: Locations of thermocouples outside the box.....	35

Fig. 3-8: Locations of thermocouples inside the box.....	36
Fig 3-9: Additional thermocouples outside the door to identify the air flow direction (dimensions are in cm).....	37
Fig. 3-10: Illustration of how to record the power input.....	38
Fig. 3-11: Horizontal screen in front of the revolving door.....	39
Fig. 3-12: Infrared camera and horizontal screen in front of the revolving door.....	40
Fig. 3-13: Vertical screen in front of the revolving door.....	40
Fig. 4-1: Experimental indoor temperature in the time interval Δt at 19.06 rpm.....	42
Fig. 4-2: Linear relationship between the volumetric air infiltration rate and the rotation speed of the experimental revolving door.....	47
Fig. 4-3: Polynomial relationship between the volumetric air infiltration rate and the rotation speed of the experimental revolving door.....	47
Fig. 4-4: Volumetric air infiltration rate vs, rotation speed of the prototype door.....	54
Fig. 4-5: Experimental air infiltration rate due to the revolution of the door vs. air flow rate of the same dimensioned centrifugal fan vs. previous study in the reduced-scale....	57
Fig. 4-6: Experimental air infiltration rate with different conditions of seals (The curves of the condition with only two vertical seals and the condition of no vertical seals are obtained by an exchange student, Alexis Aupied, using the same experimental setup as this study).....	60
Fig. 4-7: Illustration of the temperature measurement points around the revolving door.....	62

Fig. 4-8: Dimensionless temperature at thermocouple A, B, C, and D around the experimental revolving door.....	63
Fig. 4-9: Comparison of the dimensionless temperature at thermocouple B, C and M_i around the experimental revolving door.....	64
Fig. 4-10: Comparison of the dimensionless temperature at thermocouple A, D and M_o around the experimental revolving door.....	64
Fig. 4-11: Sketch showing the air flow direction.....	66
Fig. 4-12: Location of additional thermocouples to identify the air flow direction (dimensions in cm).....	67
Fig. 4-13: Temperatures in front of the door showing the air flow direction at 173.24 rpm and 18.5°C temperature difference between indoor and outdoor.....	67
Fig. 4-14: Temperatures in front of the door showing the air flow direction at 295.73 rpm and 13.98°C temperature difference between indoor and outdoor.....	68
Fig. 4-15: Temperatures in front of the door showing the air flow direction at 300.3 rpm and 42.16°C temperature difference between indoor and outdoor.....	68
Fig. 4-16: Infrared image on a horizontal screen outside the revolving door with four seals at $N = 50$ rpm.....	69
Fig. 4-17: Infrared image on a horizontal screen outside the revolving door with four seals at $N = 300$ rpm.....	70
Fig. 4-18: Infrared image on a horizontal screen outside the revolving door without vertical seals at $N = 50$ rpm.....	71

Fig. 4-19: Infrared image on a horizontal screen outside of the revolving door without vertical seals at N = 300 rpm.....	71
Fig. 4-20: Vertical infrared image on a vertical screen outside of the revolving door with four seals at N = 300 rpm.....	72
Fig. A-1: The comparison of the air velocity with and without the box in the chamber...	89
Fig. B-1: Illustration of the position of thermocouples.....	91
Fig. B-2: The temperature difference between indoor and outdoor environment in the experiment of 19.06 rpm.....	98
Fig. B-3: Volumetric air flow rate vs. the rotation speed of the experimental revolving door.....	100
Fig. C-1: The location of the thermocouple round the revolving door.....	101

LIST OF TABLES

Table 2-1: Maximum air leakage rate of entrance doors in four standards.....	6
Table 2-2: Air infiltration rate of four revolving doors and standard provisions (Zmeureanu et al., 2001).....	11
Table 3-1: Data for the revolving door no. 1 of the first university building.....	24
Table 3-2: Data for the revolving door no. 2 of the second university building.....	24
Table 3-3: Data for the revolving door no. 3 of an office building.....	25
Table 3-4: UA-value at different indoor air temperatures.....	38
Table 4-1: Infiltration air flow rate at different rotation speeds at indoor temperature around 20°C in the reduce-scale model.....	45
Table 4-2: Infiltration air flow rate at different rotation speeds around 40°C and 25°C indoor temperature in the reduced-scale model.....	46
Table 4-3: Error analysis of the experimental data.....	53
Table 4-4: Air infiltration rate at different rotation speeds in the reduced-scale model and prototype.....	55
Table 4-5: Experimental air infiltration rate due to the revolution of the revolving door vs. air flow rate of a same dimensioned centrifugal fan.....	59
Table 4-6: Example of the dimensionless temperature distribution near the revolving door at indoor temperature around 20°C and 40°C.....	62

Table 4-7: The dimensionless temperature of each test point at different experimental rotation speeds.....	65
Table 4-8: Data from experiments vs. simulated data from correlation equation in prototype with four seals condition.....	75
Table 4-9: Data from experiments vs. simulated data from correlation equation in prototype with no vertical seals.....	77
Table A-1: Air velocity near the front of the box (tested with the box in the chamber)...	86
Table A-2: Air velocity near the front of the box (tested after removing the box).....	87
Table A-3: The air velocity vs. the height.....	88
Table B-1: U-value calculated from the experiments vs. reference value.....	90
Table B-2: The air flow rate with different rotation speeds with one layer of insulation.....	91
Table B-3: The temperature distribution and temperature difference between inside and outside of the revolving door with different rotation speed with one layer of insulation.....	92
Table B-4: The air flow rate with different rotation speed with two layers of insulation.....	93
Table B-5: The temperature distribution around the revolving door with two layers of insulation.....	94
Table B-6: Air flow rate at different rotation speeds in the model.....	99
Table C-1: The temperature distribution at $T_i = 20^\circ\text{C}$	101

Table C-2: The temperature distribution at $T_i = 25^\circ\text{C}$ or 40°C	106
Table D-1: Dimensionless temperature around the revolving door with full seals.....	107
Table D-2: Dimensionless temperature around the revolving door without vertical seals.....	108
Table D-3: Correlation-based model of air infiltration when the revolving door has four seals.....	109
Table D-4: Correlation equations of air infiltration when the revolving door does not have vertical seals.....	110

NOMENCLATURE

A	Total exterior surface area of the experimental box	(m^2)
C	Flow coefficient	(-)
c_p	Specific heat of air	($J/kg \cdot ^\circ C$)
D	Diameter of the revolving door	(m)
D_p	Diameter of the revolving door in prototype	(m)
D_m	Diameter of the revolving door in model	(m)
f_o	Air displacement as fraction of segment volume when a segment is exposed to outdoor environment	(-)
f_i	Air displacement as fraction of segment volume when a segment is exposed to indoor environment	(-)
h_o	Head of air at the beginning of opening cycle	(m)
$I_{heater,j}$	Electric current to the heater at each reading step j	(A)
$I_{fan,j}$	Electric current to the heater at each reading step j	(A)
K	Coefficient of the air exchange through revolving door	(-)
m_{inf}	Mass air flow rate through a revolving door	(kg/s)
m_1	Mass of air inside the box at the beginning of the calculation time interval	(kg)
m_2	Mass of air inside the box at the end of the calculation time interval	(kg)
m_I	Mass of air in segment I	(kg)
m_{II}	Mass of air in segment II	(kg)

$m_{o,I}$	Mass of air entering segment I from outside	(kg)
$m_{II,I}$	Mass of air from segment II transferred to segment I	(kg)
$m_{i,II}$	Mass of air entering segment II from inside	(kg)
$m_{I,II}$	Mass of air from segment I transferred to segment II	(kg)
N	Rotation speed of the revolving door	(rpm)
N_{model}	Average rotation speed during the time interval Δt in model	(rpm)
N_p	Rotation speed of a revolving door in prototype	(rpm)
N_{total}	Total number of rotations during the time interval Δt	(rpm)
Q	Volumetric air flow rate	(m^3/s)
q	Net air infiltration from outdoor to indoor	(m^3)
q_1	Volume of air exchange between door segments and environments at the opening cycle	(m^3)
q_2	Volume of air exchange between door segments and environments at the closing cycle	(m^3)
$q_{\text{correlation}}$	Volumetric air flow rate in prototype from correlation-based model	(L/s)
Q_{door}	Heat loss of the box due to air infiltration through the revolving door over the time Δt when door moves	(J)
Q_{fan}	Heat generated by the small fan over the time Δt	(J)
Q_{heater}	Heat generated by heater over the time interval Δt	(J)
q_{inf}	Volumetric air infiltration rate through the revolving door	(m^3/s)
$q_{\text{inf_prototype}}$	Volumetric air infiltration rate in prototype	(L/s)
Q_{loss}	Heat loss of the box walls over the time Δt	(J)

q_{segment}	Volume of air exchange between one door segment and environments	(m^3)
$q_{o,I}$	Volumetric air flow from outdoor to the segment I	(m^3)
$q_{I,i}$	Volumetric air flow from segment I to indoor	(m^3)
R	Door radius	(m)
Re	Reynolds number	$(-)$
R^2	Coefficient of determination	$(-)$
$Se_{y/x}$	Standard error of the correlation-based model	$(-)$
T_i	Indoor air temperature	$(^{\circ}C)$
T_o	Outdoor air temperature	$(^{\circ}C)$
T_x	Air temperature at test point x	$(^{\circ}C)$
T_1	Average temperature inside the box at the beginning of the time interval Δt	$(^{\circ}C)$
T_2	Average temperature inside the box at the end of the time interval Δt	$(^{\circ}C)$
T_I	Air temperature in segment I	$(^{\circ}C)$
T_{II}	Air temperature in segment II	$(^{\circ}C)$
U	Overall heat transfer coefficient	$[W/(m^2 \cdot K)]$
V	Mean fluid velocity	(m/s)
V_m	Mean fluid velocity in reduced-scale model	(m/s)
V_p	Mean fluid velocity in prototype	(m/s)
V_{box}	Inside volume of the experimental box	(m^3)
V_{segment}	Volume of one door segment	(m^3)

$V_{fan,j}$	Voltage to the small fan at each reading step	(V)
$V_{heater,j}$	Voltage to the heater at each reading step	(V)
Greek symbols		
α	Percentage of the cold air coming from outdoor in segment I	(-)
θ_x	Dimensionless air temperature index	(-)
θ_{Ah}	Dimensionless air temperature index at high location A	(-)
θ_{Al}	Dimensionless air temperature index at low location A	(-)
θ_{Bh}	Dimensionless air temperature index at high location B	(-)
θ_{Bl}	Dimensionless air temperature index at low location B	(-)
θ_{Ch}	Dimensionless air temperature index at high location C	(-)
θ_{Cl}	Dimensionless air temperature index at low location C	(-)
θ_{Dh}	Dimensionless air temperature index at high location D	(-)
θ_{Dl}	Dimensionless air temperature index at low location D	(-)
θ_{Mo}	Dimensionless air temperature index at the middle height outside of the revolving door	(-)
θ_{Mi}	Dimensionless air temperature index at the middle height inside of the revolving door	(-)
λ_L	Geometric ratio	(-)
λ_V	Velocity ratio	(-)
λ_ω	Angular velocity factor	(-)
μ	Dynamic fluid viscosity	(Pa·s)
ν	Kinematic fluid viscosity	(m ² /s)
ν_p	Kinematic fluid viscosity in prototype	(m ² /s)

ν_m	Kinematic fluid viscosity in model	(m^2/s)
ρ	Density of the fluid	(kg/m^3)
$\rho_{segment}$	Air density in the door segment at the beginning of the opening cycle	(kg/m^3)
ρ_i	Air density in the room	(kg/m^3)
ρ_{ref}	Reference density of air	(kg/m^3)
ρ_1	Air density at the beginning of the time interval Δt	(kg/m^3)
ρ_2	Air density at the end of the time interval Δt	(kg/m^3)
ω	Angular speed	(rad/s)
ω_p	Angular speed of the revolving door in prototype	(rad/s)
ω_m	Angular speed of the revolving door in model	(rad/s)
$\omega\%$	Relative standard error of the correlation-based model	$(\%)$
ΔQ	Energy change inside the box in the time interval Δt	(J)
Δt	Time interval	(s)
Δt_{step}	Time step between each recording	(s)

CHAPTER 1

INTRODUCTION

1.1. Revolving Doors

Revolving doors are widely used as entrances of large public buildings which have high numbers of users, such as office buildings, shopping malls and hotels. A revolving door usually consists of three or four segments. The transparent doors separating the segments are called wings, and there are curved walls surrounding the wings. This configuration keeps the entrance closed all the time, and allows large numbers of people to pass through orderly. Comparing to other kinds of doors, such as swinging or sliding doors, revolving doors reduce the air infiltration and minimize the energy needs for heating and cooling caused by the entrance (Stalder, 2009).

Although there is no direct connection between indoor and outdoor environments, air exchange still occurs. In winter, the cold air brought into the building can still affect the heating loads and causes thermal discomfort in the adjacent area. Previous research (Schutrum et al., 1961, Zmeureanu et al., 2001) expressed the air leakage through a revolving door as a combination of (1) air infiltration through the gaps and seals between the wings and the door housing, and (2) air displacement due to the revolution of the door. The infiltration through door seals depends on the indoor-outdoor pressure difference and position of the door wings, i.e. whether all four or only two wings are in contact with the housing. The air displacement when door is revolving depends on the door speed, temperature difference, outside wind velocity and indoor air movement.

Schutrum et al. (1961) showed their results in terms of air infiltration under different conditions – door still, with different indoor-outdoor pressures and door moving with different rotation speeds and temperature differences. For more than 40 years, this was the only source of information available for the estimation of heating load due to air infiltration through this type of doors. ASHRAE Standard 90.1 (ASHRAE, 1999) and Load Calculation Manual by McQuinston and Spitler (1992) presented the air infiltration rates through revolving doors of commercial or institutional buildings based on the study by Schutrum et al. (1961). Zmeureanu et al. (2001) measured the air leakage of existing revolving doors of an institutional building when the doors are still and found out that the air leakage through gaps and seals was much bigger than the recommendations in some standards. Allgayer and Hunt (2004) observed the air flow pattern driven by a reduced-scale revolving door which links two water-chambers when the door rotates. However, there is no following research providing experimental data about the air exchange due to their motion of revolving doors since Schutrum et al. (1961).

1.2. Research Objectives

The objectives of the present study are as follows:

- To measure the air exchange rate caused by the rotation of the door in a reduced-scale model and to convert the experimental data to full scale prototype.
- To develop an easily-applied methodology for the calculation of the air exchange rate due to the motion of revolving doors in prototype.

- To propose more reliable data to be implemented in standards concerning the air leakage of revolving doors. These data is needed for the estimation of the heat loss through this type of doors in order to properly size the HVAC system.

1.3. Thesis Outline

This thesis is organized in the following way.

- Chapter 2: Reviews of previous researches about the air infiltration through revolving doors. Energy-related regulations for this type of doors are also described.
- Chapter 3: The experiments were designed by using a 1/10 reduced-scale model of revolving door. This chapter explains the setup details of the reduced-scale model, the dimensions of the model, the experimental conditions, the method of measurements and calculations, and the instruments used in the experiments. Field studies were carried out to find out the possible range of the rotation speed in the experiments. The similarity ratios connecting the reduced-scale model and prototype door are defined. The air infiltration through the revolving door due to the movement of the door was calculated on the basis of heat balance of the indoor air environment.
- Chapter 4: A series of experiments were carried out with different rotation speeds. The air infiltration rates were calculated based on the experimental measurements and the results were converted into prototype according to the similarity ratios. The analysis of dimensionless temperatures around the revolving door indicates the air flow direction when the door turns. Infrared pictures give a better

visualization of the air flow pattern around the door. This chapter also includes the correlation equations concluded from the dimensionless temperatures, which will provide an easier way to calculate the air exchange rate due to the motion of prototype revolving doors.

- Chapter 5: This chapter includes the conclusions of the study, as well as recommendations for future work on this topic.

CHAPTER 2

LITERATURE REVIEW

Generally, air flow entering or leaving buildings is due to the pressure difference between indoor and outdoor environments. In the winter, heated indoor air rises up to the top of a building. Conventional swing or sliding doors provide openings on the ground floor every time when people pass through, allowing cold outdoor air to enter into the building. Cooled indoor air flows out of the building through the front doors in the summer. Revolving doors are widely introduced as a solution of allowing people passing through entrances while minimizing the undesirable air flow. The first part of this chapter summarizes recommendations of air infiltration rates through entrances from four standards and regulations. The second part covers previous studies of air flow through revolving doors by full-scale measurements, reduced-scale simulation and analytical models. A study of potential energy savings by improving the usage rate of revolving doors in a university building is also presented.

2.1. Standards

The ASHRAE standard 90.1 (ASHRAE, 1989) specifies that the air leakage for commercial entrance swinging doors or revolving doors shall not exceed $6.3 \text{ L}/(\text{s}\cdot\text{m}^2$ of the door area) when tested at 75 Pa pressure difference. This value was modified to $5.0 \text{ L}/(\text{s}\cdot\text{m}^2$ of the door area) in the more recent ASHRAE standard 90.1 (ASHRAE, 1999). The Model National Energy Code of Canada for Buildings (MNECCB, 1997) specifies that air leakage rate through swinging, revolving and sliding doors should not be more

than 17 L/s for each meter of the door crack. The Energy Conservation Building Code (ECBC) 2006 (IIEC, 2006) specifies: “Air leakage for glazed swinging entrance doors and revolving doors shall not exceed 5.0 L/(s·m²).” The standards are vague about the conditions of the application of the recommended values. It can be assumed that, for swinging and sliding doors, the recommendations are made for when the doors are closed. However, since revolving doors are considered as closed all the time, it is not clear whether the values should apply when doors are still or also when they turn. The comparison of values from these standards is shown as Table 2-1 and the values in bold are the original number from each standard. The other values in the table are calculated based on the dimensions of a typical revolving door. The ECBC 2006 and ASHRAE standard 90.1 are much more restrictive than the MNECCB.

Table 2-1: Maximum air leakage rate of entrance doors in four standards

Standards	L/ (s·m ² of the door area)	L/(s·m of the door crack)
ASHRAE standard 90.1 (1989)	6.3	1.58
ASHRAE standard 90.1 (1999 - present)	5.0	1.25
MNECCB (1997)	68	17
ECBC (2006)	5.0	1.25

2.2. Full-Scale Study

Schutrum et al. (1961) carried out experimental research on air infiltration through a revolving door installed at the entrance of a laboratory, for experimental purposes, under

heating and cooling conditions. An exhausting system was used to provide required pressure differences. A tracer gas technique with hydrogen was used to measure the net air infiltration. The air exchange through revolving doors was presented as the combination of two components in their research: (1) air infiltration through the gaps and seals between the wings and the door housing; and (2) air displacement due to the motion of the door. The first component was measured under the stationary condition. Tests for the second component were carried out for the motor-driven and the manually-operated doors, respectively.

At the stationary condition, tests were made with two sets of new seals and one set of worn seals, but there were no visible cracks for both new and used seals. The magnitude of air infiltration through the gaps was presented by a graph under different pressure differentials that either two wings or four wings were touching the door housing (Fig. 2-1). It was concluded that the air infiltration past door seals depends on the condition of seals and the indoor-outdoor pressure difference.

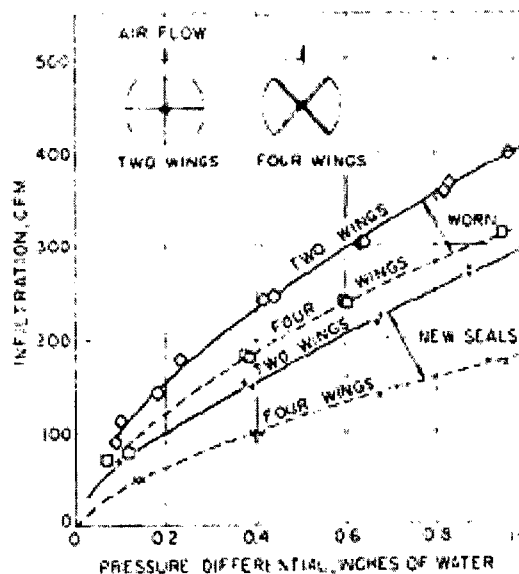


Fig. 2-1: Infiltration through new and worn door seals (door is not rotating) (Schutrum et al., 1961)

At the rotating condition, the air infiltration of a motor-operated revolving door was presented as a function of temperature difference and constant rotation speed at the indoor air movement of 0.18 m/s (35 fpm) and an outdoor wind velocity of 0.9 m/s (2 mph) (Min,1958) (Fig. 2-2). The infiltration of the manually-operated revolving doors was also measured under different traffic rates and temperature differentials at the same indoor and outdoor air movement conditions as the motor-operated door (Fig. 2-3). The traffic flow rate was obtained by two observers recording the number of people passing through and the time for a given rotation speed (50 rpm or 100 rpm) in 19 field tests of 7 buildings. It was concluded that the air displacement when door is revolving depends on the door speed, temperature difference, outside wind velocity and indoor air movement.

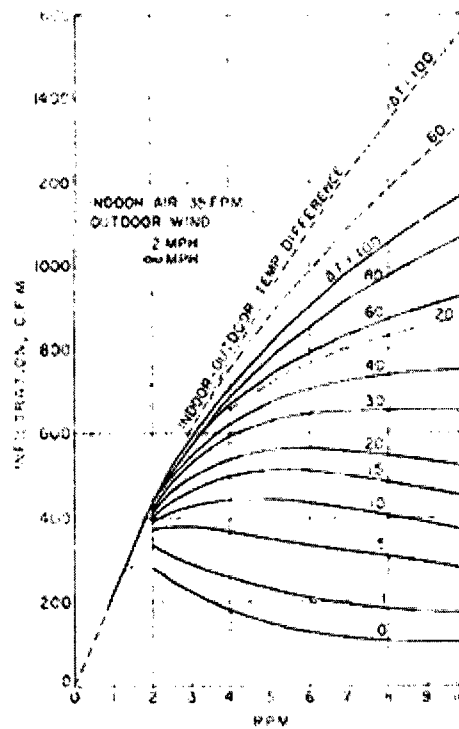


Fig. 2-2: Infiltration vs. rpm and indoor-outdoor air temperature difference for motor-operated revolving door (air leakage past seals deducted) (Schutrum et al., 1961)

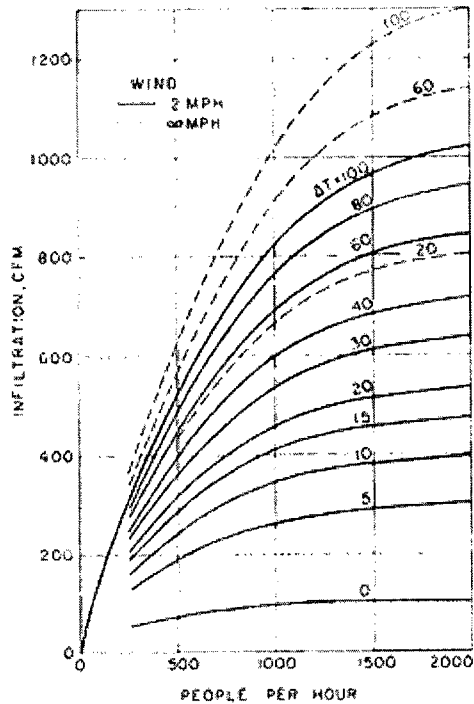


Fig. 2-3: Infiltration through manually-operated revolving doors (air movement 35 fpm indoors, air leakage past door seals deducted) (Schutrum et al., 1961)

In accordance with Schutrum et al. (1961), the total air exchange through a revolving door is the sum of the air infiltration past seals due to the pressure difference and the air exchange due to the temperature difference (which is the part due to the motion of the door). Examples were presented of a building with a pressure differential of 69 Pa (0.46 in. of water) in their paper. However, based on the National Building code of Canada (NRCC, 1995), the force on the door must not exceed 90 N in order to make sure the doors are easy to open, which means that the pressure difference should not exceed 20 Pa for a 4.2 m² doorway. Thus, the basis of their examples is unrealistic. If assume the pressure differential is 20 Pa (0.08 in. of water) for a building with a manually-operated revolving door moving, when the indoor temperature is 20°C (68°F), the outdoor temperature is 0°C (32°F) and the traffic rate is 1000 people/hr, the air infiltration

through the gaps and seals is 24 L/s (50 cfm) from Fig. 2-1. The air infiltration by temperature difference of 35°F is 263 L/s (560 cfm) from Fig. 2-3. As a consequence, the total air exchange by the revolving door in this example is 24 L/s plus 263 L/s which equals to 287 L/s. The infiltration through gaps is 8% of the total air exchange.

The study concluded that there was only insignificant change in gap leakage with door movement compared with the stationary condition, however, specific values were not provided.

2.3. Full-scale measurement

Until 2001, further experiments were carried out by Zmeureanu et al., who measured the air infiltration through gaps and seals of four revolving doors of a university building, at stationary condition, by using the blower door technique. The door seals had different states of repair conditions. The air infiltration rate of those four doors were compared with recommendations from ASHRAE Standard 90.1 (ASHRAE 1989) and the MNECCB (NRCC 1997), as well as with the air infiltration rate of a new revolving door tested by an independent consultant at a manufacturer's facility (Table 2-2). The leakage rates for all four doors greatly exceeded the values specified by both standards and the importance of good quality seals on the energy efficiency of revolving doors was highlighted.

Table 2-2: Air infiltration rate of four revolving doors and standard provisions (Zmeureanu et al., 2001)

Door	$\Delta p = 75 \text{ Pa}$	
	L/(s·m)	L/(s·m ²)
No. 1	47.0	111.3
No. 2	72.0	150.6
No. 3	89.6	213.6
No. 4	29.3	75.6
New door tested by independent consultant	1.2 – 1.4	4.8-5.4
ASHRAE (1989)	–	6.3
MNECCB (NRCC 1997)	17.0	–

The measured infiltration rates through gaps between wings and door housing of the four existing doors by Zmeureanu et al. (2001) are not only exceed the limitations in standards, but also much higher than the results from Schutrum et al. (1961) (Fig. 2-4). It was mentioned by Zmeureanu et al. (2001) that the used doors have been operating more than 30 years and the seals lack of maintenance, while the door used by Schutrum et al. (1961) was installed properly for the experimental purposes. Both studies concluded that the air leakage through the gaps and seals does not change significantly with the movement of the door.

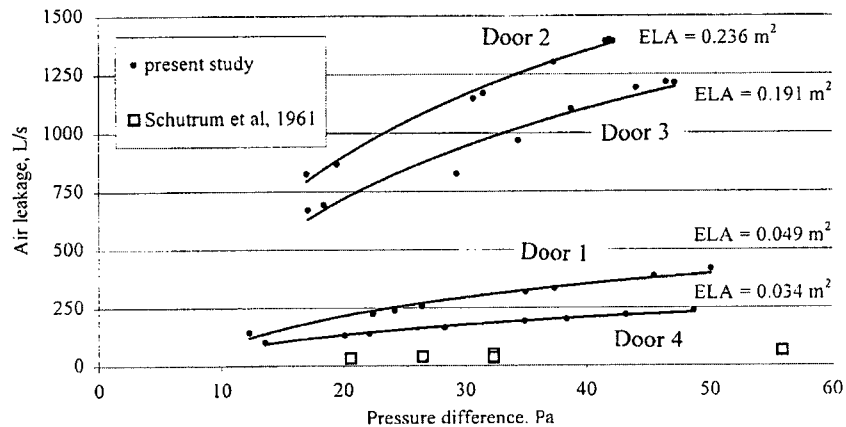


Fig. 2-4: Comparison of the air leakage of four doors and results of Schutrum et al. (1961) (Zmeureanu et al., 2001)

The heating energy costs due to the air infiltration through the four doors were also estimated and compared with the new doors by using recommended values in standards for two cases: (1) the cold air is brought from outdoor environment through the four doors by natural pressure difference of 10 Pa; and (2) the warm air leaves the pressurized building at 20 Pa pressure difference. Both cases were assumed in winter conditions and indoor temperature of 18°C. The estimated annual energy costs of heating the infiltrated air through the four revolving doors are much higher than the costs corresponding to new doors as well as the costs calculated with the maximum infiltration rates from standards. For example, the annual heating cost through the four doors at natural pressure difference is from \$47 – \$124/(m of cracks), while the new door only costs \$3/(m of cracks), and the cost by using recommended value from ASHRAE standard (ASHRAE, 1989) and MNECCB (NRCC, 1997) is \$4/(m of cracks) and \$35/(m of cracks), respectively.

2.4. Reduced-scale model

The results from Schutrum et al. (1961) and Zmeureanu et al. (2001) were based on full-scale measurements. However, it is impractical to build a full-scale version of a building for each experiment. For this reason, reduced-scale modeling techniques can be employed.

Air flow through a revolving door when it rotates was examined in a water chamber by Allgayer and Hunt (2004) using a scaled model approximately 1/10th of the full size. A transparent tank was partitioned into two compartments and a rectangular opening in the partition housed the revolving door. The fresh- and salt-water solution, which produced the density difference, was used to represent temperature difference through the

doorway. The density difference between the two rooms in the tank was analyzed. This experiment focused on detail observations of the flow patterns and the effect of the door rotation rate and temperature difference across the doorway.

When a door segment faces the inside compartment, the cold air flows out from bottom part of the segment and is replaced by warm buoyant air which enters the top of the door segment. When a door segment faces the outside compartment, the warm air in the segment rises up going outside and is displaced by the cold outdoor air entering at the bottom of the door segment.

It was concluded from the experimental results that when the rotation speed exceeds a critical rotation rate, at same indoor-outdoor temperature difference, the exchange rate becomes independent of the rotation speed and it remains constant. For the rotation rate lower than the critical value, the air exchange increases with the increasing of the rotation speed. This was based on the assumption that the air exchange process only depends on the buoyancy force resulting from the temperature difference between the indoor and outdoor environments. For a given temperature difference and door geometry, the critical rotation rate is reached when the time taken for a segment to be flushed by the buoyancy forces is equal to the time that the segment is connected to the indoor or outdoor environment. The study found that the air flow caused by infiltration through seals is small compared to the total air flow, actually less than 20% of the total air flow, when the door is rotating.

2.5. Analytical Model

Schutrum et al. (1961) also developed an analytical model to estimate the air exchange between the door segments and environment. When a segment is turned to indoor environment, the air exchange occurs because of the buoyancy forces due to the temperature difference between the cold air in the segment and warm air in the room. The process was separated into two cycles: the opening cycle, when the exposure to indoor increases; and closing cycle, when the exposure to indoor decreases.

The volumetric air exchange q_1 from one segment during the opening cycle is expressed as follows (Schutrum et al., 1961):

$$\frac{dq_1}{dt} = Kt \left(\frac{V - q_1}{V} \right) \sqrt{\frac{V - q_1}{V} - \frac{L^2}{2gVh_o} \frac{d^2q_1}{dt^2}} \quad (2-1)$$

The volumetric air exchange q_2 from one segment during the closing cycle is expressed as follows (Schutrum et al., 1961):

$$\frac{dq_2}{dt} = K \left(\frac{1}{4N} - t \right) \left(\frac{V - q_2}{V} \right) \sqrt{\frac{V - q_2}{V} - \frac{L^2}{2gVh_o} \frac{d^2q_2}{dt^2}} \quad (2-2)$$

where, q_1 = volume of air exchange between door segments and environments at the opening cycle, m^3 ;

q_2 = volume of air exchange between door segments and environments at the closing cycle, m^3 ;

$$K = CL\pi RN\sqrt{2gh_o};$$

$$h_0 = 0.5L \frac{\rho_{segment} - \rho_i}{\rho_{ref}}, \text{ head of air at the beginning of opening cycle, at } t = 0, \text{ in m;}$$

C = flow coefficient;

L = door height, m;

R = door radius, m;

$V_{segment}$ = volume of one segment, m^3 ;

$\rho_{segment}$ = air density in the door segment at the beginning of the opening cycle, kg/m^3 ;

ρ_i = air density in the room, kg/m^3 ;

$\rho_{ref} = 0.075$, reference density of air, kg/m^3 ;

N = rotation speed, rpm.

The net air infiltration due to door movement is calculated as the difference between the quantities of outdoor air in the opening cycle and the closing cycle.

$$q = \frac{4Nf_i f_o V}{1 - (1 - f_o)(1 - f_i)} \quad (m^3/h) \quad (2-3)$$

where, $f_o = \frac{q_1 + q_2}{V}$ outdoors, air displacement as fraction of segment volume when

segment is exposed to outdoors;

$f_i = \frac{q_1 + q_2}{V}$ indoors, air displacement as fraction of segment volume when

segment is exposed to indoors;

A modified model for prediction of the net air infiltration rate through revolving doors was presented by Schijndel et al. (2003) based on the original model by Schutrum et al. (1961) and the relation of mass air exchange between segments and environments (Fig. 2-5).

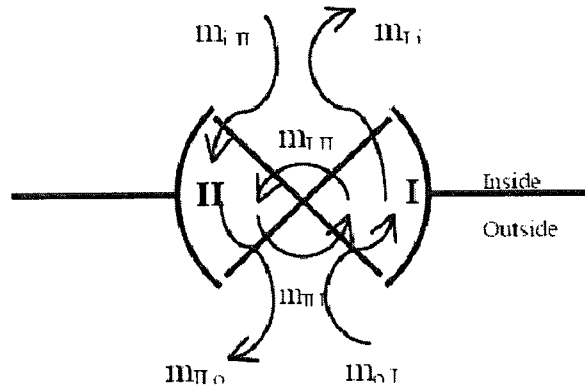


Fig. 2-5: Schematic displacement as a result of the movement of the door (Schijndel et al., 2003)

The heat balance equations for segments I and II are as follows (Schijndel et al., 2003):

$$\text{Segment I:} \quad m_I T_I c_{pI} = m_{o,I} T_o c_{po} + m_{II,I} T_{II} c_{pII} \quad (2-4)$$

$$\text{Segment II:} \quad m_{II} T_{II} c_{pII} = m_{i,II} T_i c_{pi} + m_{I,II} T_I c_{pI} \quad (2-5)$$

where, m_I , m_{II} = mass of air in segment I and II, kg;

$m_{o,I}$ = mass of air entering segment I from outside, kg;

$m_{II,I}$ = mass of air from segment II transferred to segment I, kg;

$m_{i,II}$ = mass of air entering segment II from inside, kg;

$m_{I,II}$ = mass of air from segment I transferred to segment II, kg;

T_I, T_{II}, T_i, T_o = air temperature in segment I, segment II, indoor and outdoor, respectively, °C.

According to the conservation of mass principle, $m_{o,I} = m_{II,o}$, from which the volumetric air flow from outdoor to the segment I is: $q_{o,I} = m_{II,o}/\rho_o$. So the percentage of the cold air coming from outdoor in segment I is: $\alpha = q_{o,I}/V_{\text{segment}}$.

The net air infiltration was estimated as the product between the volumetric rate from segment to indoor and the percentage of cold air in segment (Equation 2-4).

$$q = 4 \cdot 60 \cdot N \cdot \alpha \cdot q_{I,i} = 240 \cdot N \frac{q_{o,I} \cdot q_{I,i}}{V} \quad (\text{m}^3/\text{h}) \quad (2-4)$$

In order to account for the effect of outdoor wind and indoor air movement, Schutrum et al. (1961) assumed that the average non-directional air velocity head $v^2/2g$ is equal to a buoyancy head with equal magnitude. The velocity heads were converted to temperature difference heads and a trial and error approach was used to determine the effect of wind and indoor air movement. Although the same assumption was used, Shijndel et al. (2003) introduced a different process to estimate the impact of air movement in adjacent environment. The results were presented in terms of temperature differences as well. The study compared the air infiltration due to the door movement with the infiltration through seals using the data presented by Zmeureanu et al. (2001) and Schutrum et al. (1961). The air infiltration through gaps and seals between wings and door holder was estimated to be about 30% of total infiltration in the case of old doors and about 10% for a new door.

2.6. Estimation of Energy Savings by Using Revolving Doors

How big a difference can using a revolving door make? Cullum et al. (2006) developed a research to promote usage rate of revolving doors on MIT campus as much as possible to save energy consumption caused by entrances. However, it was observed that people tend to use the swinging doors more than revolving doors. A survey indicated that the usage ratio of the revolving door of a university building was only 23% of the total door-usage. The annual energy consumption used to heat or cool the air leakage through both revolving and swinging doors in this building was estimated as 98,912.8 kWh, by using the graphs by Schutrum et al. (1961) for revolving doors and the graphs by Min (1958) for swinging doors. This energy is enough to heat 6.5 single-family houses in one year, or to light a 100W bulb for 37.8 years. The study also estimated how much of this energy consumption could be saved if the revolving door usage were higher than 23%. If the revolving door usage is 50%, the annual energy consumption is reduced by 14.5%; if the revolving door usage is 75%, the annual energy consumption is reduced by 38.7%; and if the revolving door usage is up to 100%, the annual energy consumption is reduced by 74.0%.

2.7. Conclusion

In high-rise buildings, a large amount of outdoor air comes into the buildings through frequently used entrance doors in winter, which causes a substantial amount of energy consumption. Revolving doors work without establishing a direct connection between the indoor and outdoor environments. Therefore, they potentially reduce heat losses compared with other types of door. However, researches on the air flow through

revolving doors seem to have been given comparatively little attention in the previous studies.

There is still not sufficient information about the amount of the air infiltration due to the motion of the door. Therefore, further search on the air infiltration when door is revolving is necessary. Only by knowing this amount of air flow rate, appropriate recommendations can be given in standards, and the total air exchange can be estimated for calculating the energy consumption due to the air infiltration.

CHAPTER 3

DESIGN OF THE REDUCED-SCALE MODEL

3.1. Similitude and Modeling Methodologies

3.1.1. Similitude

It is usually not very convenient to use full-scale buildings for the purpose of experimental studies, so reduced-scale models are created to simulate the full-scale prototype. The goal of the reduced-scale modeling is to gather data at a more manageable, smaller size, and apply the data for usage in the full-scale systems. However, certain scaling issues need to be resolved before the experiment takes place. Only if the flow in the model is “similar” to that of the full-scale prototype, the results from a reduced-scale model can be used. There are three levels of similarity that must be satisfied between scaled model and full-scale prototype: geometric, kinematic, and dynamic similarity. Geometric similarity requires that the model and prototype be of the same shape, and that all linear dimensions of the model be related to corresponding dimensions of the prototype by a constant scale factor. Kinematic similarity requires the velocities at corresponding points of the model and prototype be in the same direction and related in magnitude by a constant scale factor. When two flows have force distributions such that identical types of forces are parallel and are related in magnitude by a constant scale factor at all corresponding points, the flows are dynamically similar.

To validate the model for application in buildings, there must be similar in the velocity distribution, airflow patterns, and linear dimensions between the prototype building and the model (Fox and McDonald, 1998). Only when the independent dimensionless groups are the same in scaled-model and prototype, relationships between scaled model and full-scale prototype are correct.

3.1.2. Dimensionless Group

It is important to match as many as possible of the dimensionless groups that may determine the accuracy of scaled-model. Reynolds number (Re) is defined as the ratio of inertia force to viscous force. It is one of the most important dimensionless parameters in fluid mechanics problems, and provides a criterion to determine the flow regime or the dynamic similitude for modeling studies. Re is defined as follows (Fox and McDonald, 1998):

$$\text{Re} = \frac{\text{inertia force}}{\text{viscous force}} = \frac{\rho VD}{\mu} = \frac{VD}{\nu} \quad (3-1)$$

where, V = mean fluid velocity, m/s;

D = diameter of revolving door as the characteristic length of the flow field geometry, D = 0.21 m;

μ = dynamic fluid viscosity, Pa·s;

$\nu = \mu/\rho$, kinematic fluid viscosity, m²/s; and

ρ = density of the fluid, kg/m³.

The typical Re number for this case is about 2900.

3.1.3. Scale Ratios

The model used in this experiment is 1/10 scaled model, so geometric ratio λ_L is:

$$\lambda_L = \frac{D_p}{D_m} = 10 \quad (3-2)$$

where the subscript p refers to the prototype (real life dimension) and m refers to the reduced scale model.

The geometric ratio $\lambda_L = 10$ means the size of the model is 10 times smaller than the prototype.

The scaled model and the prototype keep the same Re number:

$$\text{Re} = \frac{V_p D_p}{\nu_p} = \frac{V_m D_m}{\nu_m} \quad (3-3)$$

The experimental environment was designed with the same type of fluid as the prototype, the air, with temperature from 0°C to 25°C. The kinematic viscosity of air from 0°C to 25°C varies only from $1.33 \cdot 10^{-5} \text{ m}^2/\text{s}$ to $1.55 \cdot 10^{-5} \text{ m}^2/\text{s}$. Since the difference is quite small (14%), the average value of $1.44 \cdot 10^{-5} \text{ m}^2/\text{s}$ is used in this study. The kinematic viscosity is the same in the reduced-scale model and the prototype. So, the lineal velocity ratio is obtained from Equation 3-3 as it follows:

$$\lambda_v = \frac{V_p}{V_m} = \frac{D_m}{D_p} = \frac{1}{10} \quad (3-4)$$

Using angular speed, ω , and the diameter of the revolving door, D, to represent Re number, Equation 3-4 becomes (Halliday et al., 2001):

$$\text{Re} = \frac{(\omega_p \cdot \frac{D_p}{2}) \cdot D_p}{v_p} = \frac{(\omega_m \cdot \frac{D_m}{2}) \cdot D_m}{v_m} \quad (3-5)$$

The angular velocity factor λ_ω is:

$$\lambda_\omega = \frac{\omega_p}{\omega_m} = \left(\frac{D_m}{D_p}\right)^2 = \frac{1}{100} \quad (3-6)$$

The fan law can be written as follows (Fox and McDonald, 1998):

$$\frac{Q_p}{\omega_p D_p^3} = \frac{Q_m}{\omega_m D_m^3} \quad (3-7)$$

where, Q = the volumetric flow rate, m³/s.

The air flow ratio λ_Q is:

$$\lambda_Q = \frac{Q_p}{Q_m} = \frac{\omega_p D_p^3}{\omega_m D_m^3} = \frac{1}{100} \cdot 10^3 = 10 \quad (3-8)$$

3.2. Design of Experiment

3.2.1. Field Study

To obtain information of manually operated revolving doors, several field observations were made on the revolving doors of one office building and two university buildings. The number of people passing through the revolving doors and the number of rotations in each five-minutes-interval were recorded for several hours for each building. Data collected was converted to the traffic rate, in persons per hour, and the average rotation speed N in rotations per minute (rpm) (Tables 3-1, 3-2 and 3-3).

Table 3-1: Data for the revolving door no. 1 of the first university building

From	To	Traffic flow (persons)	Traffic rate (persons/hr)	Rotation speed (rpm)	From	To	Traffic flow (persons)	Traffic rate (persons/hr)	Rotation speed (rpm)
7:50	7:55	17	204	2.38	5:40	5:45	14	168	1.98
7:55	8:00	10	120	1.7	5:45	5:50	8	96	0.8
8:00	8:05	10	120	1.35	5:50	5:55	10	120	1.2
8:05	8:10	14	168	1.98	5:55	6:00	17	204	1.5
8:10	8:15	15	180	2.1	6:00	6:05	11	132	1.1
8:15	8:20	13	156	1.78	6:05	6:10	9	108	0.88
8:20	8:25	11	132	1.5	6:10	6:15	21	252	2
8:25	8:30	44	528	4.53	6:15	6:20	38	456	3.9
8:30	8:35	11	132	1.78	6:20	6:25	28	336	2.45
8:35	8:40	12	144	1.7	6:25	6:30	26	312	2.6
8:40	8:45	6	72	1	6:30	6:35	10	120	1.08
8:45	8:50	15	180	2.8	6:35	6:40	17	204	1.7
Maximum									4.53
Minimum									0.8

Table 3-2: Data for the revolving door no. 2 of the second university building

From	To	Traffic flow (persons)	Traffic rate (persons/hr)	Rotation speed (rpm)	From	To	Traffic flow (persons)	Traffic rate (persons/hr)	Rotation speed (rpm)
8:30	8:35	63	756	5.2	9:15	9:20	50	600	4.2
8:35	8:40	77	924	6.2	9:20	9:25	11	132	0.8
8:40	8:45	49	588	4.4	9:25	9:30	48	576	4.1
8:45	8:50	69	828	5.2	9:30	9:35	38	456	3.2
8:50	8:55	46	552	3.8	9:35	9:40	38	456	3.2
8:55	9:00	54	648	4.8	9:40	9:45	19	228	1.6
9:00	9:05	73	876	5.8	9:45	9:50	47	564	4.2
9:05	9:10	39	468	3.4	9:50	9:55	17	204	1.7
9:10	9:15	64	768	4.8	9:55	10:00	19	228	1.3
Maximum									6.2
Minimum									0.8

Table 3-3: Data for the revolving door no. 3 of an office building

From	To	Traffic flow (persons)	Traffic rate (persons/hr)	Rotation speed (rpm)	From	To	Traffic flow (persons)	Traffic rate (persons/hr)	Rotation speed (rpm)
7:45	7:50	15	180	2.8	8:45	8:50	12	144	2.63
7:50	7:55	9	108	2	8:50	8:55	7	84	1.75
7:55	8:00	9	108	1.8	8:55	9:00	6	72	1.4
8:00	8:05	12	144	2.43	9:00	9:05	15	180	2.48
8:05	8:10	11	132	2.13	9:05	9:10	12	144	1.9
8:10	8:15	12	144	2.4	9:10	9:15	9	108	1.83
8:15	8:20	6	72	1.13	9:15	9:20	8	96	1.48
8:20	8:25	17	204	2.73	9:20	9:25	5	60	1.05
8:25	8:30	11	132	2.58	9:25	9:30	6	72	1.28
8:30	8:35	9	108	1.85	9:30	9:35	4	48	0.88
8:35	8:40	9	108	2.33	9:35	9:40	5	60	1.03
8:40	8:45	8	96	1.58	9:40	9:45	8	96	1.70
Maximum									2.8
Minimum									0.88

The rotation speed of revolving doors in the field studies varied from 0.8 to 6.2 rpm. The most frequent rotation speed was about 2 rpm for the 1st university building and the office building, and 5 rpm for the 2nd university building (Fig 3-1). The maximum rotation speed in the field study is 6.2 rpm.

Schutrum et al. (1961) carried out 19 field tests on seven revolving doors in Cleveland to obtain the performance of motor-operated revolving doors. They recorded the time of a given number of revolutions (50 or 100), time of idle period, and the number of people passing through the door. The average rotation speed presented by Schutrum et al. (1961) excluded the idle time, thus at same traffic rate, it is larger compared to the average rotation speed in present field studies, which include the idle time. For instance, at 800 persons/hour, Schutrum et al. (1961) found the rotation speed of about 7 rpm, while this study found 5.3 rpm (Fig. 3-2). At lower traffic rate (e.g. 400 persons/hour) the difference from Schutrum et al. (1961) is even larger.

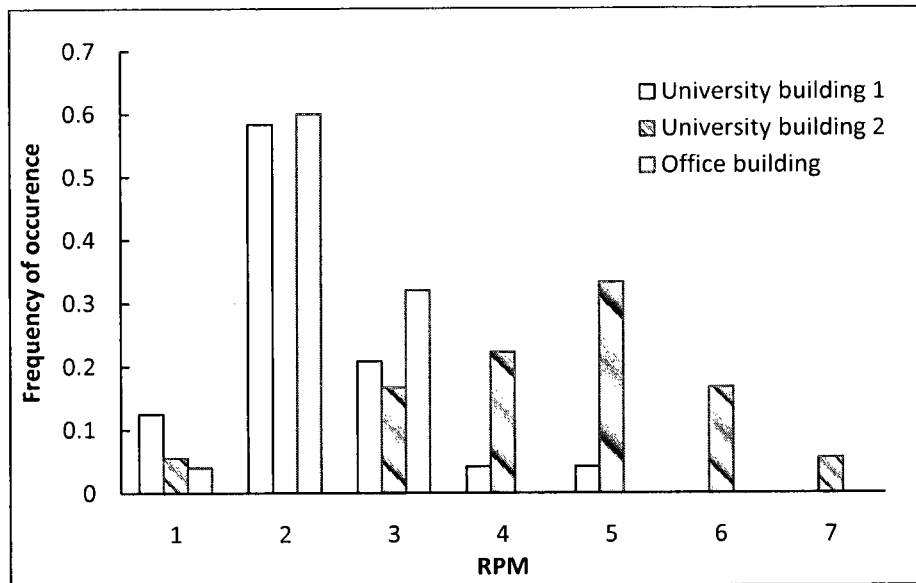


Fig. 3-1: Frequency of occurrence of rotation speed of the revolving doors from field study

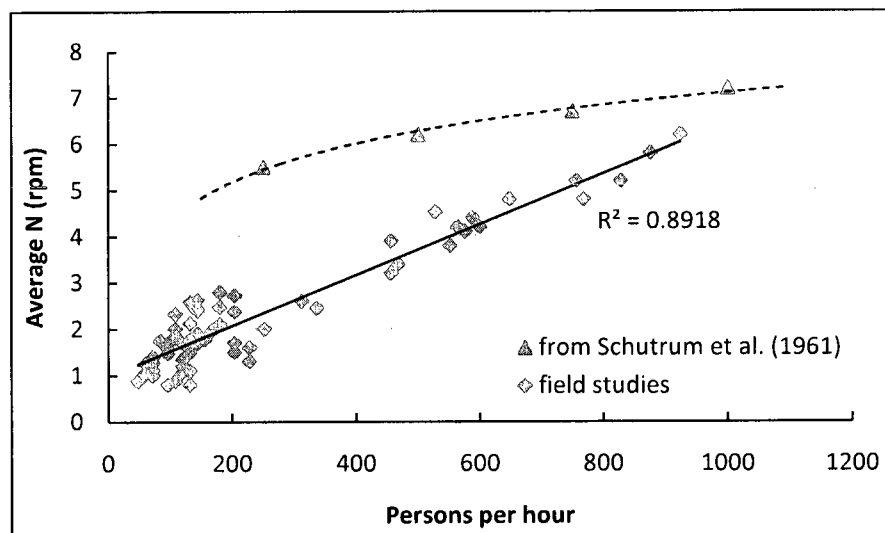


Fig. 3-2: Average rotation speed vs. traffic rate from the field study

The results from present field studies represent the traffic flow rate of all university/institutional buildings and office buildings. The traffic rate passing through the revolving doors is high at places such as airports and shopping malls, which have much more people coming in and out all the time. For the office buildings, a lot of people drive

their cars to work, therefore there is a considerable number of people coming into the building by driving directly into the garage, so they do not use the revolving doors. For the university buildings, there is a big difference of traffic flow rate between the rush time 5 to 15 minutes before or after classes and the time during the classes.

3.2.2. Dimensions of the Experimental Model

The experiment was designed by using a 1/10 reduced-scale model to simulate and to measure the air exchange of a revolving door. An airtight box with a revolving door on the front side was installed in a climatic chamber. The box represented the hall of a building, and the climatic chamber represented the outdoor environment. The inside dimensions of the box are $50 \times 58.5 \times 50$ cm (Fig. 3-3). The inside dimensions of the chamber are $3.65 \times 2.45 \times 2.03$ m.

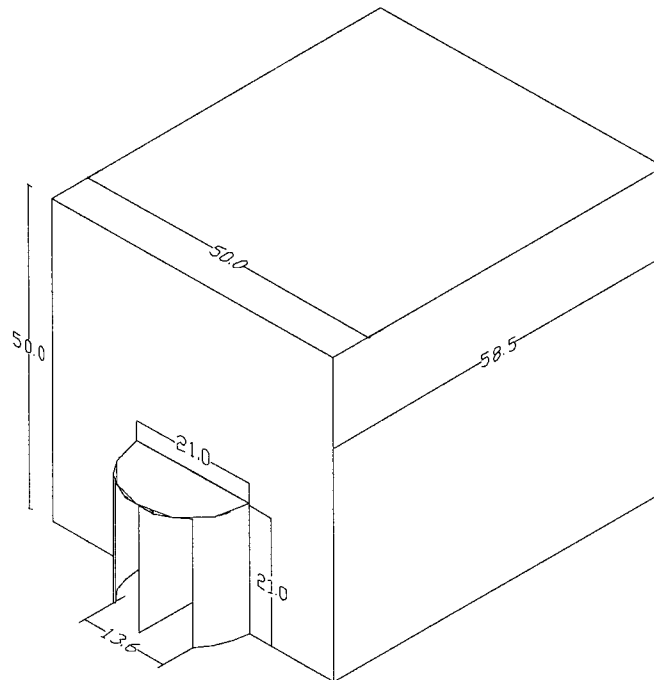


Fig. 3-3: Dimensions of the experimental box and revolving door without outside insulation (dimensions are in cm)

The height and diameter of the revolving door is 21 cm and 21 cm, respectively. The location of the box inside the chamber is presented in Fig. 3-4.

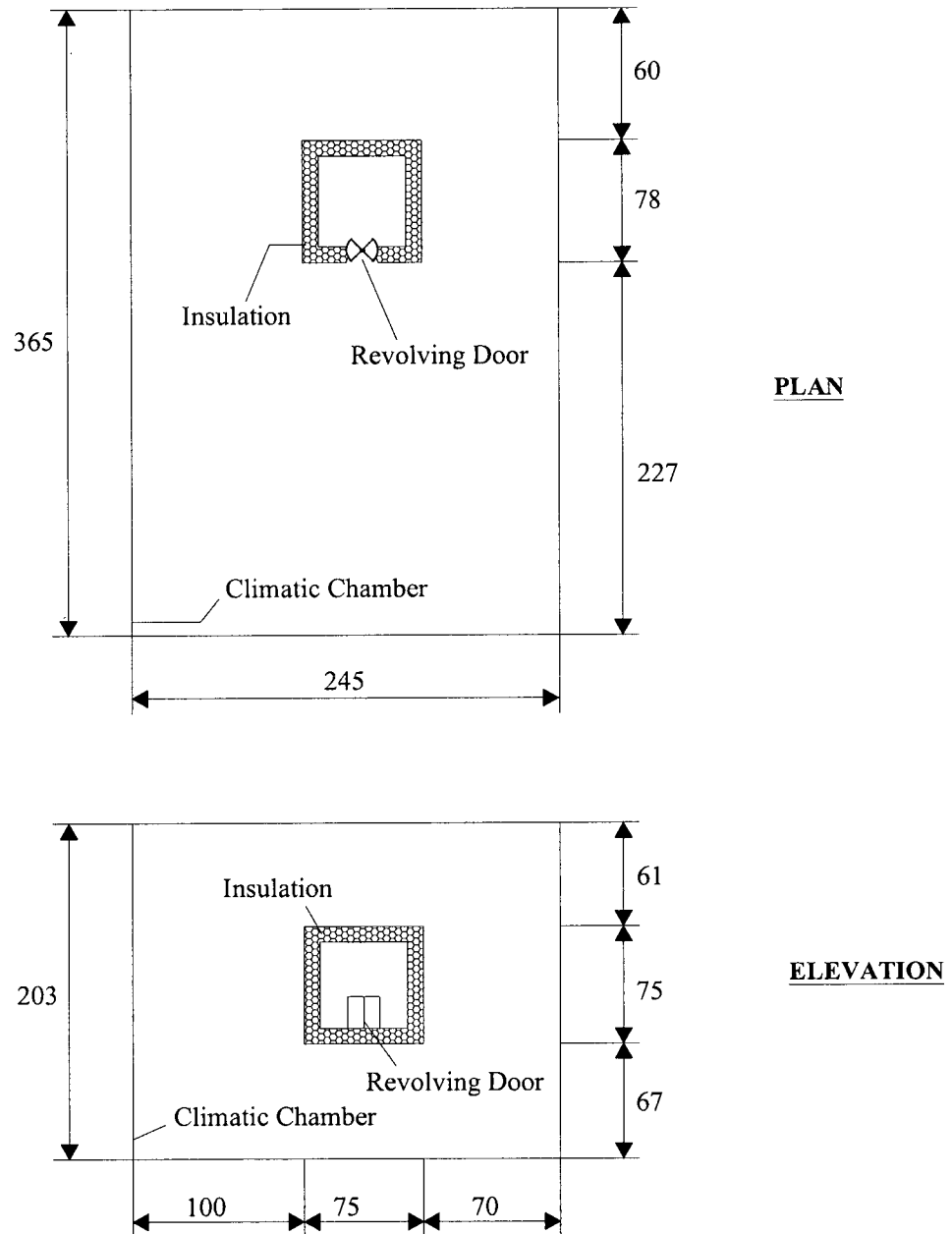


Fig. 3-4: Box position inside the environmental chamber (dimensions are in cm)

Fig. 3-5 (a) shows one of the four wings and the size of the seals. A motor is installed on the vertical axis of the revolving door to drive the door turning. Fig. 3-5 (b) shows the detailed dimensions of the 1/10 scaled revolving door.

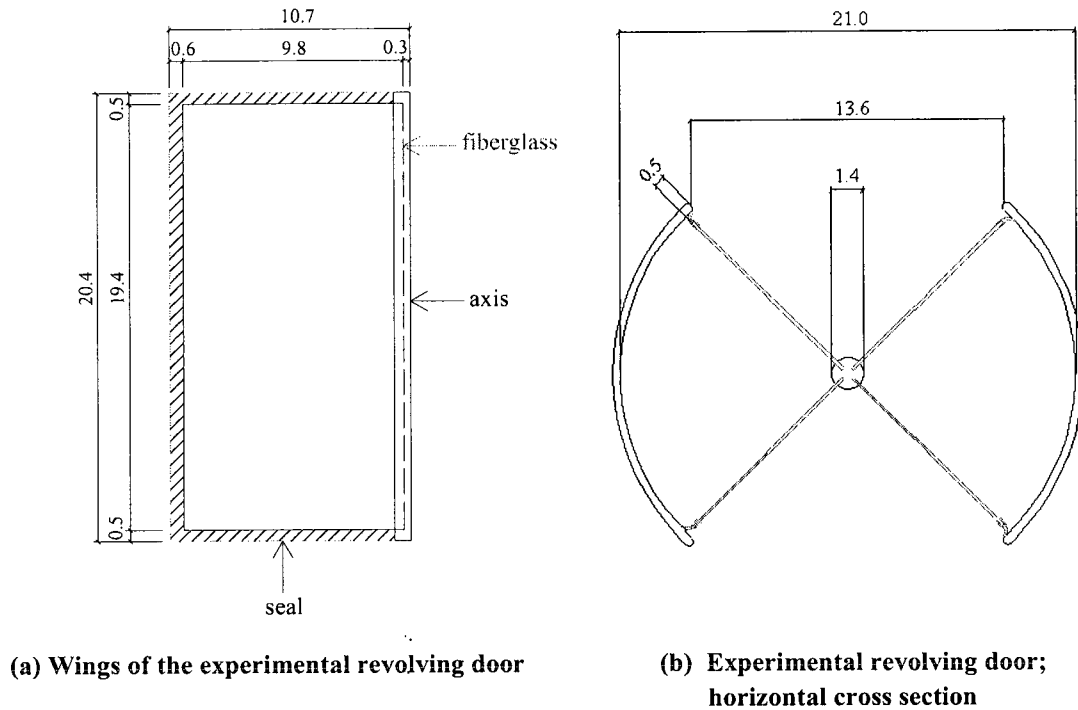


Fig. 3-5: Dimensions of the experimental model (dimensions are in cm)

To find out if the presence of the box inside the chamber will affect the air velocity field, the air velocity in the chamber when it is on was measured with and without the experimental model. The comparison shows that the presence of the box did not affect the air movement in the climatic chamber. Details are presented in Appendix A.

3.3. Experimental Approach

The experiment was designed to measure the mass air flow rate (m_{inf}) by measuring the corresponding heat loss of the box due to the usage of revolving door in the winter

condition. The overall heat balance equation is applied to the box when the door is moving during a period of time (Δt): the energy change inside the box is equal to the heat generated by heater and fan, installed in the box, minus the heat loss through walls and the heat loss due to the air infiltration through the revolving door.

$$\Delta Q = Q_{heater} + Q_{fan} - Q_{loss} - Q_{door} \quad (3-9)$$

where, ΔQ = the energy change inside the box in the time interval Δt , J;

$Q_{heater} = \Delta t_{step} \cdot \sum_j V_{heater,j} \cdot I_{heater,j}$; is the heat generated by heater over the time Δt ,

J; $\Delta t_{step} = 10s$ is the time step between each recording j ; V is the voltage, V; I is the electric current, A;

$Q_{fan} = \Delta t_{step} \cdot \sum_j V_{fan,j} \cdot I_{fan,j}$, is the heat generated by the small fan over the time

Δt , J;

Q_{loss} = the heat loss through the box walls, over the time Δt , J;

Q_{door} = the heat loss of the box due to air infiltration through the revolving door, when door is moving over the time Δt , J.

The experimental data is recorded every 10-second step. Each time step the voltage and current to the heater and fan, the average indoor air temperature of the box and the average outdoor air temperature in the environmental chamber are recorded.

The heat change inside the box in the time period Δt is calculated as follows:

$$\Delta Q = m_2 \cdot c_p \cdot T_2 - m_1 \cdot c_p \cdot T_1 = \rho_2 \cdot V_{box} \cdot c_p \cdot T_2 - \rho_1 \cdot V_{box} \cdot c_p \cdot T_1 \quad (3-10)$$

where, ρ_1 = the air density at the beginning of the time interval Δt , kg/m^3 ;

ρ_2 = the air density at the end of the time interval Δt , kg/m³;

$V_{\text{box}} = 0.5 \cdot 0.5 \cdot 0.585 = 0.146 \text{ m}^3$, is the internal volume of the box;

T_1 = the initial temperature inside the box at the beginning of the time interval Δt , °C;

T_2 = the final temperature inside the box at the end of the time interval Δt , °C;

c_p = the specific heat of air, 1005 J/kg·°C.

The heat loss Q_{loss} , including the heat loss through envelope and the heat loss due to the air leakage through the gaps around the door, is calculated by using the UA-value:

$$Q_{\text{loss}} = U \cdot A \cdot \Delta t_{\text{step}} \cdot \sum_j (T_i - T_o)_j \quad (3-11)$$

where, U = the overall heat transfer coefficient, W/(m²·K);

A = the total exterior surface area of the box, m²;

T_i = the average indoor air temperature of the box, °C;

T_o = the average air temperature of the environmental chamber, °C.

The heat loss caused by the air infiltration through the door is calculated as follows:

$$Q_{\text{door}} = m_{\text{inf}} \cdot c_p \cdot \Delta t_{\text{step}} \cdot \sum_j (T_i - T_o)_j \quad (3-12)$$

where, m_{inf} = the mass air flow rate through the revolving door, kg/s.

The air volumetric flow rate through the revolving door q_{inf} , m³/s, is:

$$q_{\text{inf}} = \frac{m_{\text{inf}}}{\rho} \quad (3-13)$$

where, ρ is air density, which is 1.29 kg/m^3 at 1°C (the average temperature in the environmental chamber) and atmospheric pressure (Fox and McDonald, 1998).

Equation 3-9 becomes:

$$\begin{aligned} \rho_2 \cdot V_{box} \cdot c_p \cdot T_2 - \rho_1 \cdot V_{box} \cdot c_p \cdot T_1 = & \left[\sum_j (V_{heater} \cdot I_{heater} + V_{fan} \cdot I_{fan})_j \right. \\ & \left. - U \cdot A \cdot \sum_j (T_i - T_o)_j - m_{int} \cdot c_p \cdot \sum_j (T_i - T_o)_j \right] \cdot \Delta t_{step} \end{aligned} \quad (3-14)$$

The unknown variable to be calculated is the air mass flow rate m_{inf} , provided that all other variables are measured. The UA-value is identified by using the steady-state heat balance equation from some separate tests when the door does not move (still position):

$$\sum_j (V_{heater} \cdot I_{heater} + V_{fan} \cdot I_{fan})_j = Q_{loss} = U \cdot A \cdot \sum_j (T_i - T_o)_j \quad (3-15)$$

Two layers of Styrofoam (5 cm for each layer) were applied to the outside surface of the box by duct tape. One layer of aluminum paper was finally taped outside the Styrofoam insulation to reduce the heat exchange by radiation between the box and environmental chamber. The outside dimensions of the box after insulation were $0.75 \times 0.78 \text{ m}$, with the height of 0.75 m .

In order to calculate the UA-value (Equation 3-15) and the air mass flow rate m_{inf} (Equation 3-14), the following variables must be measured: the average inside and outside air temperature, and electric input power to the heater and fan installed in the box, the total number of revolutions, and the time step of reading.

A Data Acquisition System (DAS) type 34970 (Agilent) was used for collecting the measured data and controlling the revolving speed (Fig 3-6). Two modules with 20 channels on each module to record temperature and electrical current, and one

multifunction module to record the total number of rotations of the door were installed in the DAS unit. An adjustable heater was placed inside the box. The voltage and current signals were recorded by the DAS. Several type T thermocouples were installed inside and outside the box as well as around the revolving door to measure the air temperature, and the results were also recorded by the DAS. The range of thermocouples is from 0 to 350°C with absolute error of $\pm 0.5^\circ\text{C}$ or relative error of $\pm 0.4\%$. All the small “T”s in circle in Fig. 3-6 represent the locations of the thermocouples in the experiment. To help the air temperature inside the box be uniform, a small fan of 0.4 W power input was installed inside the box. The fan and the door motor shared one power supply system, and their voltages and currents were recorded by DAS as well. The DAS not only reads the voltage input to the motor, but also can control the revolving speed by setting up the needed voltage input to the motor. The time and the cumulative number of rotations of the door were recorded, so that the rotation speed can be calculated.

the door, and T_{15} and T_{16} were installed at the higher position farther from the door. The indoor air temperature was calculated as the average of test results by these six T_{11} to T_{16} thermocouples. Because of the fan, the indoor temperature inside the box is uniform.

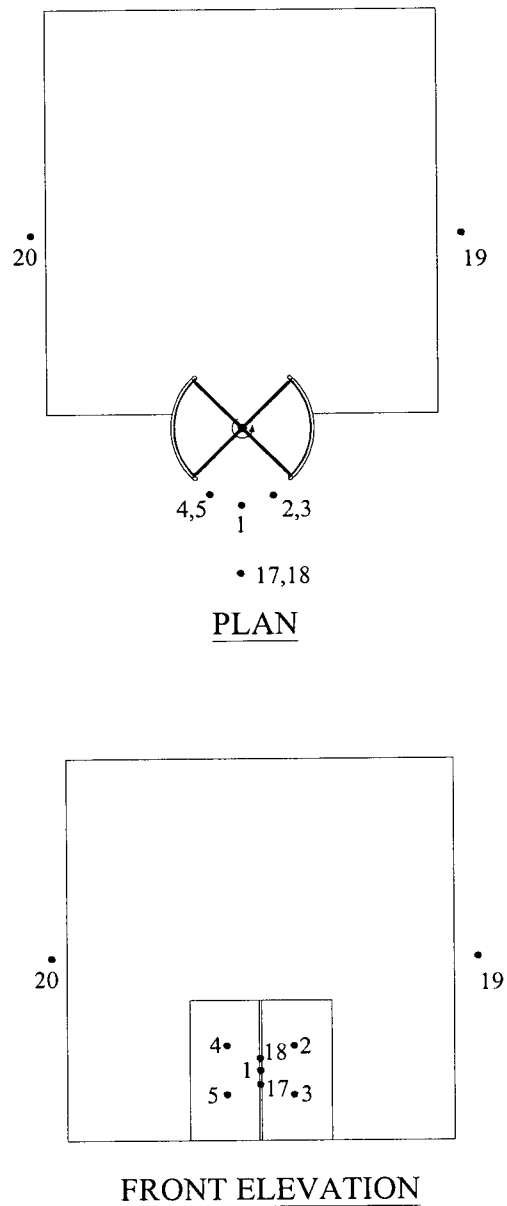


Fig. 3-7: Locations of thermocouples outside the box

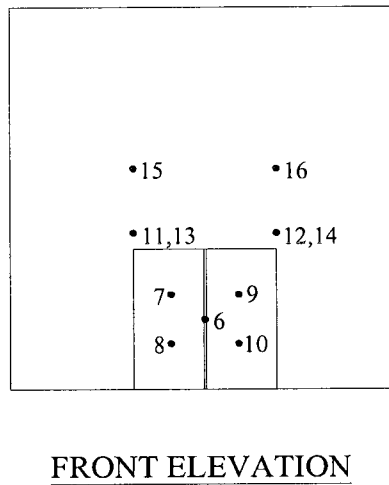
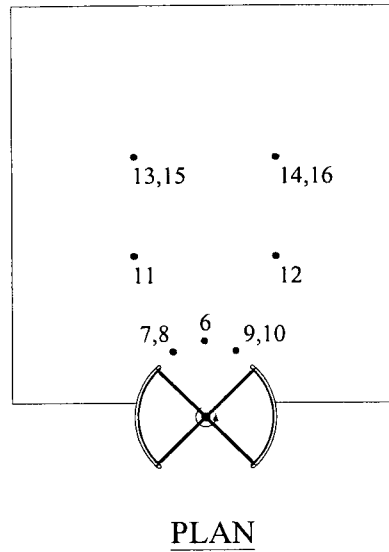
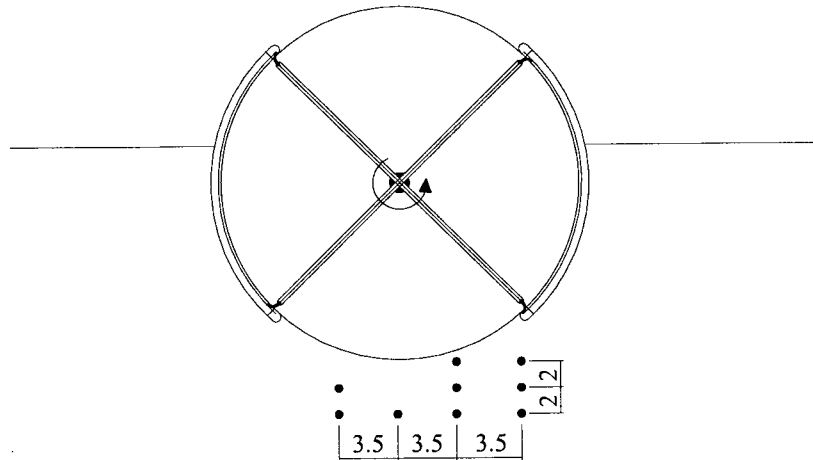


Fig. 3-8: Locations of thermocouples inside the box

In addition to those thermocouples, nine thermocouples were installed in a horizontal plan in the front center outside the revolving door, to identify the direction of air movement, generated by the revolving door (Fig. 3-9).



**Fig 3-9: Additional thermocouples outside the door to identify the air flow direction
(dimensions are in cm)**

3.3.2. Measurement of Electric Power Input

Inside the box there are two devices, the heater, which controls the air temperature, and the fan, which circulates the air to have a uniform temperature. Since the DAS can only record the voltage difference, in order to measure the current, a small resistance of 0.1Ω was installed on each circuit, (1) of the heater, and (2) of the fan. The voltage difference between the two ends of the resistance can be recorded by DAS, so that the current can be calculated by dividing the voltage by the resistance (Fig. 3-10). Every 10 seconds time step, channels 01 and 03 read the voltage differences through the resistances to calculate the current through the heater and fan, and channels 02 and 04 read the voltage difference of the heater circuit and fan circuit, respectively. Those values are recorded, exported to Excel file and the electric input power is calculated.

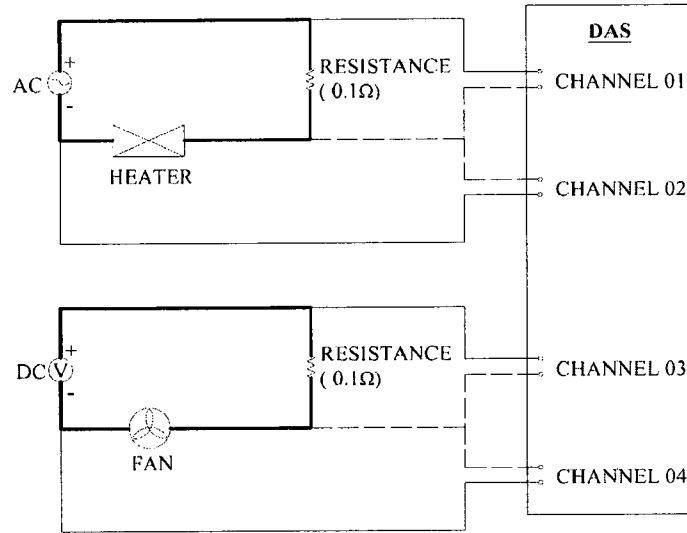


Fig. 3-10: Illustration of how to record the power input

3.3.3. Identification of the Overall UA-value of the Insulated Box

The overall UA-value is used to calculate the heat loss, when the door is still, which includes the heat loss through envelope and the heat loss due to the air leakage through the gaps around the door. From Equation 3-15, the UA-value is calculated as follows:

$$U \cdot A = \frac{\sum_j (V_{heater} \cdot I_{heater} + V_{fan} \cdot I_{fan})_j}{\sum_j (T_i - T_o)_j} \quad (3-16)$$

Tests were carried out at outdoor air temperature between 0°C and 2°C and indoor temperatures from about 20°C to 40°C when the door was not rotating, and the calculated UA-value are presented in Table 3-4.

Table 3-4: UA-value at different indoor air temperatures

Test	Average indoor temperature (°C)	UA-value [W/(m ² ·K)]
1	43.33	1.261
2	30.46	1.061
3	24.73	0.878

Based on these tests, the relationship between the overall UA-value and the indoor temperature T_i , at $T_o = 0 - 2^\circ\text{C}$ can be expressed as follows:

$$UA = 0.4181 + 0.0197 \cdot T_i \quad (\text{with } R^2 = 0.96) \quad (3-17)$$

3.3.4. Setup of Infrared Camera

To visualize the air flow direction when it leaves the revolving door, the infrared thermography was used, and infrared images were recorded at different rotation speeds and with different conditions of seals – with full seals around the wings and with no vertical seals on the side of wings. A mosquito screen fixed on a frame was placed in horizontal or vertical position outside of the revolving door. The air flow coming from indoor environment results in different temperature distribution on the net and this temperature difference can be shown by the colorful infrared pictures.

Figures 3-11 and 3-12 show the horizontal position of the screen in front and center outside the revolving door. The infrared camera was placed above the screen.

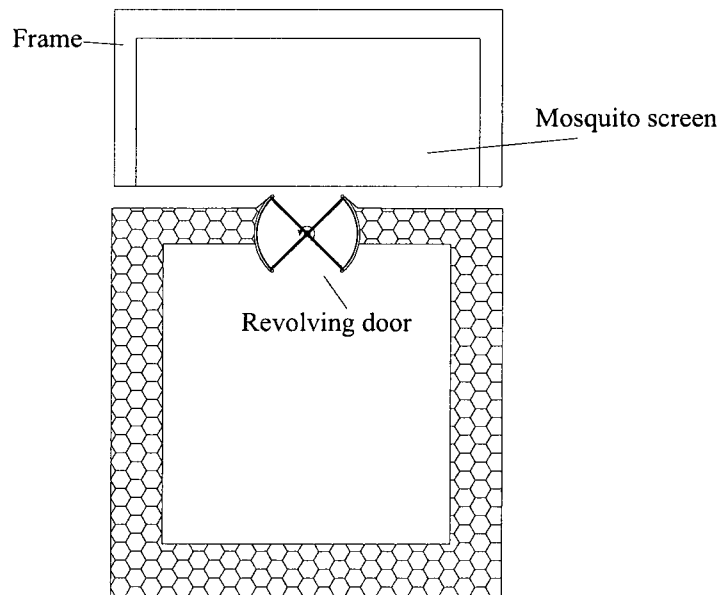


Fig. 3-11: Horizontal screen in front of the revolving door

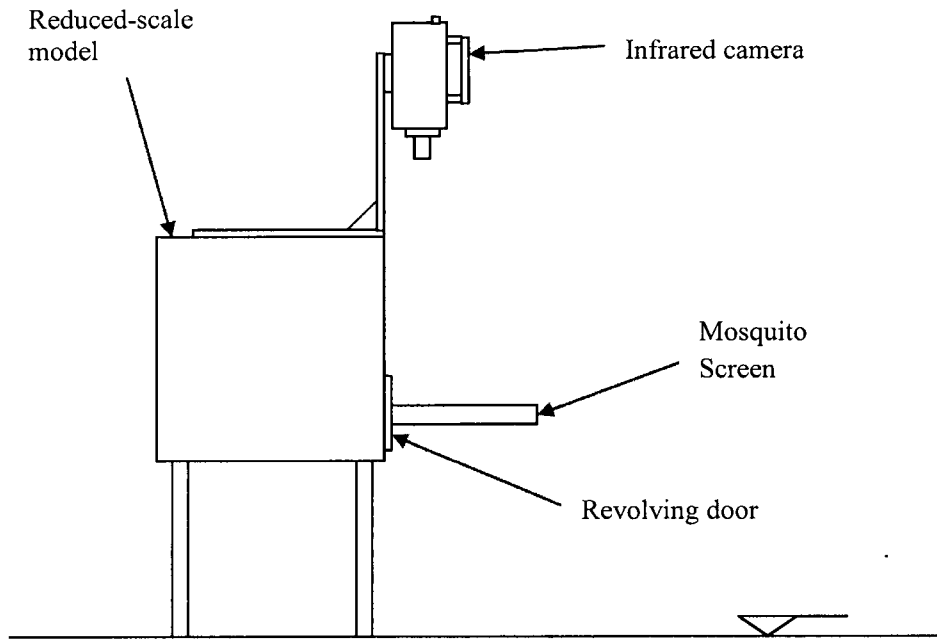


Fig. 3-12: Infrared camera and horizontal screen in front of the revolving door

Fig. 3-13 indicates the vertical position of the mosquito net outside of the revolving door. The infrared camera was perpendicular on the screen.

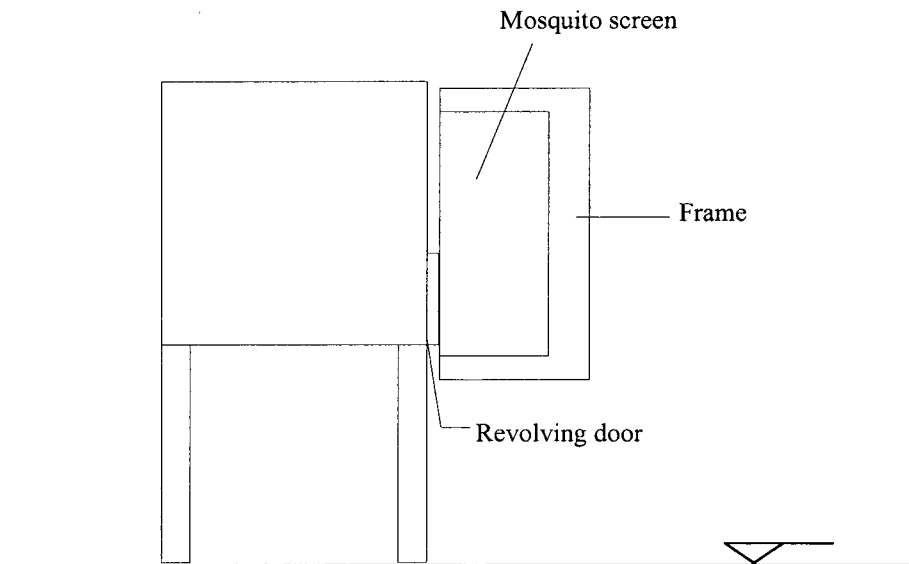


Fig. 3-13: Vertical screen in front of the revolving door

CHAPTER 4

EXPERIMENTAL RESULTS AND DISCUSSION

4.1. Data Measurement and Analysis

The experiments were carried out at different rotation speeds N of the revolving door. The conversion of the maximum rotation speed in the field study of 6 rpm gives an experimental rotation speed of 600 rpm. However, limited by the condition of the experimental revolving door, the highest rotation speed in the experiment was only 370 rpm, which is 3.7 rpm in prototype.

The outdoor temperature (the temperature in the climatic chamber) varied slightly from 0.5 to 2°C, and the experiments started from different indoor temperatures ranging from 16 to 22°C. The air infiltration rate is calculated by an integral method which is based on the heat balance equation over a period of time Δt when door rotates (Equation 3-14):

$$\begin{aligned} \rho_2 \cdot V_{box} \cdot c_p \cdot T_2 - \rho_1 \cdot V_{box} \cdot c_p \cdot T_1 = & [\sum_j (V_{heater} \cdot I_{heater} + V_{fan} \cdot I_{fan})_j \\ & - U \cdot A \cdot \sum_j (T_i - T_o)_j - m_{inf} \cdot c_p \cdot \sum_j (T_i - T_o)_j] \cdot \Delta t_{step} \end{aligned} \quad (3-14)$$

4.1.1. Experimental Results

Experiments were conducted in the reduced-scale model at different rotation speed N from 19 to 368 rpm with indoor temperature from 15.5 to 22.6°C and outdoor

temperature from 0.5 to 2°C. All data for calculations are summarized in Table 4-1. The experimental results at 19.06 rpm are presented as an example of calculation. Data used in this calculation are from 50th time step (16:32:45) to 275th time step (17:10:25) (Fig. 4-1). Based on measurements, the relation between the indoor temperature (T_i) and measurement time (t) is expressed as:

$$T_i = -0.0018 \cdot t + 19.734 \quad (\text{with } R^2 = 0.9065) \quad (4-1)$$

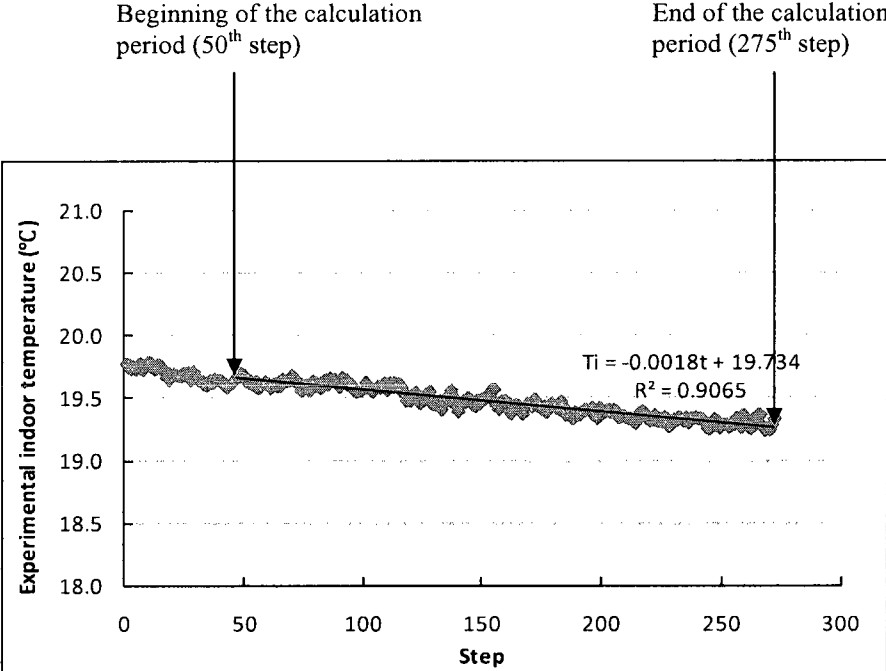


Fig. 4-1: Experimental indoor temperature in the time interval Δt at 19.06 rpm

The calculation steps are as follows:

- 1) Time interval recorded:

$$\Delta t = 17:10:25 - 16:32:45 = 37.67 \text{ min} = 2260 \text{ s}$$

- 2) Total number of rotations during the time interval Δt :

$$N_{total} = 870(\text{at } 17:10:25) - 152(\text{at } 16:32:45) = 718 \text{ rotations}$$

3) The average rotation speed during the time interval:

$$N_{model} = \frac{N_{total}}{\Delta t} = \frac{718}{37.67} = 19.06 \text{ rpm}$$

4) The average indoor temperature:

At the beginning of time interval Δt : $T_1 = 19.73^\circ\text{C}$;

At the end of time interval Δt : $T_2 = 19.73 - 0.0018 \cdot 225 = 19.32^\circ\text{C}$

5) The inside volume of the box:

$$V_{box} = 0.146 \text{ m}^3$$

6) The total heat generated by heater and fan in the time interval $\Delta t = 2260 \text{ s}$:

$$\sum_j (V_{heater} \cdot I_{heater} + V_{fan} \cdot I_{fan})_j \cdot \Delta t_{step} = 46639.47 \text{ J}$$

7) The summation of the temperature difference between indoor and outdoor:

$$\sum_j (T_i - T_o)_j \cdot \Delta t_{step} = 40317.09^\circ\text{C} \cdot \text{s}$$

8) The UA-value from Equation 3-17 (using the average value of the initial and final temperature inside the box):

$$U \cdot A = 0.4181 + 0.0197 \cdot (19.73 + 19.32)/2 = 0.80 \text{ W}/^\circ\text{C} \quad (4-2)$$

9) The mass air infiltration rate is calculated from the heat balance equation over the time interval ($\Delta t = 2260 \text{ s}$):

$$m_{\text{inf}} = \frac{\sum_j (V_{\text{heater}} \cdot I_{\text{heater}} + V_{\text{fan}} \cdot I_{\text{fan}})_j \cdot \Delta t_{\text{step}} - (\rho_2 \cdot T_2 - \rho_1 \cdot T_1) \cdot V_{\text{box}} \cdot c_p - U \cdot A \cdot \sum_j (T_i - T_o)_j \cdot \Delta t_{\text{step}}}{c_p \cdot \sum_j (T_i - T_o)_j \cdot \Delta t_{\text{step}}} \quad (4-3)$$

$$= \frac{46639.47 - (1.214 \cdot 19.32 - 1.213 \cdot 19.73) \cdot 0.146 \cdot 1005 - 0.80 \cdot 40317.09}{1005 \cdot 40317.09}$$

$$= 0.356 \times 10^{-3} \text{ kg/s}$$

From where:

$$q_{\text{inf}} = \frac{m_{\text{inf}}}{\rho_o} = \frac{0.361 \times 10^{-3}}{1.25} = 0.284 \text{ L/s} \quad (4-4)$$

Table 4-1: Infiltration air flow rate at different rotation speeds at indoor temperature around 20°C in the 1/10 reduced-scale model

Average rotation speed (rpm)	Time interval Δt (s)	$Q_{heater}+Q_{fan}$ (J)	Initial indoor temperature T_1 (°C)	Final indoor temperature T_2 (°C)	Overall UA-value (W/°C)	$\Sigma(T_i-T_o) \cdot \Delta t_{step}$ (°C · s)	Volumetric flow rate q_{inf} (L/s)
19.06	2260	46639.47	19.65	19.25	0.80	40317.09	0.284
19.17	2500	51299.65	19.84	19.56	0.81	44363.60	0.280
31.76	500	10587.20	19.24	19.21	0.80	8993.30	0.303
38.88	1505	30693.02	20.53	20.23	0.82	28294.29	0.213
47.85	3006	61361.68	20.94	20.64	0.83	57505.25	0.191
48.55	2000	41900.61	19.14	18.96	0.79	36002.82	0.296
51.96	2070	42527.61	19.76	19.52	0.81	36987.27	0.275
61.10	1110	22666.78	20.25	20.02	0.81	20682.13	0.225
76.29	200	4094.90	20.80	20.71	0.83	3945.90	0.211
79.68	4005	82582.80	19.62	19.30	0.80	72944.20	0.264
85.37	2000	40837.46	20.96	20.32	0.82	37789.89	0.206
108.37	2001	40963.78	19.98	19.80	0.81	35667.75	0.270
116.44	3015	61735.99	20.44	20.08	0.82	53159.42	0.275
157.70	1500	30564.79	21.29	21.00	0.83	27555.41	0.220
173.87	15010	308063.74	19.63	18.80	0.80	251878.01	0.340
187.06	10010	208381.77	18.12	17.22	0.77	165588.42	0.393
192.39	4000	81503.12	19.44	19.12	0.80	70334.68	0.288
221.59	6010	123809.31	17.74	16.78	0.76	97407.67	0.410
247.36	1000	20768.20	19.00	18.84	0.79	17944.30	0.293
284.99	500	1047.10	20.07	19.96	0.81	9262.50	0.255
287.37	3000	62157.39	20.24	19.58	0.81	48592.03	0.375
295.73	1000	20996.00	16.24	16.13	0.74	15160.00	0.517
303.75	5010	103193.78	16.52	15.72	0.74	76857.80	0.485
308.51	1000	20750.00	19.49	19.27	0.80	17629.01	0.302
322.84	6000	123600.20	19.00	17.86	0.78	99409.87	0.370
333.03	4020	83947.55	15.42	14.98	0.72	57967.60	0.583
333.03	2007	41285.08	17.18	16.82	0.75	32611.40	0.410
333.78	4000	82585.30	15.95	15.19	0.72	59039.14	0.538
347.77	1000	20770.00	19.09	18.83	0.79	17365.00	0.324
368.31	3005	62284.53	17.97	16.98	0.76	48129.45	0.426

The data acquired from other three tests at indoor temperature around 40°C and one test at indoor temperature of 25°C are presented in Table 4-2.

Table 4-2: Infiltration air flow rate at different rotation speeds around 40°C and 25°C indoor temperature in the reduced-scale model

Average rotation speed (rpm)	Time interval Δt (s)	$Q_{\text{heater}}+Q_{\text{fan}}$ (J)	Initial indoor temperature T_1 (°C)	Final indoor temperature T_2 (°C)	Overall UA-value (W/°C)	$\Sigma(T_i-T_o) \cdot \Delta t_{\text{step}}$ (°C · s)	Volumetric flow rate q_{inf} (L/s)
152.98	2000	138477.20	42.82	42.74	1.26	85993.37	0.287
155.17	5000	126124.00	25.53	25.28	0.91	98944.30	0.288
270.75	5000	351156.40	40.58	40.83	1.22	200550.10	0.436
300.30	7010	479534.07	42.52	41.82	1.25	287339.90	0.346

Fig. 4-2 shows all calculated volumetric air infiltration rates under different rotation speeds and the different indoor temperatures. The results at indoor temperature of 25°C and 40°C are within the same range of the results as experiments around 20°C. This result indicates that the air infiltration rate due to the rotation of the door is independent from the indoor and outdoor temperature difference. Hence, the results from this study can be applied to other air temperature differences.

The experimental air infiltration rate (q_{inf}), in L/s, and the experimental rotation speed (N), in rpm, can be expressed by a linear relationship (Fig. 4-2):

$$q_{\text{inf}} = 0.0006 \cdot N + 0.2148 \quad (\text{with } R^2 = 0.51) \quad (4-5)$$

Or by a polynomial trendline (Fig. 4-3):

$$q_{\text{inf}} = 10^{-6} \cdot N^2 - 8 \cdot 10^{-5} \cdot N + 0.2456 \quad (\text{with } R^2 = 0.53) \quad (4-6)$$

Since it is concluded that the air infiltration caused by the motion of the door is independent to indoor and outdoor temperature difference, Equations 4-5 and 4-6 are valid at all temperature differences.

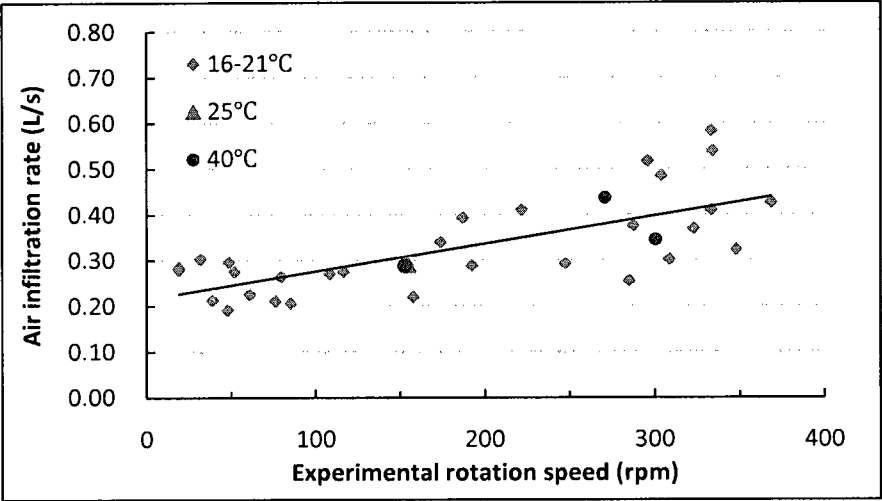


Fig. 4-2: Linear relationship between the volumetric air infiltration rate and the rotation speed of the experimental revolving door

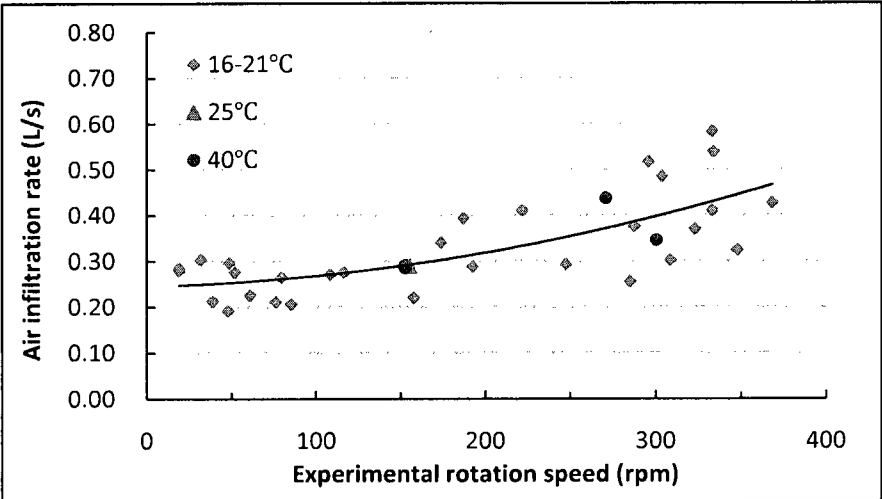


Fig. 4-3: Polynomial relationship between the volumetric air infiltration rate and the rotation speed of the experimental revolving door

From the linear trendline (Equation 4-5), the experimental air flow rate due to the motion of the door increases by 0.21 L/s (from 0.226 to 0.437 L/s) when the rotation speed of the model door increases by 349 rpm (from 19 to 368 rpm).

Another calculation approach, using data from the steady state thermal condition after a long time, is presented in Appendix B. However, in some experiments, the steady state conditions were never reached. Therefore the integral method gives more accurate results.

4.1.2. Error Analysis

Assuming that the two directly measured quantities are X and Y, with absolute errors Δx and Δy , respectively. The measurements X and Y are independent of each other. The relative error (E) is the value of the absolute error divided by the measured value of the quantity (e.g., $E_x = \Delta x/X$). If Z is calculated from X and Y, the calculation of the errors of Z follows these three rules:

$$\text{Rule 1: if } Z = X + Y \text{ or } Z = X - Y, \text{ then } \Delta z = \sqrt{\Delta x^2 + \Delta y^2}. \quad (4-7)$$

$$\text{Rule 2: if } Z = X \times Y \text{ or } Z = X/Y, \text{ then } \frac{\Delta z}{Z} = \sqrt{\left(\frac{\Delta x}{X}\right)^2 + \left(\frac{\Delta y}{Y}\right)^2}. \quad (4-8)$$

$$\text{Rule 3: if } Z = X^n, \text{ then } \Delta z = n \cdot x^{n-1} \cdot \Delta x \text{ and } \frac{\Delta z}{Z} = n \frac{\Delta x}{X}. \quad (4-9)$$

$$\text{From Rule 1, if } Z = \sum_1^n X_n \text{ then } \Delta Z = \sqrt{\sum_1^n (\Delta x_n)^2} \text{ and } Z = \frac{\sqrt{\sum_1^n (\Delta x_n)^2}}{\sum_1^n X_n}. \quad (4-10)$$

The air infiltration rate is calculated based on several laboratory measurements of physical variables. The mass infiltration rate caused by the revolution of the experimental revolving door is calculated based on the heat balance equation during a period of time Δt :

$$m_{\text{int}} = \frac{\sum_j (V_{\text{heater}} \cdot I_{\text{heater}} + V_{\text{fan}} \cdot I_{\text{fan}})_j \cdot \Delta t_{\text{step}} - (\rho_2 \cdot V_{\text{box}} \cdot c_p \cdot T_2 - \rho_1 \cdot T_1) \cdot V_{\text{box}} \cdot c_p - U \cdot A \cdot \sum_j (T_i - T_o)_j \cdot \Delta t_{\text{step}}}{c_p \cdot \sum_j (T_i - T_o)_j \cdot \Delta t_{\text{step}}} \quad (4-3)$$

The measured physical quantities are: voltage inputs to the heater and fan installed inside the box; currents of the heater and fan (by means of adding a 0.1 Ω electricity resistance in each electric circuit); dimension of the box; air temperature; and time. The reading error of DC voltage is $\pm 0.004\%$ for the fan and the reading error of AC voltage is $\pm 0.06\%$ for the heater by the data acquisition system (Agilent). The 0.1 Ω electricity resistance installed in the circuits has a relative error of $\pm 1\%$. The relative error of the thermocouple for the temperature measurement (T type, special limit) is $\pm 0.4\%$ of range from 0 to 350°C.

The equation for calculating the air infiltration rate is complicated (having a large number of summation over the period of time involved) and the error analysis was accomplished in spreadsheets of Excel. The calculation of rotation speed of 19.06 rpm is taken to illustrate the error analysis process.

- (1) The relative error of voltage input to the heater: $E_{V_{heater}} = \pm 0.06\%$, relative error of voltage input to the fan: $E_{V_{fan}} = \pm 0.004\%$.
- (2) The currents of heater and fan are calculated by dividing the voltage to the small electricity resistance with a relative error of $\pm 1\%$. The relative error of the current to the heater and the fan is:

$$E_{I_{heater}} = \sqrt{0.06\%^2 + 1\%^2} = \pm 1.002\%$$

$$E_{I_{fan}} = \sqrt{0.004\%^2 + 1\%^2} = \pm 1\%$$

- (3) Based on Rules 1 and 2 (Equations 4-7 and 4-8), the absolute error of the energy generated by the heater and fan at each recording step can be calculated. The value is different between each step, depending on the data recorded by the Data Acquisition System. The absolute error of the summation of the energy generated by heater and fan can be calculated based on Equation 4-10.

$$\Delta[\sum_j (V_{heater} \cdot I_{heater} + V_{fan} \cdot I_{fan})_j \cdot \Delta t_{step}] = \pm 30.44 J$$

- (4) The reading error of a ruler for measuring the dimension of the experimental box is 0.1 mm. The relative error of the volume of inside box is:

$$E_V = \sqrt{\left(\frac{0.0001}{0.5}\right)^2 + \left(\frac{0.0001}{0.5}\right)^2 + \left(\frac{0.0001}{0.58}\right)^2} = \pm 0.17\%$$

- (5) The relative error and absolute error of the energy change inside the box is:

$$E_{(\rho_2 T_2 - \rho_1 T_1) c_p V_{box}} = \pm 0.27\%$$

$$\Delta(\rho_2 \cdot T_2 - \rho_1 \cdot T_1) \cdot c_p \cdot V_{box} = 0.27\% \cdot (-67.43) = -0.18 \text{ J}$$

- (6) The relative error of the thermocouples for the temperature measurement is 0.4%. The relative error of the summation of temperature difference between indoor and outdoor is:

$$E_{\sum_j (T_i - T_o)_j \cdot \Delta t_{step}} = \frac{\Delta[\sum_j (T_i - T_o)_j \cdot \Delta t_{step}]}{\sum_j (T_i - T_o)_j \cdot \Delta t_{step}} = \pm 0.29\%$$

- (7) The overall UA-value is calculated from Equation 3-17:

$$\begin{aligned} U \cdot A &= 0.4181 + 0.0197 \cdot (T_1 + T_2) / 2 = 0.4181 + 0.0197 \cdot (19.65 + 19.25) / 2 \\ &= 0.80 \text{ W/}^\circ\text{C} \end{aligned}$$

So the relative error of the UA-value is:

$$E_{UA} = \frac{\sqrt{(\Delta T_1)^2 + (\Delta T_2)^2}}{T_1 + T_2} = \frac{\sqrt{(E_T \cdot T_1)^2 + (E_T \cdot T_2)^2}}{T_1 + T_2} = \frac{\sqrt{(0.4\% \cdot 19.65)^2 + (0.4\% \cdot 19.25)^2}}{19.65 + 19.25} = \pm 0.28\%$$

- (8) The relative error of the heat loss through the envelope of the experimental box is:

$$E_{U A \sum_j (T_i - T_o)_j \cdot \Delta t_{step}} = \sqrt{(0.28\%)^2 + (0.034\%)^2} = \pm 0.282\%$$

$$\Delta[U \cdot A \cdot \Delta t_{step} \cdot \sum_j (T_i - T_o)_j] = 0.282\% \cdot 32301.04 = \pm 90.94 \text{ J}$$

- (9) The absolute error and the relative error of numerator in Equation 4-3 is:

$$\Delta_{numerator} = \sqrt{30.44^2 + 0.28^2 + 90.94^2} = \pm 95.89 \text{ J}$$

$$E_{numerator} = 95.89/434161 = \pm 0.022\%$$

- (10) The relative error of the air infiltration rate through the model door due to the revolution of the door is:

$$E_{m_{inf}} = \sqrt{0.022\%^2 + 0.029\%^2} = \pm 0.037\%$$

The relative errors of calculated air infiltration rate in all the experiments are shown in Table 4-3. The application of the integral method decreases the relative error of the experimental results dramatically. Besides, the data acquisition system already has really high accuracy. The relative error of most cases varies from 0.023% to 0.050%. The confidence interval is 95%.

Table 4-3: Error analysis of the experimental data

Experimental rotation speed (rpm)	Experimental air infiltration (L/s)	Relative Error (±%)
19.06	0.284	0.037
19.17	0.280	0.037
31.76	0.303	0.028
38.88	0.213	0.043
47.85	0.191	0.035
48.55	0.296	0.037
51.96	0.275	0.038
61.10	0.225	0.050
76.29	0.211	0.040
79.68	0.264	0.031
85.37	0.206	0.039
108.37	0.270	0.039
116.44	0.275	0.035
152.98	0.287	0.038
155.17	0.288	0.026
157.70	0.220	0.045
173.87	0.340	0.024
187.06	0.393	0.023
192.39	0.288	0.032
221.59	0.410	0.031
247.36	0.293	0.0025
270.75	0.437	0.024
284.99	0.255	0.028
287.37	0.375	0.035
295.73	0.517	0.035
300.30	0.345	0.028
303.75	0.485	0.025
308.51	0.302	0.039
322.84	0.370	0.027
333.00	0.583	0.026
333.00	0.410	0.035
333.78	0.538	0.027
347.77	0.324	0.033
368.31	0.426	0.031
Maximum relative error		±0.050%
Minimum relative error		±0.023%

4.1.3. Conversion of the Experimental Results to the Prototype Air Infiltration Rate

According to the dimensionless analysis in section 3.1, the air flow rate through prototype door is 10 times greater than the experimental result, and the corresponding rotation speed is only 1/100 of the rotation speed in the model. When the experimental results are converted to prototype, the volumetric air infiltration rate is expressed as follows (Fig. 4-4):

$$q_{\text{inf_prototype}} = 0.61 \cdot N_p + 2.15 \quad (4-11)$$

where, $q_{\text{inf_prototype}}$ = the volumetric air infiltration rate in prototype, L/s;

N_p = the rotation speed in prototype, rpm.

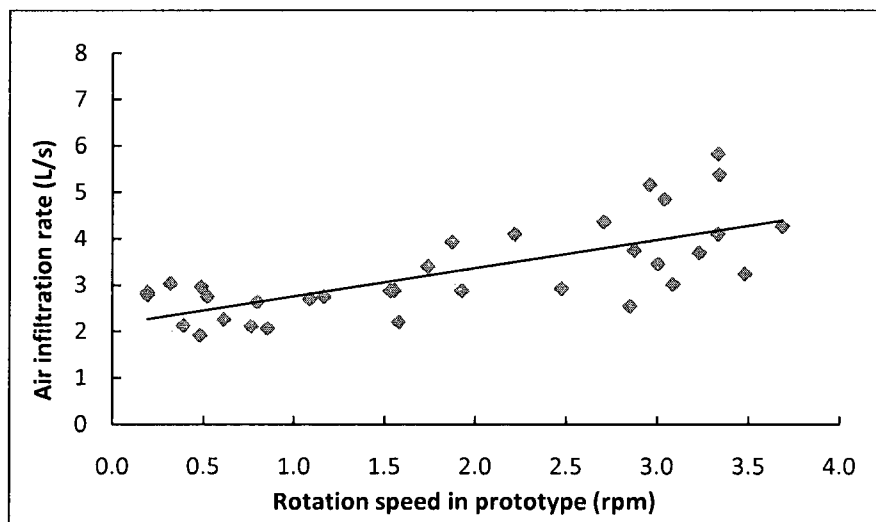


Fig. 4-4: Volumetric air infiltration rate vs, rotation speed of the prototype door

The air infiltration rates at different rotation speeds in the scaled-model and prototype are presented in Table 4-4.

Table 4-4: Air infiltration rate at different rotation speeds in the reduced-scale model and prototype

In reduced-scale model		In prototype	
Rotation speed (rpm)	Air infiltration rate (L/s)	Rotation speed (rpm)	Air infiltration rate (L/s)
19.06	0.28	0.19	2.84
19.17	0.28	0.19	2.80
31.76	0.30	0.32	3.03
38.88	0.21	0.39	2.13
47.85	0.19	0.48	1.91
48.55	0.30	0.49	2.96
51.96	0.28	0.52	2.75
61.10	0.23	0.61	2.25
76.29	0.21	0.76	2.11
79.68	0.26	0.80	2.64
85.37	0.21	0.85	2.06
108.37	0.27	1.08	2.70
116.44	0.27	1.16	2.75
152.98	0.29	1.53	2.87
155.17	0.29	1.55	2.88
157.70	0.22	1.58	2.20
173.87	0.34	1.74	3.40
187.06	0.39	1.87	3.93
192.39	0.29	1.92	2.88
221.59	0.41	2.22	4.10
247.36	0.29	2.47	2.93
270.75	0.44	2.71	4.37
284.99	0.25	2.85	2.55
287.37	0.38	2.87	3.75
295.73	0.52	2.96	5.17
300.30	0.35	3.00	3.45
303.75	0.48	3.04	4.85
308.51	0.30	3.09	3.02
322.84	0.37	3.23	3.70
333.03	0.58	3.33	5.83
333.03	0.41	3.33	4.10
333.78	0.54	3.34	5.38
347.77	0.32	3.48	3.24
368.31	0.43	3.68	4.26

4.1.4. Discussion

The calculated volumetric air infiltration rates at different rotation speeds are smaller than the results from Schutrum et al. (1961). For example, at rotation speed of 3.6 rpm in prototype, the air infiltration rate due to the motion of the door from Schutrum et al. (1961) is 235 L/s, while it is only 4.5 L/s from present research. Since there is no other publication available for the comparison of the data of air flow rate caused by the motion of the revolving door, in order to prove this research is reasonable and valuable, additional information is needed.

Since the centrifugal fans have similar air dynamics as revolving doors, the performance data of a centrifugal fan with similar dimensions of the experimental revolving door is collected from a manufacturer's catalogue (Elektorr Airsystems GmbH, 2009). A centrifugal fan with diameter of 204 mm gives the air flow rate of 2.7 m³/min (45 L/s) at rotation speed of 2920 rpm. Based on the fan law (Equation 3-7) (Fox and McDonald, 1998), the air flow rate at other rotation speeds can be calculated as follows (Equation 4-12):

$$q_2 = \frac{q_1 \cdot \omega_2 \cdot D_2^3}{\omega_1 \cdot D_1^3} = \frac{45 \cdot 0.21^3}{2920 \cdot 0.204^3} \cdot \omega_2 = 0.0168\omega_2 \quad (4-12)$$

Fig. 4-5 shows the experimental air infiltration rate through the model door, the air flow rate of the centrifugal fan based on fan law and the air infiltration rate converted from the results by Schutrum et al. (1961) in the reduced-scale. The air flow rate of the centrifugal fan increases linearly according to the fan law from 0.3 to 6.2 L/s, while the air infiltration rate of the door is from 0.25 to 0.48 L/s in present study. However, the air infiltration in experimental scale converted from Schutrum et al. (1961) is from 10 to 29

L/s. At the maximum rotation speed of 366 rpm, the air infiltration rate through the door is 8% of the value of the fan. The air infiltration rates in reduced-scale, converted from Schutrum et al. (1961) are not only higher than this research, but also much higher than a running centrifugal fan. However, after all, the revolving door is not designed to generate air movement as a centrifugal fan. It is impossible that a revolving door brings air flow rate air from outside to inside higher than that generated by a similar size centrifugal fan.

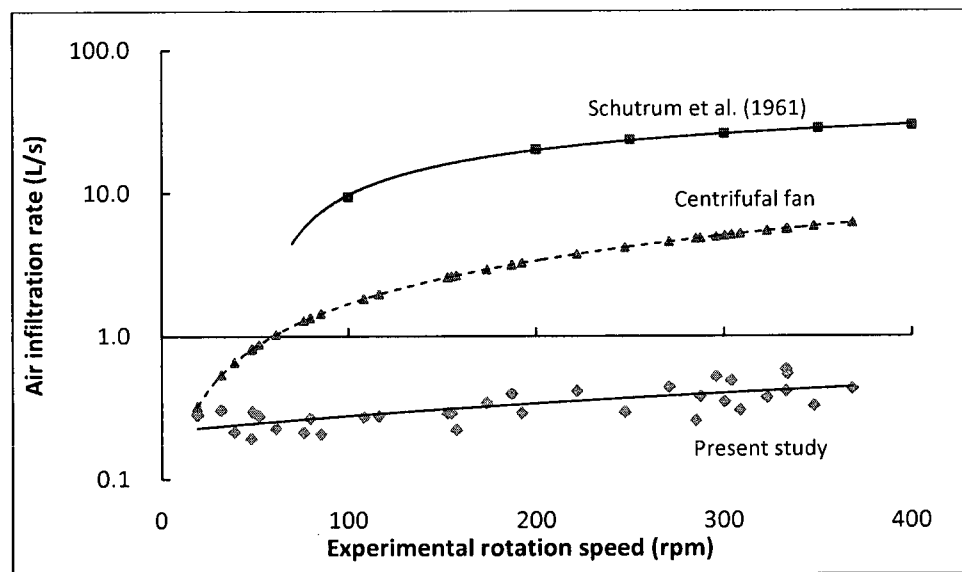


Fig. 4-5: Experimental air infiltration rate due to the revolution of the door vs. air flow rate of the same dimensioned centrifugal fan vs. previous study in the reduced-scale

Moreover, Cullum et al. (2006) estimated the energy needs for heating the infiltrated air through the revolving (using Schutrum et al. (1961)'s data) and swinging doors of one building equals the heating needs of 6.5 single-family houses over one year. The result appears to overestimate the air infiltration rate through doors.

Another simple calculation was carried out by using degree-day method and results of Schutrum et al. (1961) to calculate the energy consumption caused by a revolving door.

Assuming the revolving door is located in Montreal, the design outdoor air temperature for heating is -23°C . For the indoor air temperature of 18°C , the electric demand for heating the cold air brought into the building the revolving door is about 13 kW based on Schutrum et al. (1961). The annual heating energy usage is estimated at a huge value of 23,600 kWh by degree-day method, which equals to the average energy consumption of a house in Quebec. It shows that the air infiltration rate by Schutrum et al (1961) is overvalued. However, from present research, the electric heater for the same case is about 0.2 kW and the annual energy consumption is about 300 kWh. Therefore, the experimental data from this research is considered more reasonable. The air flow rate values at each experimental rotation speed are presented in Table 4-5.

Table 4-5: Experimental air infiltration rate due to the revolution of the revolving door vs. air flow rate of a same dimensioned centrifugal fan

Experimental rotation speed (rpm)	Air infiltration caused by the motion of the experimental revolving door (L/s)	Air flow rate of a centrifugal fan with same diameter as the experimental door (L/s)
19.06	0.284	0.320
19.17	0.280	0.322
31.76	0.303	0.534
38.88	0.213	0.653
47.85	0.191	0.804
48.55	0.296	0.816
51.96	0.275	0.873
61.10	0.225	1.026
76.29	0.211	1.282
79.68	0.264	1.339
85.37	0.206	1.434
108.37	0.270	1.821
116.44	0.275	1.956
152.98	0.287	2.570
155.17	0.288	2.607
157.70	0.220	2.649
173.87	0.340	2.921
187.06	0.393	3.143
192.39	0.288	3.232
221.59	0.410	3.723
247.36	0.293	4.156
270.75	0.437	4.549
284.99	0.255	4.788
287.37	0.375	4.828
295.73	0.517	4.968
300.30	0.345	5.045
303.75	0.485	5.103
308.51	0.302	5.183
322.84	0.370	5.424
333.03	0.583	5.595
333.03	0.410	5.595
333.78	0.538	5.608
347.77	0.324	5.843
368.31	0.426	6.188

It is also found that the air infiltration rate due to the rotation of the door is independent of the indoor and outdoor temperature difference, while Schutrum et al. (1961) concluded that the air infiltration caused by the movement of the door “may be expected as a function of temperature difference and constant rotation speed of the door” from the full-scale measurements.

4.1.5. Air Infiltration through Revolving Door with Different Conditions of Seals

The experimental revolving door has all four wings with good seals in good contact with the door housing. The results of this study are compared in Fig. 4-6 with results of A. Aupied (2009)¹ that used the same experimental setup. He carried out two series of experiments, one with the vertical seals on two wings removed, and another with all the vertical seals removed.

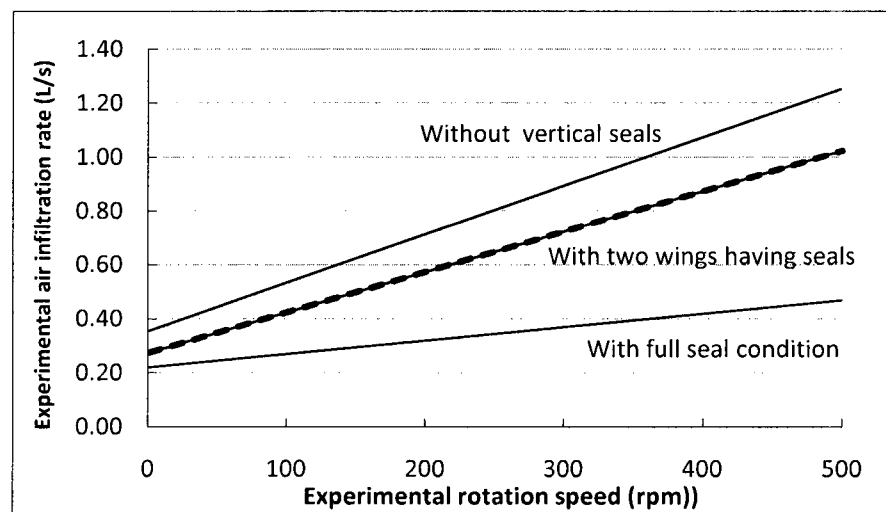


Fig. 4-6: Experimental air infiltration rate with different conditions of seals (The curves of the condition with only two vertical seals and the condition of no vertical seals are obtained by an exchange student, Alexis Aupied, using the same experimental setup in this study.)

¹ A. Aupied (2009). Exchange Student from IUT de Saint-Malo. Measurements, Calculations, Highlights and Visualization of the Heat Loss in a Building Caused by the Rotation of a Revolving Door. Supervisor: R. Zmeureanu. Concordia University.

The air infiltration rate due to the revolution of the door increases when the condition of seals gets worse, which indicates again the importance of maintaining the seals around the wings for energy saving purposes. However, the values are still within the same range of the air infiltration with full seal condition.

4.2. Dimensionless Expression of Temperature Distribution

To normalize results for different indoor and outdoor temperatures that vary from one experiment to another, the dimensionless air temperature index θ_x , which corrects the air temperature at selected location x near the door opening (Fig. 4-7) when the door rotates, is presented in this section:

$$\theta_x = \frac{T_x - T_o}{T_i - T_o} \quad (4-14)$$

where each temperature is the average value over the last five minutes of the recording period.

The revolving door is turning counterclockwise. There are four groups of thermocouples A, B, C and D, near the door holder. The “h” subscript represents a higher thermocouple, and the “l” subscript represents a lower thermocouple. For each group A, B, C and D, the dimensionless temperature is calculated using the average value of the “h” and “l” test points. There are also two thermocouples, M_o and M_i , at the middle height and center near the revolving door. M_o is the thermocouple installed outside and M_i is the thermocouple installed inside the box (Fig. 4-7).

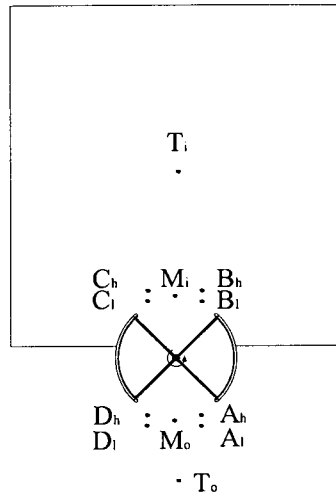
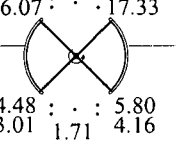
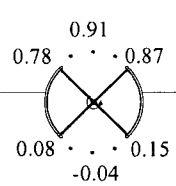
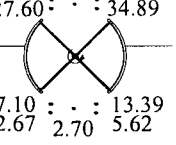
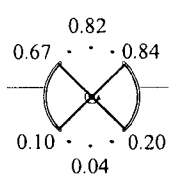


Fig. 4-7: Illustration of the temperature measurement points around the revolving door

For example, the dimensionless temperatures at 116.44 rpm, 17.62°C indoor temperature, and 152.98 rpm, 42.72°C indoor temperature in the reduced-scaled model are presented in Table 4-6. Results from all experiments are presented in Appendix C.

Table 4-6: Examples of the dimensionless temperature distribution near the revolving door at indoor temperature around 20°C and 40°C

Average rotation speed (rpm)	Indoor and outdoor temperature difference (°C)	Measured temperatures (°C)	Dimensionless temperature index θ_x (-)
116.44	17.62	20.01 IN 2.39 16.21 18.41 18.21 16.07 : : 17.33  4.48 : : 5.80 3.01 1.71 4.16	 0.91 0.78 : : 0.87 0.08 : : 0.15 -0.04
152.98	42.72	43.50 IN 0.78 31.02 35.85 38.05 27.60 : : 34.89  7.10 : : 13.39 2.67 2.70 5.62	 0.82 0.67 : : 0.84 0.10 : : 0.20 0.04

The variation of dimensionless temperature index θ_x versus the rotation speed is presented for each point, A, B, C and D, inside and outside the box (Table 4-7).

The dimensionless temperatures θ_x at B and C locations (inside the box) are higher than at A and D locations (outside the box) (Fig. 4-8). When the rotation speed is greater than 120 – 150 rpm, θ_C is almost at 0.75. Therefore the infiltration of cold air from outside does not increase with the increase of rotation speed. In the same time, θ_B shows that less cold air reaches location B as the air is directly towards location C.

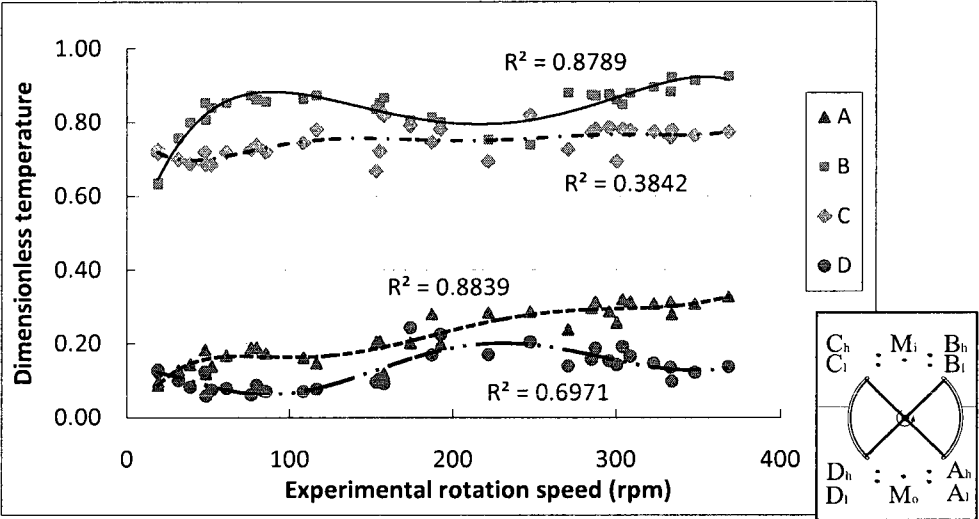


Fig. 4-8: Dimensionless temperature at thermocouple A, B, C, and D around the experimental revolving door

Figure 4-9 shows that the air leaving the revolving door has a similar impact on thermocouples at location B and M_i , compared to location C.

A similar calculation is obtained from the analysis of dimensionless temperatures at outside locations (A, D and M_o) (Fig. 4-10). The air leaving the revolving door affects mostly the location A (with higher θ_x values) than locations D and M_o .

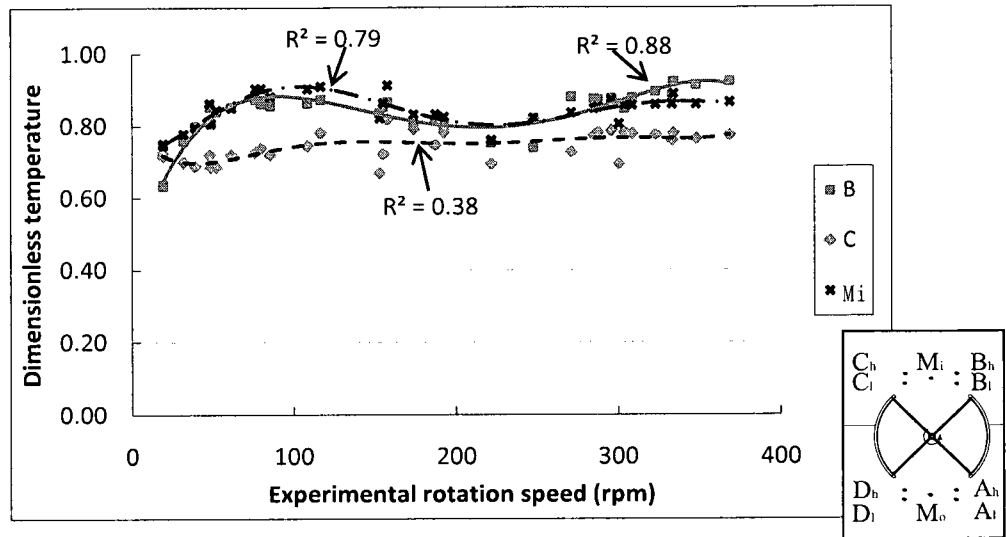


Fig. 4-9: Comparison of the dimensionless temperature at thermocouple B, C and M_i around the experimental revolving door

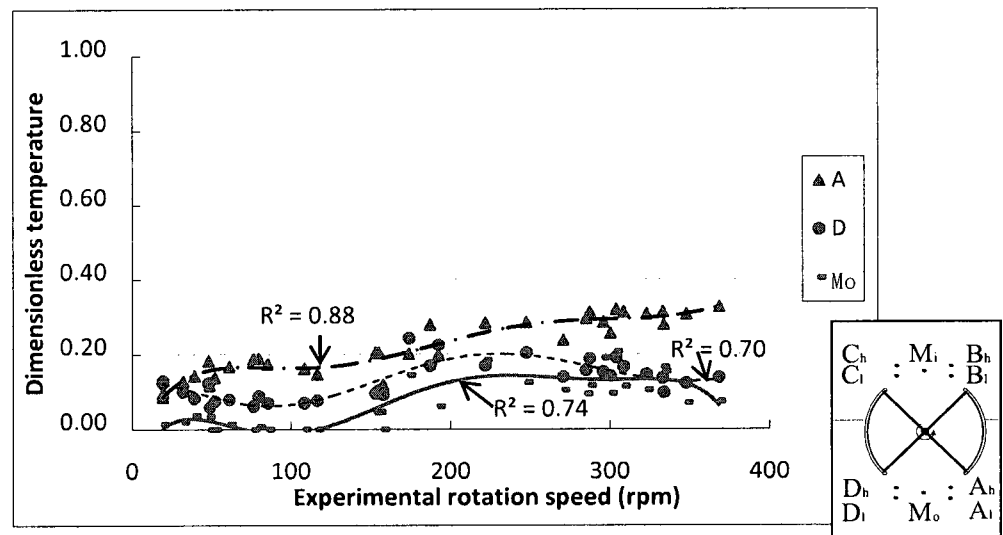


Fig. 4-10: Comparison of the dimensionless temperature at thermocouple A, D and M_o around the experimental revolving door

Table 4-7 presents the summary of all dimensionless temperatures index θ at the test points A to D and M_o and M_i . Most tests were done at the indoor temperature around 20°C. The bold numbers are the tests at the indoor temperature around 30°C and 40°C. The dimensionless values at 30°C and 40°C indoor temperature fit the variation trend of the values at 20°C, which also supports the conclusion that the indoor and outdoor

temperature difference does not influence the air infiltration due to the rotation of the door.

Table 4-7: The dimensionless temperature of each test point at different experimental rotation speeds

Experimental rotation speed (rpm)	Indoor temperature (°C)	A	B	C	D	M₀	M₁
19.06	19.45	0.09	0.64	0.73	0.12	0.01	0.75
19.17	19.70	0.10	0.63	0.72	0.13	0.00	0.75
31.76	17.54	0.13	0.76	0.70	0.10	0.02	0.78
38.88	20.38	0.14	0.80	0.69	0.08	0.04	0.80
47.85	20.79	0.18	0.85	0.72	0.12	0.03	0.86
48.55	19.05	0.12	0.81	0.69	0.06	-0.02	0.81
51.96	19.64	0.14	0.84	0.68	0.07	-0.01	0.84
61.10	20.14	0.17	0.85	0.72	0.08	0.01	0.85
76.29	21.05	0.19	0.87	0.73	0.06	-0.02	0.90
79.68	19.46	0.19	0.86	0.74	0.09	0.01	0.90
85.37	20.64	0.17	0.86	0.72	0.07	-0.02	0.88
108.37	19.89	0.16	0.86	0.74	0.07	-0.02	0.90
116.44	20.26	0.15	0.87	0.78	0.08	-0.04	0.91
152.98	42.78	0.20	0.84	0.67	0.10	0.04	0.82
155.17	25.41	0.20	0.85	0.72	0.10	0.05	0.86
157.70	21.14	0.12	0.87	0.82	0.09	-0.01	0.91
173.87	19.21	0.20	0.81	0.79	0.24	0.14	0.83
187.06	17.67	0.28	0.81	0.75	0.17	0.18	0.83
192.39	19.28	0.20	0.80	0.78	0.23	0.06	0.82
221.59	17.26	0.28	0.75	0.69	0.17	0.18	0.76
247.36	19.29	0.29	0.74	0.82	0.20	0.13	0.82
270.75	40.71	0.24	0.88	0.73	0.14	0.10	0.84
284.99	20.42	0.30	0.87	0.77	0.16	0.09	0.85
287.37	19.91	0.31	0.87	0.78	0.19	0.12	0.85
295.73	15.68	0.29	0.88	0.79	0.15	0.19	0.87
300.30	42.17	0.26	0.86	0.69	0.14	0.10	0.81
303.75	16.12	0.32	0.85	0.78	0.19	0.21	0.86
308.51	19.91	0.31	0.88	0.78	0.17	0.11	0.86
322.84	18.43	0.31	0.89	0.77	0.15	0.10	0.86
333.00	17.00	0.31	0.88	0.76	0.14	0.17	0.86
333.78	15.57	0.28	0.92	0.78	0.10	0.15	0.89
347.77	19.23	0.31	0.91	0.76	0.12	0.07	0.86
368.31	17.48	0.33	0.92	0.77	0.14	0.07	0.87

Except at very low rotation speed, the air entering the box is pushed towards point C, and the air leaving the box is pushed towards point A by the revolving door when it moves. Fig. 4-11 shows the air direction from the analysis of dimensionless temperature θ_x . The air flow direction around the door is the same direction as the door.

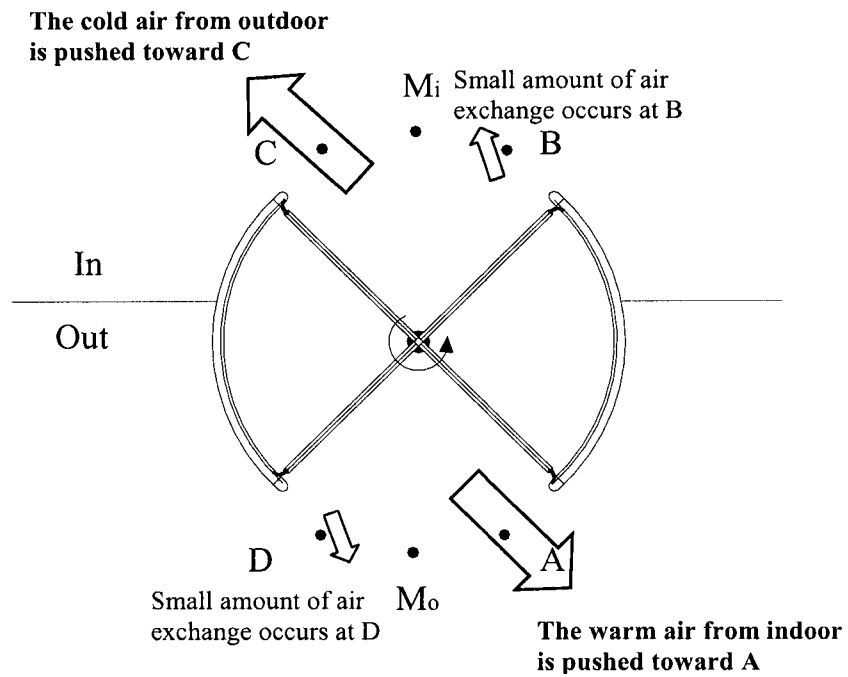


Fig. 4-11: Sketch showing the air flow direction

To illustrate the air direction more clearly, additional nine thermocouples were installed outside the revolving door in a horizontal plan (Fig. 4-12).

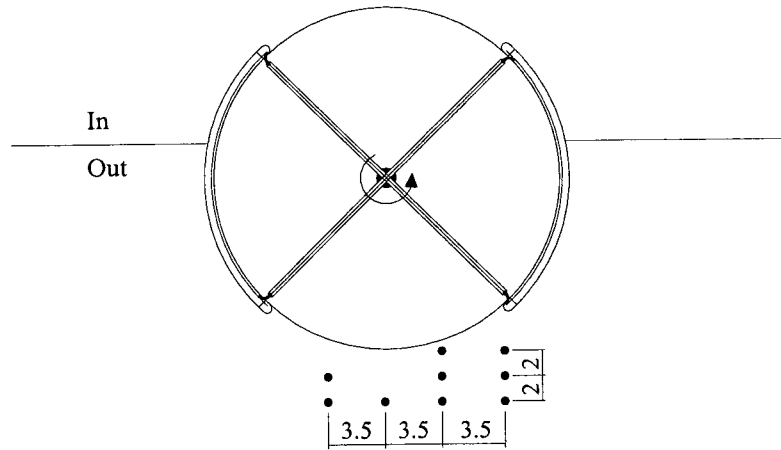


Fig. 4-12: Location of additional thermocouples to identify the air flow direction (dimensions in cm)

Two tests were carried out at the rotation speeds of 173.24 (Fig. 4-13) and 295.73 rpm (Fig. 4-14), both at the indoor air temperature of 20°C. Another test was at the rotation speed of 270.75 rpm and 40°C indoor temperature (Fig. 4-15). The values presented are the average air temperature, in °C, of last five minutes of the calculation period. The temperature at the point showed by a small “x” in the figures is the average temperature of D_h and D_l . The dimensionless temperatures are presented within brackets. In all cases, when the door rotates counterclockwise, the warm air from indoor is pushed along the tangent to the door housing. The temperatures of Fig. 4-13 suggest that a proportion of air brought by the revolving door from inside might be re-entered by the door.

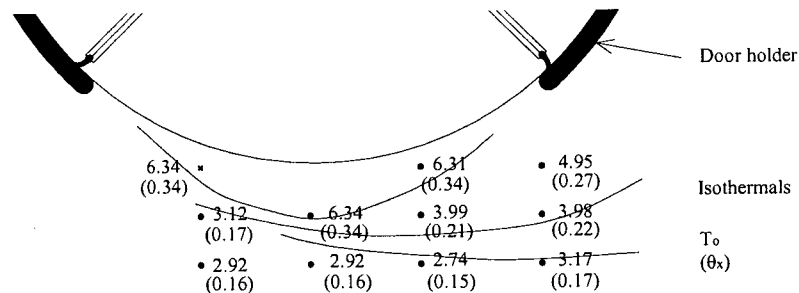


Fig. 4-13: Temperatures in front of the door showing the isothermals at 173.24 rpm and 18.5°C temperature difference between indoor and outdoor

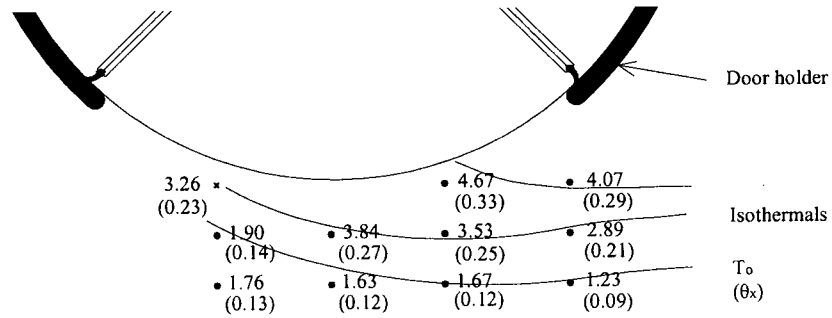


Fig. 4-14: Temperatures in front of the door showing the isothermals at 295.73 rpm and 13.98°C temperature difference between indoor and outdoor

Fig. 4-15 shows the temperature distribution outside and close to the door when the indoor temperature was around 40°C. With a higher indoor temperature, it shows more clearly that there is more heat exchange happening around test point A, and the air direction is towards A.

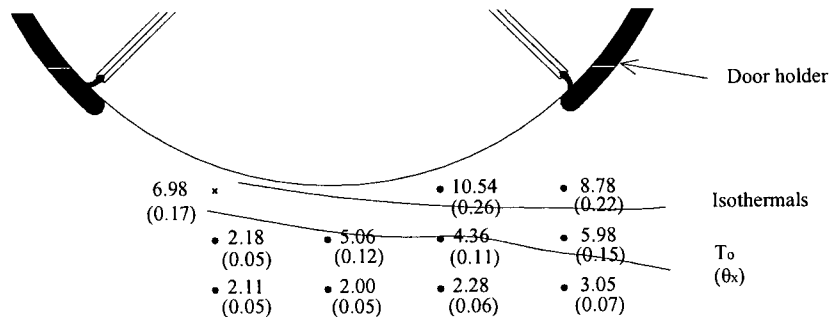


Fig. 4-15: Temperatures in front of the door showing the isothermals at 300.3 rpm and 42.16°C temperature difference between indoor and outdoor

The measurements also indicated that the temperature outside the revolving door drops very fast. At 4 cm away from the revolving door, the air temperature is already very close to the outdoor air temperature (the air temperature in the climatic chamber).

4.3. Infrared Images

A mosquito screen fixed on a frame was placed in horizontal or vertical position outside of the revolving door. Infrared images were taken at different rotation speeds and with different conditions of seals. In these images, the more reddish colour represents higher temperature and the more blueish colour represents lower temperature.

Figures 4-16 and 4-17 are the infrared images when the door has seals around the four wings, and the rotation speed of 50 and 300 rpm, respectively. The temperature scales of the images were automatically modified by computer program. It does not represent the real temperatures, more for the best image quality. However, it still can be considered as a reference for the temperature drop outside the revolving door. The door rotates counterclockwise. The infrared images show that the warm air coming from indoor to outdoor is pushed along the rotation direction towards the door housing.

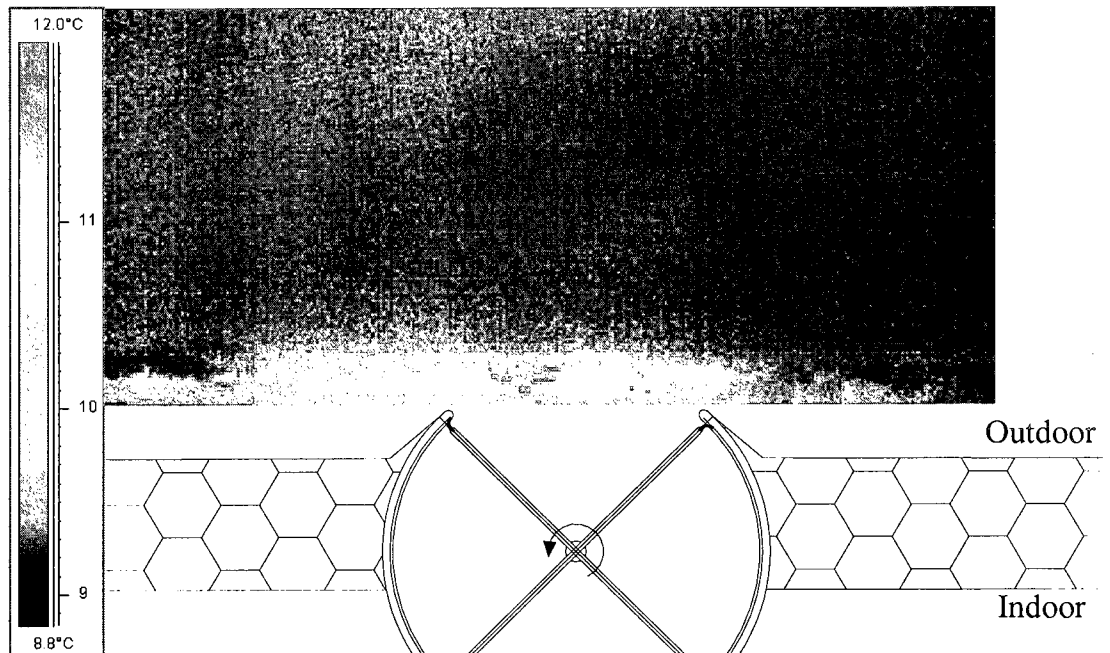


Fig. 4-16: Infrared image on a horizontal screen outside the revolving door with four seals at N = 50 rpm

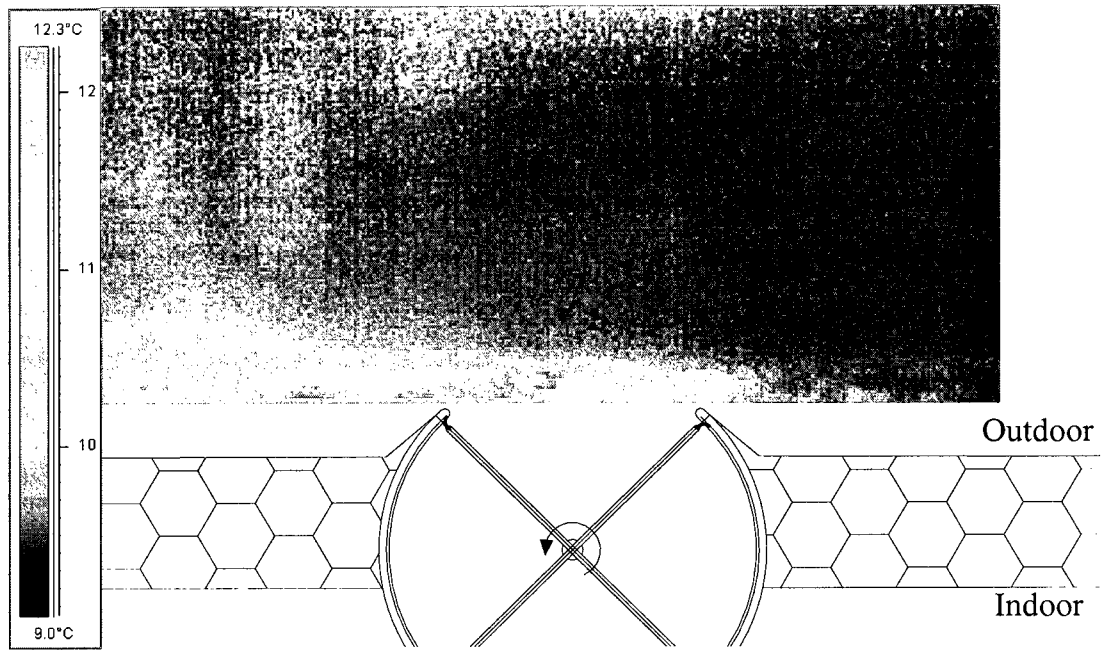


Fig. 4-17: Infrared image on a horizontal screen outside of the revolving door with four seals at $N = 300$ rpm

As the rotation speed increases, the area with higher temperature becomes longer and larger, which means the contribution of warm air coming from indoor environment increases. The warm air is pushed further counterclockwise to the outside enclosure of the box as well. As shown, the area of warm air is very narrow along the rotation direction of the door, which supports the conclusion from the measurement of the air temperature by thermocouples in section 4.2.

Infrared images were also taken at 50 and 300 rpm after removing the vertical seals on the wings (Figures 4-18 and 4-19). The images show a similar air flow pattern.

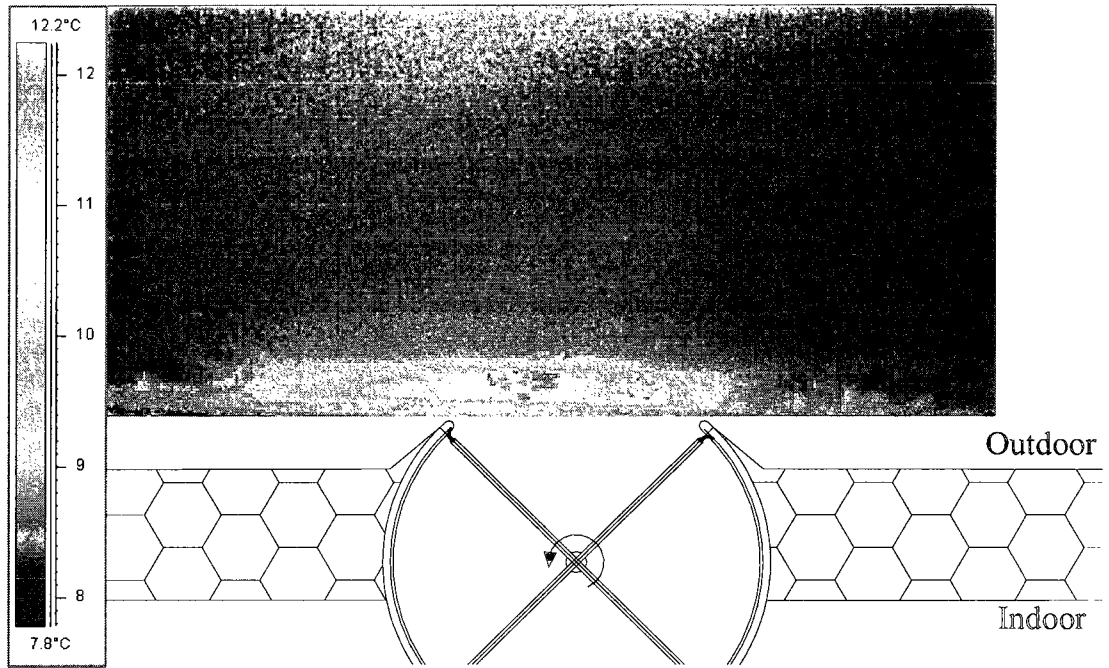


Fig. 4-18: Infrared image on a horizontal screen outside the revolving door without vertical seals at $N = 50$ rpm

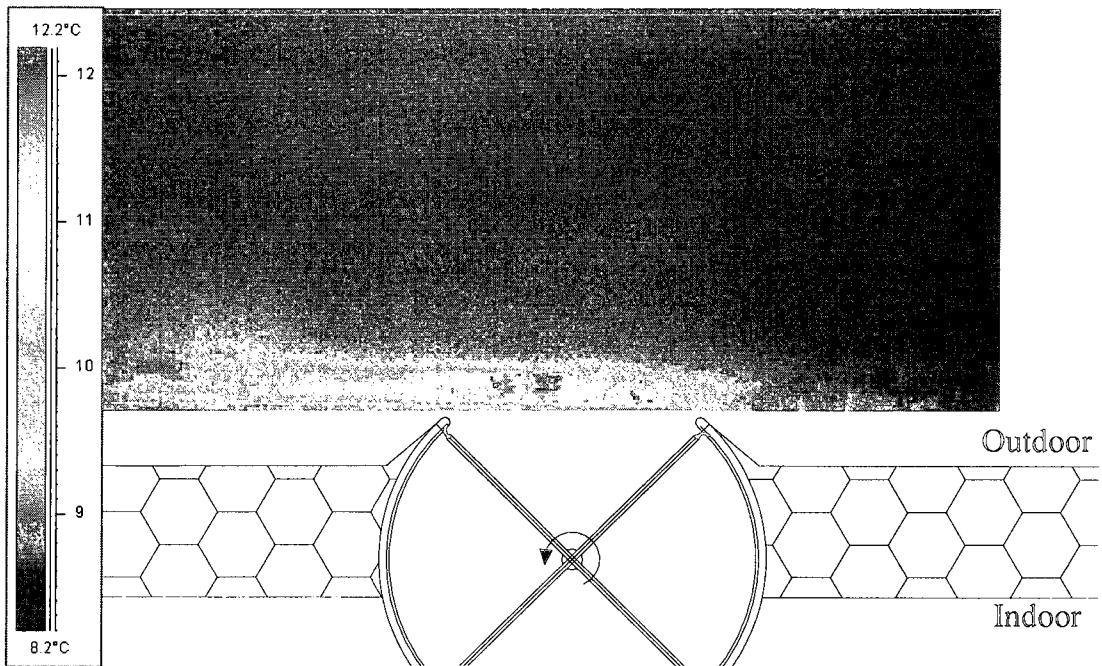


Fig. 4-19: Infrared image on a horizontal screen outside of the revolving door without vertical seals at $N = 300$ rpm

Similarly, more air is pushed toward counterclockwise as the rotation speed increases, and there is more air exchange at the closing period of the rotation. The area of warm air is very narrow which means that the temperature coming from indoor drops very fast at the outdoor environment.

Infrared images were also taken when the screen is placed at the vertical position outside the revolving door. Fig. 4-22 is the infrared image at the rotation speed of 300 rpm with all wings sealed. The vertical images were taken at different times of experiment from the horizontal images. Therefore the scales of temperature are different between vertical and horizontal images. The red area in vertical image is affected by the heating leakage through insulation from door motor.

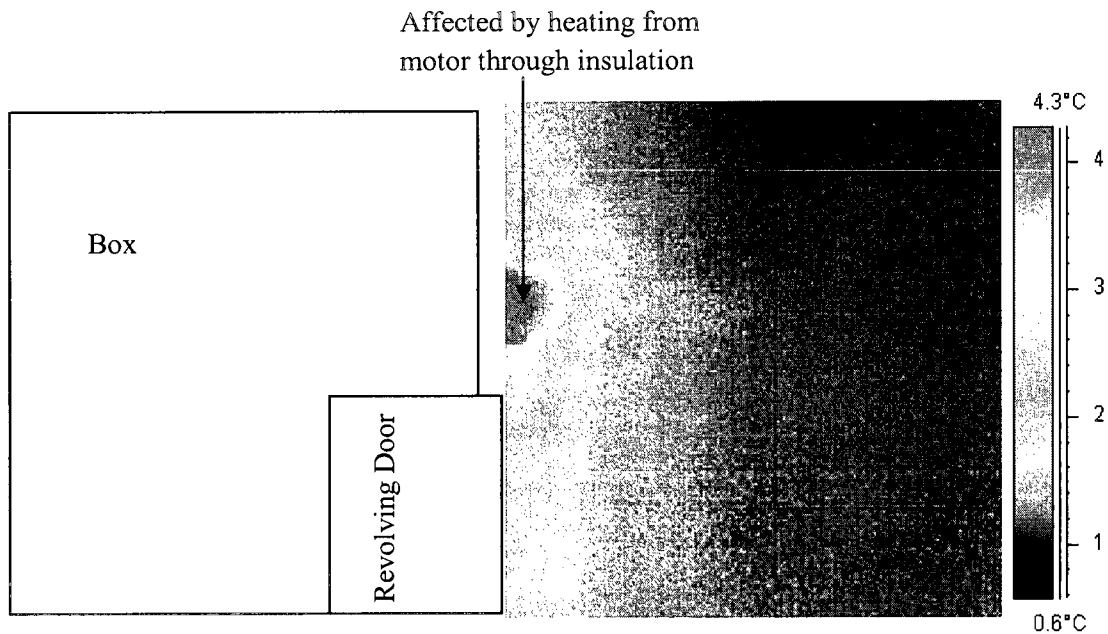


Fig. 4-22: Vertical infrared image on a vertical screen outside of the revolving door with four seals at N = 300 rpm

4.4. Correlation-Based Models

The experiments were carried out with the experimental rotation speed from 19 rpm to 360 rpm, which equals 0.19 to 3.6 rpm in the prototype. In the experiments, in order to keep the indoor temperature at a constant value, a heater was set inside the box, and the power input of the heater was used in the calculation of the air infiltration rate caused by the motion of the revolving door. However in the real (prototype) case of a large building, it is impossible to have a similar experimental setup.

It will be much more practical if the air infiltration rate can be estimated based on on-site measurements of the rotation speed and the dimensionless temperature values around the revolving door. Several correlation-based models of volumetric flow rate (L/s) expressed as function of different groups of variables (e.g.: N, dimensionless temperature θ_x) are compared in Appendix D, along with the dimensionless temperatures at each test point used to generate the models. The best correlation-based models for different seal conditions are presented in this section and are recommended for use on-site to estimate the air infiltration through existing revolving doors.

In the case of experimental revolving door with four seals, the following correlation-based model predicts the experimental air infiltration rate, in L/s, when door is rotating:

$$q_{inf} = (0.000006 \cdot N^2 - 0.0017 \cdot N - 1.96 \cdot \theta_{Ah} - 0.046 \cdot \theta_{Al} - 0.85 \cdot \theta_{Bh} + 0.35 \cdot \theta_{Bl} - 0.16 \cdot \theta_{Ch} - 0.53 \cdot \theta_{Cl} - 0.61 \cdot \theta_{Dh} + 0.31 \cdot \theta_{Dl} + 2.22 \cdot \theta_{Mo} + 1.09 \cdot \theta_{Mi} + 0.93) / \rho \quad (4-15)$$

R^2 of this correlation-based equation is 0.81, standard error is 0.075 L/s and relative error is 18.6%.

Using the similarity criteria (Section 3.1.3), the correlation-based model for prototype is as follows:

$$q_{\text{inf_prototype}} = (0.64 \cdot N^2 - 1.72 \cdot N - 19.62 \cdot \theta_{\text{Ah}} - 0.46 \cdot \theta_{\text{Al}} - 8.45 \cdot \theta_{\text{Bh}} + 3.53 \cdot \theta_{\text{Bl}} - 1.55 \cdot \theta_{\text{Ch}} - 5.27 \cdot \theta_{\text{Cl}} - 6.13 \cdot \theta_{\text{Dh}} + 3.08 \cdot \theta_{\text{Dl}} + 22.19 \cdot \theta_{\text{Mo}} + 10.85 \cdot \theta_{\text{Mi}} + 9.34) / \rho \quad (4-16)$$

Table 4-9 gives the comparison of the volumetric air infiltration rate in prototype from experimental data and the values from correlation-based model. The relative error for each group varies from -22% to 36%. The relative standard error of this correlation equation is 18.6%. Therefore, by measuring the on-site dimensionless temperature θ_x in the selected points, and the rotation speed, it is possible to estimate the net air infiltration rate through a prototype revolving door.

Table 4-8: Data from experiments vs. simulated data from correlation equation in prototype with four seals condition

Rotation speed (rpm)	Volumetric flow rate from experimental	Volumetric flow rate from correlation-based model	Relative error
	data $q_{\text{prototype}}$ (L/s)	$q_{\text{correlation}}$ (L/s)	$\frac{q_{\text{correlation}} - q_{\text{prototype}}}{q_{\text{prototype}}}$
0.19	2.84	3.05	0.04
0.19	2.80	2.63	-0.09
0.32	3.03	2.67	0.20
0.39	2.13	2.91	0.26
0.48	1.91	2.18	0.11
0.49	2.96	2.48	-0.22
0.52	2.75	2.71	-0.11
0.61	2.25	2.27	0.00
0.76	2.11	1.98	0.00
0.80	2.64	2.34	-0.10
0.85	2.06	1.77	0.01
1.08	2.70	2.35	-0.06
1.16	2.75	2.28	-0.13
1.53	2.87	2.90	0.06
1.55	2.88	2.36	-0.02
1.58	2.20	2.83	0.36
1.74	3.40	3.51	-0.02
1.87	3.93	3.66	-0.03
1.92	2.88	2.02	-0.18
2.22	4.10	4.21	0.01
2.47	2.93	3.25	0.15
2.71	4.37	3.55	-0.13
2.85	2.55	2.74	0.24
2.87	3.75	2.92	-0.13
2.96	5.17	5.25	-0.02
3.00	3.45	3.50	0.08
3.04	4.85	4.95	-0.01
3.09	3.02	3.49	0.23
3.23	3.70	3.67	0.04
3.33	5.83	4.96	-0.16
3.34	5.38	5.51	0.00
3.48	3.24	3.70	0.18
3.68	4.26	4.01	-0.08

In the case when the experiential revolving door has no vertical seals, as on extreme case, the following correlation-based model predicts the experimental air infiltration rate, in L/s:

$$q_{inf} = (0.000026 \cdot N^2 - 0.0071 \cdot N - 8.32 \cdot \theta_{Ah} - 4.36 \cdot \theta_{Al} + 8.56 \cdot \theta_{Bh} + 1.16 \cdot \theta_{Bl} + 14.3 \cdot \theta_{Ch} + 11.95 \cdot \theta_{Cl} - 13.08 \cdot \theta_{Dh} + 24.57 \cdot \theta_{Dl} + 1.24 \cdot \theta_{Mo} - 16.45 \cdot \theta_{Mi} - 9.58) / \rho \quad (4-17)$$

R^2 of this correlation-based equation is 0.99, standard error is 0.069 L/s and relative error is 6.9%.

Using the similarity criteria, the correlation-based model for the prototype for the case of no vertical seals is as follows:

$$q_{inf_prototype} = (2.62 \cdot N^2 - 7.08 \cdot N - 83.18 \cdot \theta_{Ah} - 43.57 \cdot \theta_{Al} - 85.63 \cdot \theta_{Bh} + 11.64 \cdot \theta_{Bl} + 142.97 \cdot \theta_{Ch} + 119.52 \cdot \theta_{Cl} - 130.84 \cdot \theta_{Dh} + 245.69 \cdot \theta_{Dl} + 12.35 \cdot \theta_{Mo} - 164.46 \cdot \theta_{Mi} - 95.82) / \rho \quad (4-18)$$

The air infiltration rates calculated by the correlation equation are very close to the experimental data for no seal condition (Table 4-9). The relative error between the experimental results and calculated air infiltration by correlation equation is from -5.90% to 2.56%.

Table 4-9: Data from experiments vs. simulated data from correlation equation in prototype with no vertical seals

Rotation speed (rpm)	Volumetric flow rate in prototype (L/s)	Volumetric flow rate from correlation equation (L/s)	Relative error $\frac{Q_{correlation} - Q_{prototype}}{Q_{prototype}}$
0.44	4.58	4.59	0.32
0.87	5.63	5.58	-0.89
1.31	6.61	6.63	0.27
1.73	5.43	5.36	-1.25
1.90	5.54	5.53	-0.11
2.16	7.75	7.95	2.50
2.42	7.67	7.58	-1.15
2.59	8.64	8.78	1.73
2.78	8.81	8.70	-1.23
3.05	8.70	8.80	1.08
3.35	9.07	9.16	1.07
3.46	10.92	10.28	-5.90
3.66	10.20	10.46	2.56
3.81	10.23	10.40	1.64
3.98	10.37	10.34	-0.30

Others correlation-based models with different variables were also concluded in Appendix D, as well as the dimensionless values at each point used to obtain the correlation-based models.

4.5. Conclusion

The air infiltration rate due to the revolution of the revolving door was calculated from a series of experiments by a reduced-scale model. Compared to the air infiltration through the gaps and seals between door wings and door holder, the air infiltration rate caused by the rotation of the door is very small. The air infiltration due to the motion of the door increases slightly with increasing rotation speed of the door, however, it is independent from the indoor and outdoor temperature difference. A correlation-based

model was developed for revolving doors with different seal conditions. This research is the only resource of the experimental data of the air infiltration through a revolving door by its movement since a single paper about this issue published more than 40 years ago. This may catch the attention of future research regarding the energy consumption in buildings with this type of doors or the modification of the energy standards or regulations.

The results of this study indicate that smaller air infiltration rates through revolving doors should be used to size the heating systems to compensate for heat losses, when compared with values recommended by Schutrum et al. (1961). For instance, when a revolving door with good seals rotates at 3 rpm and the indoor-outdoor air temperature difference is 20°C (36°F), results from Schutrum et al. (1961) give an air infiltration rate of about 260 L/s (550 cfm) (Fig. 2-2). The present study recommends an air infiltration rate of only 3.45 L/s. As presented in section 4.1.4, the results of Schutrum et al. (1961) overestimate the air infiltration rate due to the door revolution, significantly. If the revolving door is located in Montreal, to keep the indoor environment at constant 18°C, the electric demand for heating is about 13 kW and the annual heating energy usage is estimated at a value of 23,600 kWh by degree-day method based on the air infiltration rate from Schutrum et al. (1961), which equals to the average energy use of a house. However, the electric heater for the same case is about 0.2 kW and the annual energy usage is estimated at 300 kWh by using the air infiltration rate from present study.

CHAPTER 5

CONCLUSIONS AND RECOMMENDATIONS FOR FUTURE WORK

5.1. Summary and Conclusions

This research provides accurate laboratory data of the part of air infiltration through revolving door caused by the revolution of the door. A 1/10 reduced-scale model of a revolving door was designed for the measurements of the air infiltration rate due to the motion of revolving doors. An airtight box, where the revolving door was installed, was very well insulated to make sure that the energy exchange only occurs at the doorway. Experiments were carried out in the winter condition. The box was located in a climatic chamber which provides an outdoor temperature around 0°C. To warm up and keep the air temperature constant inside the box, a heater was installed in the box. A small motor was used to drive the door turning. Thermocouples were placed at the indoor and outdoor environments and around the revolving door. The power inputs of the instruments, the temperatures, and the total number of turns were recorded by a Data Acquisition System (Agilent).

The traffic flow rates of three revolving doors in office/university buildings were recorded in field studies. Experiments at different experimental rotation speeds from 19 rpm to 360 rpm were carried out, which gives the data for rotation speeds from 0.19 rpm

to 3.6 rpm in prototype. The air infiltration rate was calculated based on the heat balance equation of the indoor environment over a period of time.

It is found that the air infiltration increases slightly with the increase in the rotation speed. According to the experimental results, the motion of the revolving door only has a very small effect to the air infiltration rate. In prototype at the rotation speeds of 0.2 rpm to 3.6 rpm, the air infiltration caused by the rotation of the door varies from 2 L/s to 6 L/s which equals to 0.5-1.1 L/s·m² of the door area and 0.1-0.3 L/(s·m) of door crack. The recommended limitations of the air infiltration through door way in several standards presented in literature review are most likely just for the part of air infiltration through gap and seals when revolving doors are still. The air infiltration due to the revolution of the door could be included in the standard and this research provides reliable data as a reference.

Most tests were carried out at indoor temperatures around 20°C, and several tests were made at indoor temperatures around 30°C and 40°C. The calculated air infiltration rate in the conditions of 30°C and 40°C indoor environment fits the range of air infiltration rate in the condition of 20°C very well, which indicates that the temperature difference between indoor and outdoor is independent to the air infiltration rate caused by the motion of the revolving door.

To remove the effect of different outdoor and indoor temperature measurements, the dimensionless air temperature index θ_x around the revolving door is presented at different rotation speeds. The dimensionless analysis gives an idea of the air flow pattern around the revolving door and it is also a support of the conclusion that the air infiltration rate due to the motion of the door does not increase significantly with the rotation speed.

Several more thermocouples were installed in a horizontal place in front of the revolving door at the outdoor environment. The measured temperature shows the same result that the air flow direction is along the tangent towards the door housing. It is also indicated that temperature of the warm air coming from indoor drops very fast when it comes to outdoor environment. The area of warm air outside the revolving door is very narrow. The air temperature at the distance of 4 cm away from the revolving door in the experiment is already very close to the average outdoor temperature.

Infrared images presenting the air flow pattern around the revolving door were taken at different seal conditions at 50, 150, and 300 rpm. A mosquito screen was placed in horizontal and vertical position outside of the door. In the horizontal pictures, the area of warm air outside the revolving door is very narrow, and the air flow direction is towards the door housing. The vertical infrared picture outside the door indicates that the warm air coming from indoor with smaller density rises up when it comes to the outdoor environment.

To provide an easily-applied way of calculating the volumetric air flow rate due to the rotation of the door, correlation-based models of air flow rate were established as functions of rotation speed and dimensionless temperature indexes. By only measuring the air temperature around the revolving door, the volumetric air flow rate in prototype can be calculated according to the correlation-based models which are obtained from the experimental data of different seals conditions.

5.2. Future Work

Based on the experience obtained from this study, the following suggestions can be

made with respect to future work on this area.

1) Study the air infiltration rate through revolving doors when there is pressure difference between outside and inside environments.

2) Repeat this study for different geometric ratios λ_L . It would also be great if some tests were carried out in a full-scale revolving door and results compared with those from reduced-scale models. By using a full-scale door, people can really enter and leave the revolving door that the effect of people can also be observed.

3) Use other approaches for measuring the air infiltration rate. For instance, use a laminar flow meter instead of controlling T_i and T_o , and calculate the infiltration rate based on heat balance equation.

4) Based on the field studies, the rotation speed of a real-sized revolving door could be up to 7 rpm. In order to get the data for higher rotation speed, structural intensity and ability of motor controlling door turning need to be improved.

References

Allgayer, D. M., & Hunt, G. R. (2004). *Air movement by revolving doors. Roomvent 2004, Eighth International Conference on Air Distribution in Rooms, Coimbra, Portugal.*

ASHRAE (1989). *ASHRAE standard 90.1.* American Society of Heating, Refrigerating and Air-conditioning Engineers, Inc., Atlanta.

ASHRAE (1999). *ASHRAE standard 90.1.* American Society of Heating, Refrigerating and Air-conditioning Engineers, Inc., Atlanta.

Cullum, B. A., Lee, O., Sukkasi, S., & Wesolowski, D. (2006). *Modifying habits towards sustainability: A study of revolving door usage on the MIT campus.* Retrieved from http://web.mit.edu/wesolows/www/11.366_REVOLVING_DOOR_FINAL_REPORT.pdf, Cambridge, MA.

Elektror airsystems gmbh. (2009). *Elektror catalog medium pressure blower.* http://pdf.directindustry.com/pdf/elektror/product-review-24355-7697.html#pdf_7697

Fox, R. W., & McDonald, A. T. (1998). *Introduction to fluid mechanics* (Fifth ed.). John Wiley & Sons, Inc., New York.

Halliday, D., Resnick, R., & Walker, J. (2001). *Fundamentals of physics* (8th ed.). Wiley: Hoboken, NJ.

IIEC (2006). *Energy conservation building code 2006.* International Institute for Energy Conservation, U.S.

McQuiston, F. C., & Spitler, J. D. (1992). *Cooling and heating load calculation manual* (2nd ed.). American Society of Heating, Refrigerating and Air-Conditioning Engineers, Atlanta, GA.

Min, T. C. (1958). Winter infiltration through swinging-door entrances in multistory buildings. *ASHRAE Transactions*, 64, 421, American Society of Heating, Refrigerating and Air-Conditioning Engineers, Atlanta, GA.

MNECCB (1997). *Model national energy code of Canada for buildings*. National Research Council Canada (NRCC), Ottawa.

NRCC (1997). *National building code of Canada*. National Research Council Canada, Ottawa.

Schijndel, H. v., Zmeureanu, R., & Stathopoulos, T. (2003). Simulation of air infiltration through revolving doors. *Eighth International IBPSA Conference*, 1193. Eindhoven, Netherlands.

Schutrum, L. F., Ozisik, N., Baker, J. T., & Humphreys, C. M. (1961). Air infiltration through revolving doors. *ASHRAE Journal*, 3(11), 43-50.

Stalder, L. (2009). Turning architecture inside out: Revolving doors and other threshold devices. *Journal of Design History*, 22(1), 69-77.

Zmeureanu, R., Stathopoulos, T., Schopmeijer, M. E. D., Siret, F., & Payer, J. (2001). Measurements of air leakage through revolving doors of institutional building. *ASCE: Journal of Architectural Engineering*, 7(4), 131-137.

Appendix A:

Air Velocities inside the Climatic Chamber

To find out whether the presence of the box inside the chamber affects the air velocity field, the air velocity in the chamber was measured with and without the room model. First, the velocity near the front of the box was measured with the box in the chamber. The measurements started from the bottom of the box to the ceiling of the box with 5 cm interval. Then the box was removed and the same measurements were carried out. Five points above and five points below the box with same intervals were measured as well. Measurements were carried out three times at each point. The air velocities and deviations were recorded, and the average values were calculated.

Table A-1: Air velocity near the front of the box (tested with the box in the chamber)

Test Point	Air Velocity (m/s)	Average Velocity (m/s)	Deviation	Average Deviation	Test Point	Air Velocity (m/s)	Average Velocity (m/s)	Deviation	Average Deviation
1	0.2	0.233	0.09	0.083	7	0.26	0.210	0.09	0.087
	0.26		0.09			0.18		0.09	
	0.24		0.07			0.19		0.08	
2	0.23	0.243	0.07	0.083	8	0.23	0.237	0.1	0.093
	0.25		0.08			0.26		0.09	
	0.25		0.1			0.22		0.09	
3	0.18	0.223	0.08	0.077	9	0.21	0.190	0.07	0.060
	0.26		0.08			0.2		0.06	
	0.23		0.07			0.16		0.05	
4	0.22	0.200	0.08	0.073	10	0.14	0.170	0.07	0.067
	0.18		0.07			0.17		0.07	
	0.2		0.07			0.2		0.06	
5	0.24	0.217	0.08	0.083	11	0.26	0.217	0.1	0.093
	0.21		0.08			0.19		0.09	
	0.2		0.09			0.2		0.09	
6	0.23	0.237	0.1	0.080	12	0.19	0.190	0.08	0.070
	0.24		0.07			0.2		0.06	
	0.24		0.07			0.18		0.07	

Table A-2: Air velocity near the front of the box (tested after removing the box)

Test Point	Air Velocity (m/s)	Average Velocity (m/s)	Deviation	Average Deviation	Test Point	Air Velocity (m/s)	Average Velocity (m/s)	Deviation	Average Deviation
1	0.2	0.230	0.1	0.103	7	0.23	0.207	0.08	0.080
	0.25		0.12			0.18		0.09	
	0.24		0.09			0.21		0.07	
2	0.25	0.257	0.09	0.087	8	0.18	0.190	0.07	0.087
	0.25		0.08			0.16		0.11	
	0.27		0.09			0.23		0.08	
3	0.25	0.223	0.08	0.080	9	0.21	0.203	0.08	0.073
	0.21		0.08			0.16		0.07	
	0.21		0.08			0.24		0.07	
4	0.23	0.227	0.1	0.100	10	0.23	0.190	0.05	0.067
	0.23		0.09			0.16		0.09	
	0.22		0.11			0.18		0.06	
5	0.22	0.233	0.09	0.093	11	0.23	0.203	0.07	0.070
	0.24		0.09			0.21		0.07	
	0.24		0.1			0.17		0.07	
6	0.23	0.227	0.07	0.080	12	0.21	0.180	0.07	0.080
	0.23		0.09			0.15		0.08	
	0.22		0.08			0.18		0.09	
+1	0.22	0.190	0.08	0.077	-1	0.14	0.153	0.11	0.090
	0.16		0.07			0.17		0.08	
	0.19		0.08			0.15		0.08	
+2	0.24	0.217	0.08	0.073	-2	0.23	0.217	0.09	0.090
	0.22		0.07			0.21		0.08	
	0.19		0.07			0.21		0.1	
+3	0.19	0.197	0.09	0.080	-3	0.15	0.187	0.08	0.087
	0.18		0.07			0.19		0.1	
	0.22		0.08			0.22		0.08	
+4	0.25	0.217	0.09	0.073	-4	0.22	0.247	0.11	0.103
	0.19		0.06			0.23		0.09	

	0.21		0.07			0.29		0.11	
	0.26		0.06			0.26		0.1	
+5	0.2	0.237	0.1	0.087	-5	0.28	0.263	0.11	0.097
	0.25		0.1			0.25		0.08	

As showing in Table A-3, there is not a particular influence to the air velocity after setting up the model in the chamber. The average outdoor velocity is 0.214 m/s.

Table A-3: The air velocity vs. the height

No.	Distance from floor (m)	Velocity with box (m/s)	Velocity without box (m/s)
+5	1.55		0.237
+4	1.5		0.217
+3	1.45		0.197
+2	1.4		0.217
+1	1.35		0.19
1	1.3	0.233	0.23
2	1.25	0.243	0.257
3	1.2	0.233	0.223
4	1.15	0.2	0.227
5	1.1	0.217	0.233
6	1.05	0.237	0.227
7	1	0.21	0.207
8	0.95	0.237	0.19
9	0.9	0.19	0.203
10	0.85	0.17	0.19
11	0.8	0.217	0.203
12	0.75	0.19	0.18
-1	0.7		0.153
-2	0.65		0.217
-3	0.6		0.187
-4	0.55		0.247
-5	0.5		0.263
Average		0.214	0.213

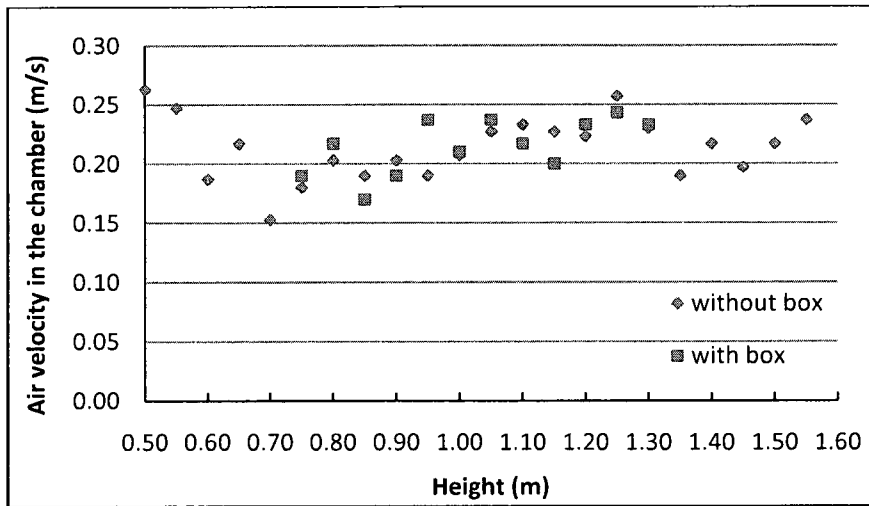


Fig. A-1: The comparison of the air velocity with and without the box in the chamber

The comparison of the air velocity with and without box shows that the presence of the box did not affect the air movement in the climatic chamber.

Appendix B:

Instantaneous Calculation Method of Experimental Air Infiltration

Tests were also carried with one layer of insulation, two layers of insulation without aluminum paper, and two layers of insulation and one layer aluminum paper but the motor was insulated as well which may affect the accuracy of the experiments. The results are presented here.

B-1. Heat loss through the envelope

The overall coefficient of heat transmission (U) of the experiments is compared with the U-valued calculated from the known thermal properties and dimensions of the insulation material, at the condition of one layer of insulation, two layers of insulation and two layers of insulation with a layer of aluminum paper.

Table B-1: U-value calculated from the experiments vs. reference value

Insulation	Thickness (cm)	$U_{\text{experiment}}$ ($\text{W}/\text{m}^2 \cdot ^\circ\text{C}$)	$U_{\text{reference}}$ ($\text{W}/\text{m}^2 \cdot ^\circ\text{C}$)
One layer of Styrofoam	5	0.61	0.416
Two layers of Styrofoam	10	0.245	0.227
Two layers of Styrofoam + aluminum paper	10	0.249	0.227

The reason why the U value from the test after one layer of insulation were much bigger than the calculated value is that the insulation was not taped tightly enough, that there were still a lot of gaps between the insulation material and experimental box. After applying another layer of machine cut insulation, all the gaps were fit nicely, and all the

gaps were taped tightly as well. The U value of two layer insulation by test is much closer to the reference value.

B-2. Tests with one layer of insulation

Table B-2 shows the air flow rate with different rotation speed. Table B-3 shows the temperature distribution.

Table B-2: The air flow rate with different rotation speeds with one layer of insulation

Rotation speed (rpm)	Indoor temperature T_i (°C)	Outdoor temperature T_o (°C)	Temperature difference $T_i - T_o$ (°C)	Heat loss through envelope q_{loss} (W)	Mass flow rate m_{inf} (g/s)	Volumetric flow rate v_{inf} (L/s)
18.32	22.83	2.48	20.35	31.64	0.123	0.099
20.57	23.878	2.103	21.775	33.86	0.028	0.022
29.32	23.185	1.81	21.375	33.24	0.091	0.072
58.48	22.62	3.77	18.85	29.31	0.337	0.27
158.02	28.99	1.96	27.03	42.03	0.231	0.185
174.4	21.51	1.57	19.94	31.01	0.125	0.1
195.31	20.37	1.5	18.87	29.34	0.244	0.195

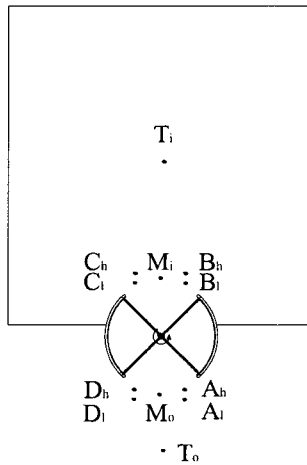


Fig. B-1: Illustration of the position of thermocouples

In Fig. B-2, the “h” subscript represents the higher thermocouple, and the “l” subscript represents lower thermocouple. There are also M_o and M_i two thermocouples in the middle height and center near the revolving door. M_o represents the thermocouple outside and M_i represents the thermocouple inside the box.

Table B-3: The temperature distribution and temperature difference between inside and outside of the revolving door with different rotation speed with one layer of insulation

Rotation speed (rpm)	Temperature Distribution	$\Delta T = T_i - T_o$	$\Delta T_{\text{goes_in}} = T_B - T_A$	$\Delta T_{\text{goes_out}} = T_c - T_D$	$\Delta T_{\text{middle}} = T_{M_i} - T_{M_o}$
	· 22.83				
18.32	<p>19.70 19.89 18.23 16.37 : : : 15.45</p> <p>5.04 : : : 4.96 3.01 1.27 2.58</p> <p>· 2.00 · 24.88</p>	20.35	13.08	14.00	16.98
20.57	<p>20.02 19.88 20.07 16.37 : : : 17.52</p> <p>4.09 : : : 5.05 2.58 1.62 2.26</p> <p>· 2.1 · 23.18</p>	21.77	15.14	14.87	18.27
29.32	<p>18.20 19.83 19.90 16.27 : : : 18.44</p> <p>3.58 : : : 5.29 2.28 1.27 2.10</p> <p>· 1.81 · 22.62</p>	21.37	15.47	14.30	18.57
58.48	<p>17.34 20.59 20.37 18.83 : : : 19.48</p> <p>4.51 : : : 7.64 4.13 3.35 4.68</p> <p>· 3.77 · 27.03</p>	18.82	13.7	13.47	17.1
158.02	<p>21.94 26.40 25.85 22.47 : : : 24.39</p> <p>3.13 : : : 6.52 2.53 1.40 3.05</p> <p>· 1.96</p>	27.03	20.33	19.37	25.00

174.4		20.37	14.86	15.6	19.25
195.31		19.70	14.82	15.52	18.88

B-3. Tests after two layers of insulation

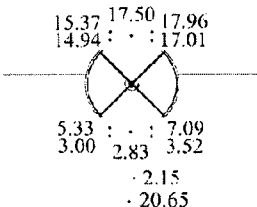
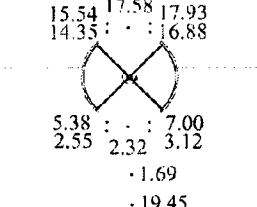
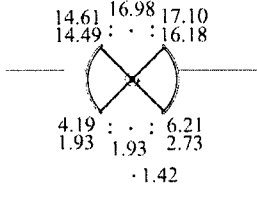
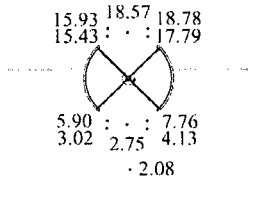
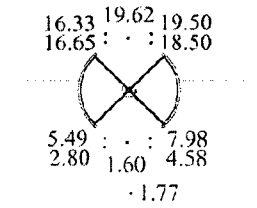
The experiments were carried out at a group of different rotation speeds. Table B-4 shows the air flow rate with different rotation speed. Table B-5 shows the temperature distribution.

Table B-4: The air flow rate with different rotation speed with two layers of insulation

Rotation speed (rpm)	Indoor temperature T_i (°C)	Outdoor temperature T_o (°C)	Temperature difference $T_i - T_o$ (°C)	Heat loss through envelope q_{loss} (W)	Mass flow rate m_{inf} (g/s)	Volumetric flow rate V_{inf} (L/s)
25.30	20.65	1.43	19.22	16.577	0.197	0.157
35.91	22.66	1.75	20.91	18.035	0.119	0.095
39.16	19.32	1.27	18.05	15.568	0.290	0.232
47.07	19.84	1.67	18.17	15.672	0.266	0.212
52.00	22.14	1.51	20.63	17.793	0.112	0.090
55.70	19.83	1.21	18.62	16.060	0.244	0.195
73.42	20.19	2.15	18.04	15.560	0.271	0.217
73.43	20.65	1.69	18.96	16.353	0.196	0.156
87.05	19.45	1.42	18.03	15.551	0.283	0.226
101.95	21.23	2.08	19.15	16.517	0.221	0.177
120.75	21.92	1.77	20.15	17.379	0.145	0.116

Table B-5: The temperature distribution around the revolving door with two layers of insulation

Rotation speed (rpm)	Temperature Distribution	$\Delta T = T_i - T_o$	$\Delta T_{\text{goes_in}} = T_B - T_A$	$\Delta T_{\text{goes_out}} = T_c - T_D$	$\Delta T_{\text{middle}} = T_{Mi} - T_{Mo}$
	- 20.65				
25.30	<p> 15.72 14.97 15.38 12.34 : : : 11.84 5.17 : : : 5.11 1.98 2.16 1.60 • 1.43 • 22.66 </p>	19.22	10.26	10.46	12.81
35.91	<p> 18.66 17.93 18.96 14.61 : : : 15.30 7.22 : : : 6.76 2.82 1.76 2.08 • 1.75 • 19.32 </p>	20.91	12.72	11.61	16.17
39.16	<p> 15.37 15.42 16.20 12.29 : : : 14.19 4.34 : : : 5.71 1.82 1.93 1.64 • 1.27 • 19.84 </p>	18.05	11.52	10.70	13.49
47.07	<p> 15.46 16.18 16.88 13.09 : : : 15.43 4.61 : : : 6.39 2.21 2.43 2.20 • 1.67 • 22.14 </p>	18.17	11.86	10.87	13.76
52.00	<p> 17.52 18.00 19.22 14.14 : : : 17.08 5.93 : : : 6.92 2.75 1.66 2.35 • 1.51 • 19.83 </p>	20.63	13.52	11.49	16.35
55.70	<p> 15.04 16.51 17.07 13.49 : : : 15.78 4.52 : : : 6.41 2.00 2.02 2.23 • 1.21 </p>	18.62	12.10	11.00	14.50

		• 20.188				
73.42		18.04	12.18	10.99	14.67	
73.43		18.96	12.34	10.98	15.26	
87.05		18.03	12.17	11.49	15.05	
101.95		19.15	12.34	11.23	15.82	
120.75		20.15	12.72	11.85	18.02	

B-4. The instantaneous method

Assuming after a long period of time, the whole system gets to steady state condition. The heat balance equation, at steady state is applied to the box: the heat

generated by heater and fan is equal to the heat loss through walls and heat loss due to the air infiltration through the revolving door, when door is moving:

$$\Delta Q = Q_{heater} + Q_{fan} - Q_{loss} - Q_{door} \quad (B-1)$$

where, $Q_{heater} = V \cdot I_{heater}$; is the power input to the heater, W. V is the voltage difference, V; I is the electric current, A

$Q_{fan} = V \cdot I_{fan}$, is the power input to the fan, W;

Q_{loss} = the heat loss through the box envelope, W;

Q_{door} = the heat loss due to air infiltration through the revolving door when door is moving, W;

The heat loss through walls is calculated as follows:

$$Q_{loss} = U \cdot A \cdot (T_i - T_o) \quad (B-2)$$

where, U = the overall coefficient of heat transmission, W/(m²·K);

A = the total exterior surface area of enclosure, m²;

T_i = average indoor room air temperature, °C;

T_o = temperature outside the box, which is the temperature inside the chamber, °C.

The heat loss caused by the air infiltration is expected as follows:

$$Q_{door} = m_{inf} \cdot c_p \cdot (T_i - T_o) \quad (B-3)$$

where, m_{inf} = the air mass flow rate through the revolving door, kg/s

c_p = the specific heat of air, 1005 J/kg·°C.

The air volumetric flow rate through the revolving door is:

$$v_{\text{inf}} = \frac{m_{\text{inf}}}{\rho} \quad (\text{B-4})$$

where, ρ is air density, which is 1.29 kg/m^3 at 1°C , which was the set-up outdoor temperature in the experiment, at atmospheric pressure (Fox and McDonald, 1998).

Equation B-1 becomes:

$$V \cdot I_{\text{heater}} + V \cdot I_{\text{fan}} = U \cdot A \cdot (T_i - T_o) + m_{\text{inf}} \cdot c_p \cdot (T_i - T_o) \quad (\text{B-5})$$

The unknown variable is to the air mass flow rate m_{inf} , provided that all other variables are measured. The UA value is identified by using the heat balance equation with the door not moving (still position):

$$V \cdot I_{\text{heater}} + V \cdot I_{\text{fan}} = q_{\text{loss}} = U \cdot A \cdot (T_i - T_o) \quad (\text{B-6})$$

The experimental results at 19.06 rpm are presented as an example of calculations. The calculation is based on the heat balance equation during a period of time with the door rotating. All the experiments were executed for enough long time to make sure the environment get to steady state. Data used in the calculation are the average values of the last five minutes interval (Fig. B-2).

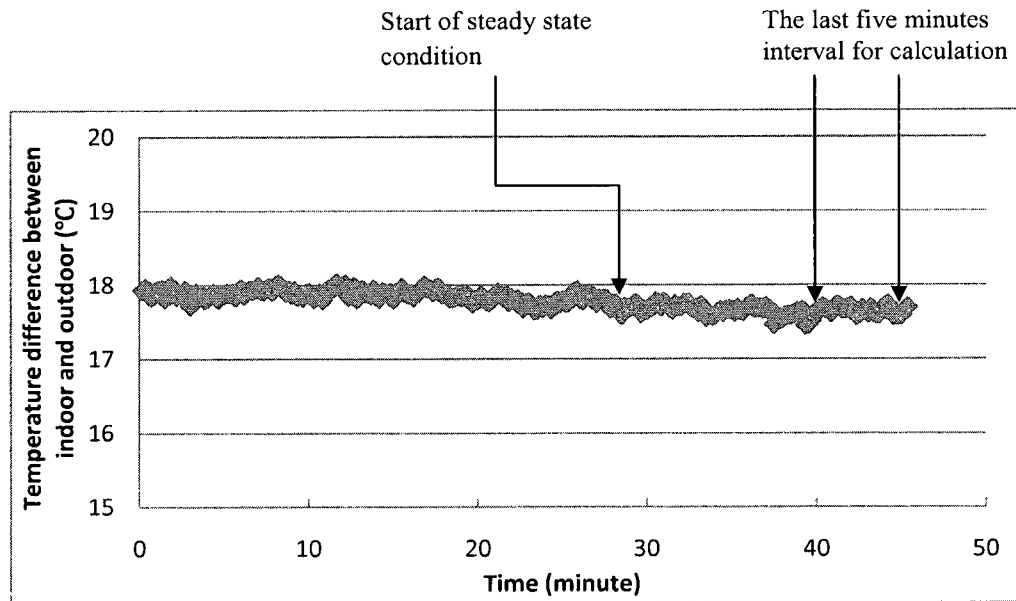


Fig. B-2: The temperature difference between indoor and outdoor environment in the experiment of 19.06 rpm

- 1) Time interval recorded:

$$\Delta t = 17:09:55 - 16:25:45 = 44.17 \text{ min}$$

- 2) Total number of rotations during the time interval Δt :

$$\Delta Rot = 860.5 \text{ (at } 17:09:55) - 18.5 \text{ (at } 16:25:45) = 842 \text{ rotations}$$

- 3) The average rotation speed during the time interval:

$$RPM_{model} = \frac{\Delta Rot}{\Delta t} = \frac{842}{44.177} = 19.06 \text{ rpm}$$

- 4) The heat balance equation at steady state:

$$V \cdot I_{heater} + V \cdot I_{fan} = U \cdot A \cdot (T_i - T_o) + m_{inf} \cdot c_p \cdot (T_i - T_o) \quad (B-5)$$

$$0.087 \cdot 4.36 + 0.96 \cdot 21.02 = 0.8625 \cdot (19.29 - 1.64) + m_{inf} \cdot 1005 \cdot (19.29 - 1.64)$$

$$m_{\text{inf}} = 0.299 \times 10^{-3} \text{ kg/s}$$

$$v_{\text{inf}} = \frac{m_{\text{inf}}}{\rho_o} = \frac{0.299 \times 10^{-3}}{1.25} = 0.239 \times 10^{-3} \text{ m}^3/\text{s} = 0.239 \text{ L/s}$$

The power inputs to the indoor environment, the indoor temperatures, outdoor temperatures and the calculated air flow rate at different rotation speeds are summarized in table B-6.

Table B-6: Air flow rate at different rotation speeds in the model

Experimental rotation speed (rpm)	$V \cdot I_{\text{heater+fan}}$ (W)	T_i (°C)	T_o (°C)	$T_i - T_o$ (°C)	$m_{\text{inf_model}}$ (g/s)	$v_{\text{inf_model}}$ (L/s)
19.06	20.53	19.29	1.64	17.65	0.299	0.239
31.76	20.32	19.01	1.54	17.47	0.299	0.239
38.88	20.40	20.20	1.67	18.53	0.237	0.190
47.85	20.44	20.74	2.33	18.41	0.247	0.197
48.55	20.75	18.95	1.08	17.87	0.297	0.238
51.96	20.5	19.57	1.86	17.71	0.294	0.235
60.10	20.28	20.04	1.75	18.29	0.245	0.196
79.68	21.16	19.29	1.08	18.21	0.298	0.238
85.37	20.48	20.39	1.8	18.59	0.238	0.190
108.37	20.4	19.82	2.09	17.73	0.287	0.229
116.44	20.37	20.01	2.39	17.62	0.292	0.234
173.87	20.37	18.64	2.39	16.25	0.389	0.311
192.39	20.26	19.06	1.67	17.39	0.301	0.241
247.36	20.45	18.87	1.11	17.76	0.288	0.230
287.37	20.65	18.86	1.57	17.29	0.330	0.264
295.73	20.04	15	3.04	11.96	0.809	0.647
308.51	20.7	19.21	1.86	17.35	0.329	0.263
322.84	20.64	18.94	1.92	17.02	0.348	0.279
347.77	20.48	18.83	1.79	17.04	0.338	0.270

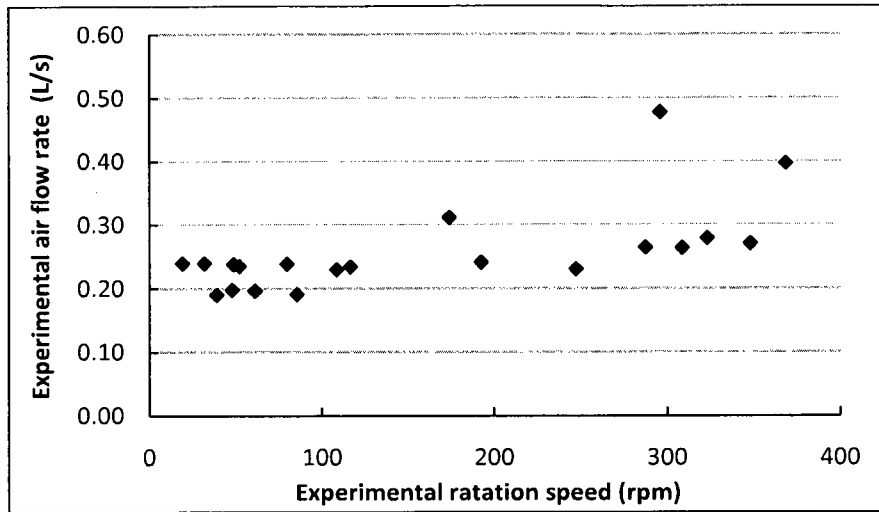


Fig. B-3: Volumetric air flow rate vs. the rotation speed of the experimental revolving door

The air infiltration rate increases slightly with the rotation speed (Fig. B-3), which means that the rotation speed only has a small impact on the air infiltration.

Appendix C:

Measured Temperatures and Dimensionless Temperatures around the Experimental Revolving Door

Thermocouples were installed around the revolving doors (Fig. C-1). The air temperature at each test point, the average value of each group: A, B, C, D, M_o and M_i , and the dimensionless temperature of each group of the final experiments are showing below in table C-1.

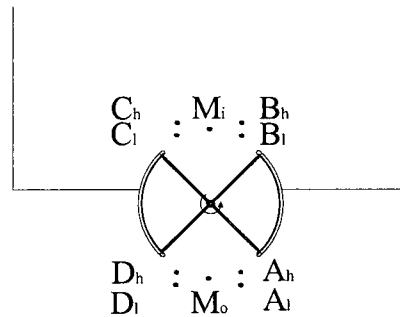
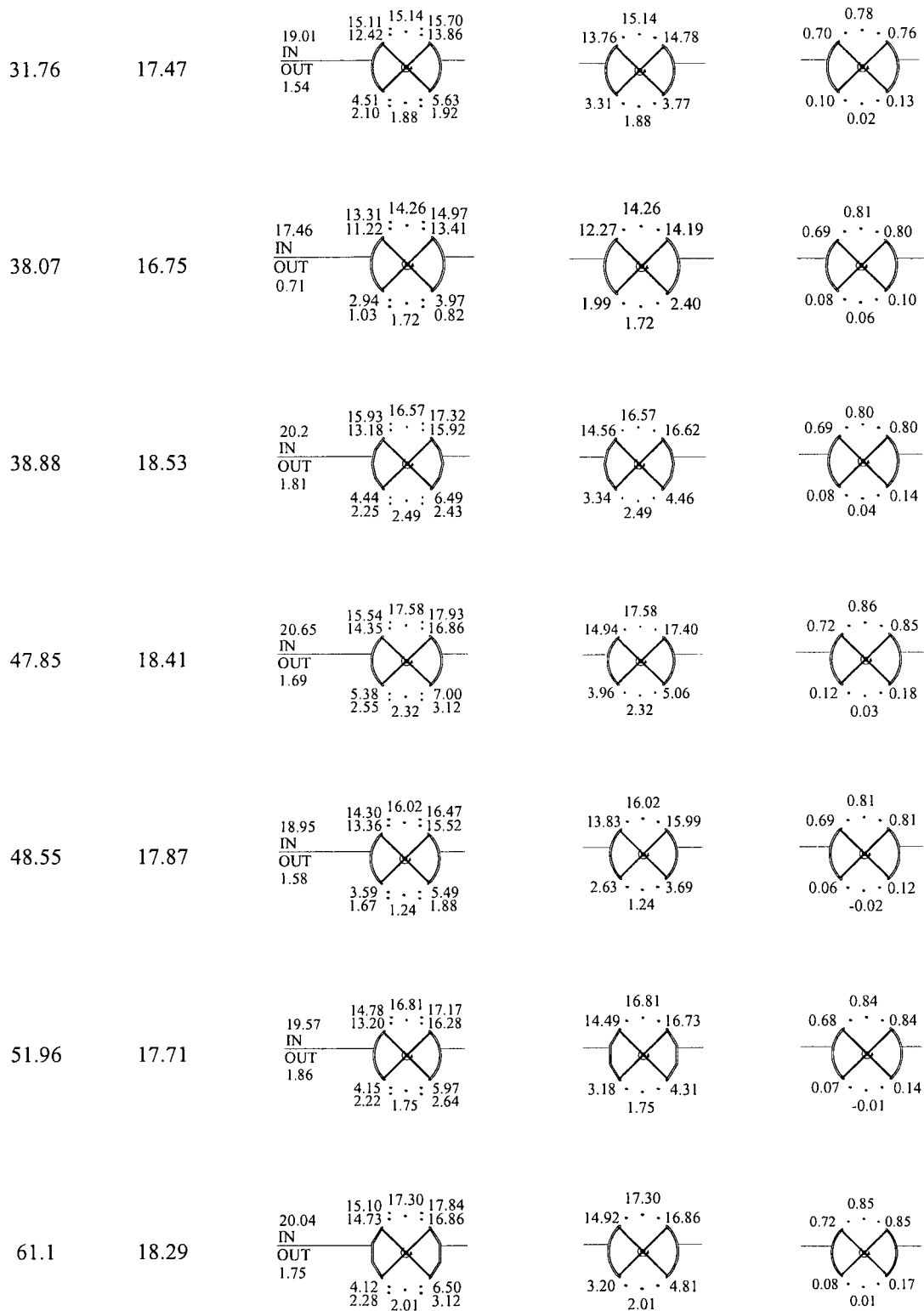
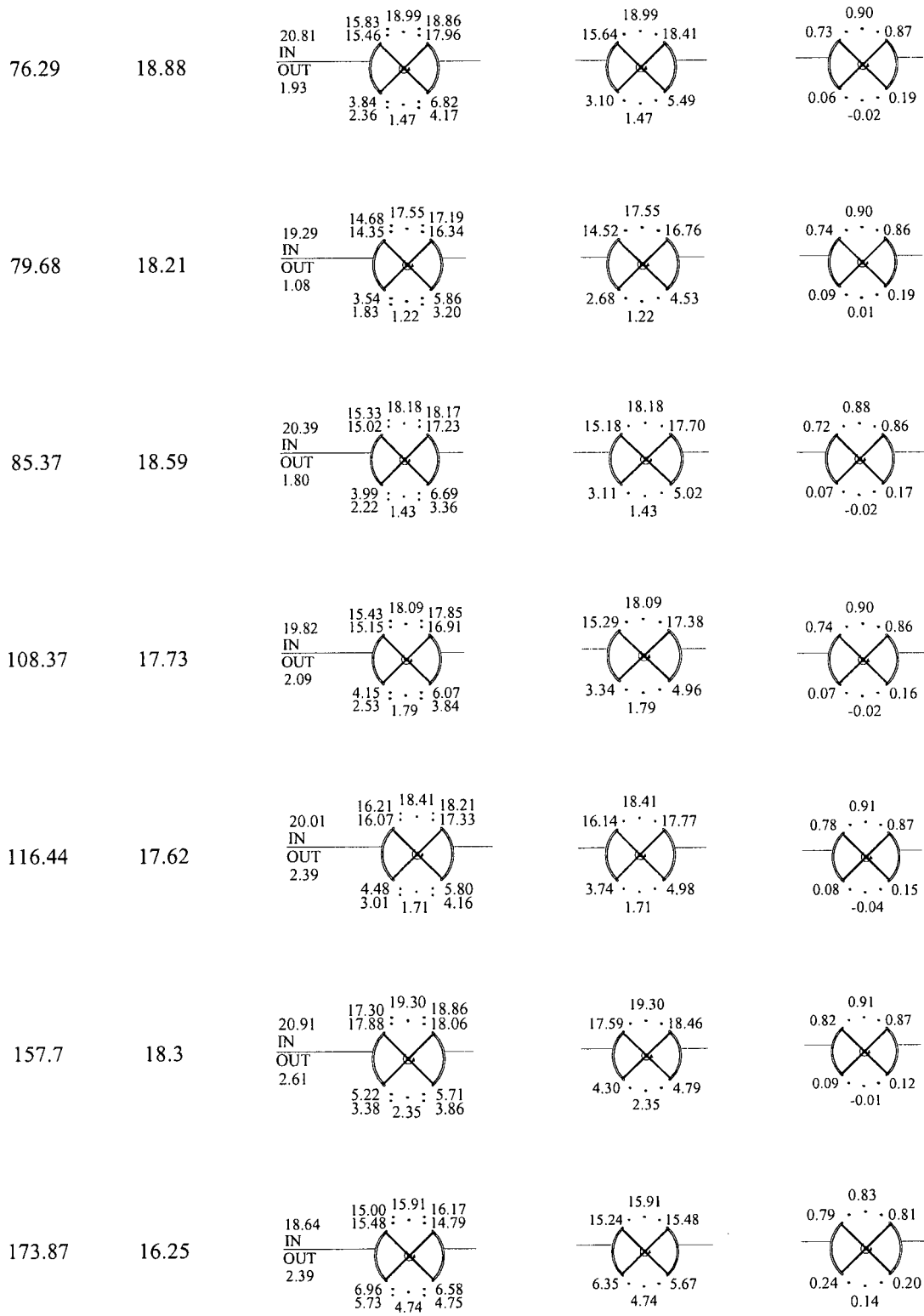


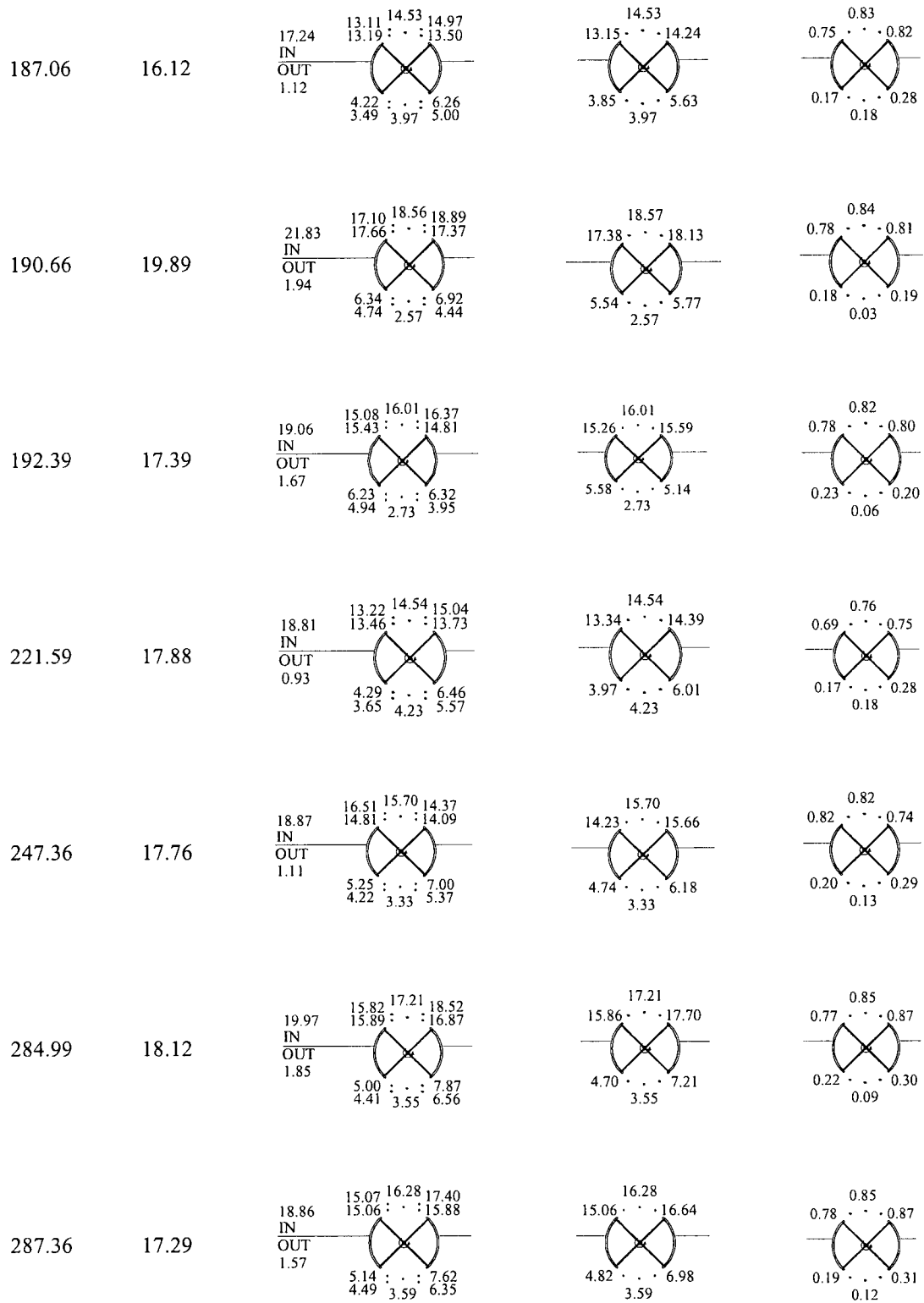
Fig. C-1: The location of the thermocouple round the revolving door

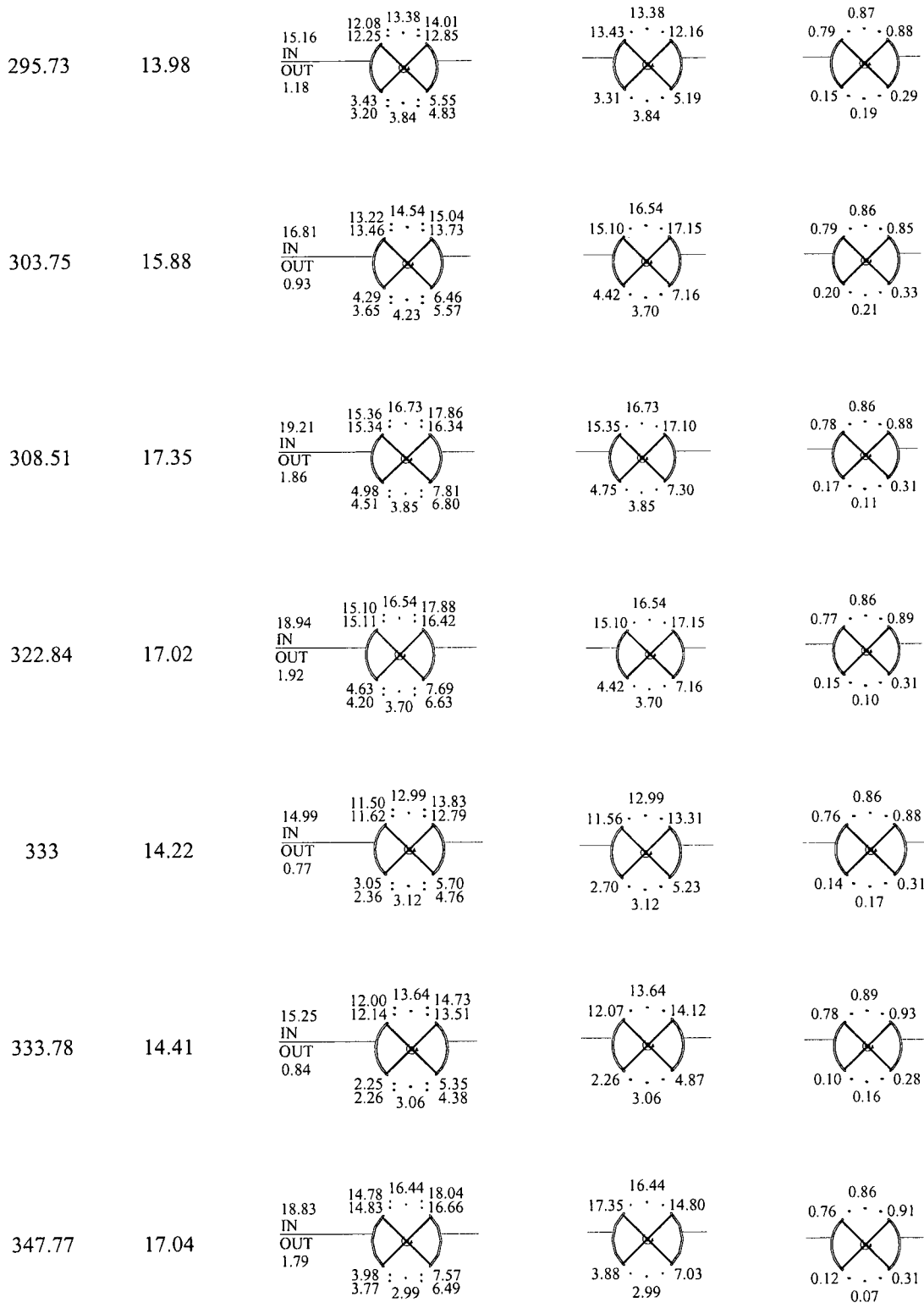
Table C-1: The temperature distribution at $T_i = 20^\circ\text{C}$

RPM	$\Delta T = T_i - T_o$	Temperature Distribution	Average Temperature	Dimensionless Temperature
19.06	17.65	<div style="display: flex; align-items: center; justify-content: center;"> <div style="margin-right: 10px;">19.29 IN OUT 1.64</div> </div>	<div style="display: flex; align-items: center; justify-content: center;"> </div>	<div style="display: flex; align-items: center; justify-content: center;"> </div>
19.17	17.91	<div style="display: flex; align-items: center; justify-content: center;"> <div style="margin-right: 10px;">19.59 IN OUT 1.99</div> </div>	<div style="display: flex; align-items: center; justify-content: center;"> </div>	<div style="display: flex; align-items: center; justify-content: center;"> </div>









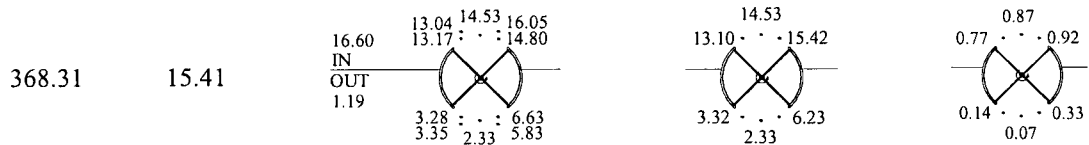


Table C-2: The temperature distribution at $T_i = 25^\circ\text{C}$ or 40°C

RPM	$\Delta T = T_i - T_o$	Temperature Distribution	Average Temperature	Dimensionless Temperature
152.98	42.72			
270.75	40.04			
300.3	40.74			
155.17	24.91			

Appendix D:

Correlation-based Models Obtained from Experimental Data

The dimensionless temperatures used for the establishment of the correlation at the condition with seals around all wings are presented in Table D-1. The numbers in Table D-2 are the dimensionless temperatures when the door has no vertical seals on the four wings.

Table D-1: Dimensionless temperature around the revolving door with full seals

N	θ_{Ah}	θ_{Al}	θ_{Bh}	θ_{Bl}	θ_{Ch}	θ_{Cl}	θ_{Dh}	θ_{Dl}	θ_{Mo}	θ_{Mi}
19.06	0.17	0.00	0.74	0.53	0.82	0.63	0.22	0.03	0.01	0.75
19.17	0.19	0.01	0.73	0.53	0.80	0.63	0.22	0.04	0.00	0.75
31.76	0.23	0.02	0.81	0.71	0.78	0.62	0.17	0.03	0.02	0.78
38.07	0.19	0.01	0.85	0.76	0.75	0.63	0.13	0.02	0.06	0.81
38.88	0.25	0.03	0.84	0.76	0.76	0.61	0.14	0.02	0.04	0.80
47.85	0.29	0.08	0.88	0.82	0.75	0.69	0.20	0.05	0.03	0.86
48.55	0.22	0.02	0.83	0.78	0.71	0.66	0.11	0.01	-0.02	0.81
51.96	0.23	0.04	0.86	0.81	0.73	0.64	0.13	0.02	-0.01	0.84
61.10	0.26	0.07	0.88	0.83	0.73	0.71	0.13	0.03	0.01	0.85
76.29	0.26	0.12	0.90	0.85	0.74	0.72	0.10	0.02	-0.02	0.90
79.68	0.26	0.12	0.88	0.84	0.75	0.73	0.14	0.04	0.01	0.90
85.37	0.26	0.08	0.88	0.83	0.73	0.71	0.12	0.02	-0.02	0.88
108.37	0.22	0.10	0.89	0.84	0.75	0.74	0.12	0.02	-0.02	0.90
116.44	0.19	0.10	0.90	0.85	0.78	0.78	0.12	0.04	-0.04	0.91
152.98	0.30	0.11	0.87	0.80	0.71	0.63	0.15	0.04	0.04	0.82
155.17	0.28	0.13	0.88	0.83	0.74	0.70	0.15	0.06	0.05	0.86
157.70	0.17	0.07	0.89	0.84	0.80	0.83	0.14	0.04	-0.01	0.91
173.87	0.26	0.15	0.85	0.76	0.78	0.81	0.28	0.21	0.14	0.83
187.06	0.32	0.24	0.86	0.77	0.74	0.75	0.19	0.15	0.18	0.83
190.66	0.25	0.13	0.85	0.78	0.76	0.79	0.22	0.14	0.03	0.84
192.39	0.27	0.13	0.85	0.76	0.77	0.79	0.26	0.19	0.06	0.82
221.59	0.31	0.26	0.79	0.72	0.69	0.70	0.19	0.15	0.18	0.76
247.36	0.33	0.24	0.75	0.73	0.87	0.77	0.23	0.18	0.13	0.82
270.75	0.30	0.17	0.90	0.85	0.75	0.71	0.18	0.10	0.10	0.84
284.99	0.33	0.26	0.92	0.83	0.77	0.77	0.17	0.14	0.09	0.85
287.37	0.35	0.28	0.92	0.83	0.78	0.78	0.21	0.17	0.12	0.85
295.73	0.31	0.26	0.92	0.83	0.78	0.79	0.16	0.14	0.19	0.87

300.30	0.32	0.19	0.89	0.83	0.72	0.66	0.19	0.10	0.10	0.81
303.75	0.35	0.29	0.89	0.81	0.77	0.79	0.21	0.17	0.21	0.86
308.51	0.34	0.28	0.92	0.83	0.78	0.78	0.18	0.15	0.11	0.86
322.84	0.34	0.28	0.94	0.85	0.77	0.77	0.16	0.13	0.10	0.86
333.00	0.35	0.28	0.92	0.85	0.75	0.76	0.16	0.11	0.17	0.86
333.78	0.31	0.25	0.96	0.88	0.77	0.78	0.10	0.10	0.15	0.89
347.77	0.34	0.28	0.95	0.87	0.76	0.77	0.13	0.12	0.07	0.86
368.31	0.35	0.30	0.96	0.88	0.77	0.78	0.14	0.14	0.07	0.87

Table D-2: Dimensionless temperature around the revolving door without vertical seals

N	θ_{Ah}	θ_{Al}	θ_{Bh}	θ_{Bl}	θ_{Ch}	θ_{Cl}	θ_{Dh}	θ_{Dl}	θ_{Mo}	θ_{Mi}
44.06	0.25	0.05	0.79	0.78	0.73	0.74	0.12	0.03	0.04	0.82
87.18	0.29	0.13	0.86	0.86	0.73	0.81	0.11	0.03	0.04	0.86
130.53	0.28	0.22	0.88	0.90	0.75	0.83	0.16	0.06	0.05	0.89
173.36	0.33	0.32	0.87	0.91	0.77	0.85	0.20	0.10	0.09	0.90
190.37	0.32	0.30	0.90	0.93	0.79	0.85	0.20	0.09	0.10	0.93
216.42	0.31	0.28	0.90	0.92	0.80	0.85	0.19	0.09	0.07	0.95
242.00	0.30	0.22	0.87	0.88	0.76	0.82	0.16	0.07	0.07	0.89
258.92	0.31	0.24	0.88	0.90	0.77	0.83	0.17	0.07	0.07	0.90
277.61	0.34	0.29	0.89	0.90	0.79	0.84	0.20	0.12	0.10	0.96
305.00	0.31	0.28	0.88	0.91	0.79	0.84	0.18	0.10	0.09	0.98
335.01	0.29	0.26	0.88	0.91	0.79	0.84	0.16	0.08	0.06	0.98
346.37	0.28	0.26	0.86	0.90	0.77	0.82	0.16	0.09	0.06	0.95
365.94	0.27	0.26	0.84	0.89	0.74	0.80	0.16	0.10	0.07	0.94
381.41	0.28	0.26	0.83	0.88	0.74	0.79	0.15	0.10	0.06	0.93
398.24	0.29	0.26	0.83	0.88	0.73	0.79	0.16	0.10	0.07	0.93

Table D-3 presents several correlation-based models for the case when the experimental revolving door has four seals, which were developed from the experimental data, using the statistical capability of EXCEL spreadsheet, and verified with Matlab. The fifth model that uses as independent variables N^2 , N , θ_{Ah} , θ_{Al} , θ_{Bh} , θ_{Bl} , θ_{Ch} , θ_{Cl} , θ_{Dh} , θ_{Dl} , θ_{Mo} , θ_{Mi} , gives the highest R^2 value of 0.81 and the relative error is 18.6%. It is important to note that at location A, B, C, D, M_i and M_o , two temperature values are used, at high and low locations.

Table D-3: Correlation-based model of air infiltration when the revolving door has four seals

	Model	R²	Standard error Se_{y/x}	Relative standard error ω%
1	$q_{inf} = (0.00098N - 1.26\theta_A - 0.42\theta_B + 0.099\theta_C - 1.81\theta_D + 2.24\theta_{M0} + 0.1\theta_{Mi} + 0.77) / \rho$	0.75	0.077	19.1%
2	$q_{inf} = (0.000004N^2 - 0.00054N - 1.49\theta_A - 0.55\theta_B - 0.14\theta_C - 1.12\theta_D + 2.32\theta_{M0} + 0.93\theta_{Mi} + 0.4) / \rho$	0.73	0.072	18%
3	$q_{inf} = (0.000003N^2 - 0.00023N + 0.122\theta_A - 0.52\theta_B - 0.058\theta_C - 0.35\theta_D + 0.8) / \rho$	0.42	0.115	28.7%
4	$q_{inf} = (0.001N - 0.75\theta_{Ah} - 0.83\theta_{Al} + 0.23\theta_{Bh} - 0.77\theta_{Bl} + 0.05\theta_{Ch} - 0.5\theta_{Cl} - 1.62\theta_{Dh} + 0.26\theta_{Dl} + 2.14\theta_{M0} + 0.77\theta_{Mi} + 0.74) / \rho$	0.77	0.08	20%
5	$q_{inf} = (0.000006 \cdot N^2 - 0.0017 \cdot N - 1.96 \cdot \theta_{Ah} - 0.046 \cdot \theta_{Al} - 0.85 \cdot \theta_{Bh} + 0.35 \cdot \theta_{Bl} - 0.16 \cdot \theta_{Ch} - 0.53 \cdot \theta_{Cl} - 0.61 \cdot \theta_{Dh} + 0.31 \cdot \theta_{Dl} + 2.22 \cdot \theta_{M0} + 1.09 \cdot \theta_{Mi} + 0.93) / \rho$	0.81	0.075	18.6%
6	$q_{inf} = (0.000004N^2 - 0.0013N - 2.48\theta_{Ah} + 1.49\theta_{Al} - 0.17\theta_{Bh} + 0.3\theta_{Bl} - 0.06\theta_{Ch} - 1.27\theta_{Cl} - 0.55\theta_{Dh} + 1.45\theta_{Dl} + 1.72) / \rho$	0.51	0.11	28.6%

The correlation-based models when the door has no seal around the vertical side of the wings are also generated (Table D-4). The experimental data used for establishing the models for no vertical seals was provided by A. Aupied (2009), which used the same experimental setup as this research. The R² values of all models are between 0.95 and 0.99.

Table D-4: Correlation equations of air infiltration when the revolving door does not have vertical seals

	Equation	R ²	Standard error Se _{y/x}	Relative standard error ω%
1	$q_{inf} = (0.0024N - 4.89\theta_A + 3.86\theta_B - 1.3\theta_C + 6.03\theta_D - 2.87\theta_{Mo} - 1.93\theta_{Mi} - 1.01)/\rho$	0.95	0.081	8.1%
2	$q_{inf} = (-0.00001N^2 + 0.006N - 2.81\theta_A + 2.02\theta_B - 6.52\theta_C + 3.82\theta_D - 3.3\theta_{Mo} + 2.6\theta_{Mi} + 1.71)/\rho$	0.95	0.083	8.3%
3	$q_{inf} = (-0.000002N^2 + 0.0034N + 5.57\theta_A + 4.9\theta_B - 3.07\theta_C + 4.48\theta_D - 0.62)/\rho$	0.95	0.078	7.8%
4	$q_{inf} = (0.0026N - 3.33\theta_{Ah} - 5.04\theta_{Al} + 1.12\theta_{Bh} + 3.39\theta_{Bl} + 1.53\theta_{Ch} + 3.95\theta_{Cl} - 2.65\theta_{Dh} + 13.82\theta_{Dl} - 2.85\theta_{Mo} - 3.47\theta_{Mi} - 3.15)/\rho$	0.98	0.078	7.8%
5	$q_{inf} = (0.000026N^2 - 0.0071N - 8.32\theta_{Ah} - 4.36\theta_{Al} + 8.56\theta_{Bh} + 1.16\theta_{Bl} + 14.3\theta_{Ch} + 11.95\theta_{Cl} - 13.08\theta_{Dh} + 24.57\theta_{Dl} + 1.24\theta_{Mo} - 16.45\theta_{Mi} - 9.58)/\rho$	0.99	0.069	6.9%
6	$q_{inf} = (-0.000004N^2 + 0.0038N - 4.9\theta_{Ah} - 5.04\theta_{Al} + 0.18\theta_{Bh} + 1.78\theta_{Bl} - 3.04\theta_{Ch} + 5.27\theta_{Cl} + 0.54\theta_{Dh} + 9.7\theta_{Dl} - 1.65)/\rho$	0.97	0.08	8%